Diss. ETH No. 13429

Behavior of Iodine Species in Oxidative Processes During Drinking Water Treatment

A dissertation submitted to the
SWISS FEDERAL INSTITUTE OF TECHNOLOGY ZURICH
for the degree of
Doctor of Natural Sciences

presented by
YVES BICHSEL
Dipl. Chem. ETH
born December 30, 1971
citizen of Eggiwil

accepted on the recommendation of
Prof. Dr. Bernhard Wehrli, examiner
Prof. Dr. Willem H. Koppenol, co-examiner
Dr. Urs von Gunten, co-examiner
Dr. Auguste Bruchet, co-examiner

2000

Dank

Mein herzlicher Dank geht an Urs von Gunten, der mich während der vergangenen vier Jahre betreut hat. Auch in turbulenten Reorganisationszeiten an der EAWAG hat er immer Zeit für meine Arbeit gehabt.

Ebensosehr danke ich meinen Kolleginnen und Kollegen aus der Forschungsgruppe für die gute Zusammenarbeit und Mithilfe für das Gelingen dieser Arbeit: Juan Acero, Silvio Canonica, Mike Elovitz, Hervé Gallard, Edi Höhn, Suzanne Mettler, Yvonne Oliveras, Uli Pinkernell, Lisa Salhi, Konrad Stemmler. Weitere Personen an der EAWAG haben mich in verschiedenster Hinsicht unterstützt: Urs Jans, Hans Kramer, Hans-Ueli Laubscher, Hermann Mönch, Henning Raschke, Csaba Reisinger, Winfried Suske, Monika Zemp.

Je voudrais remercier Auguste Bruchet de la Lyonnaise des Eaux pour l'intérêt qu'il a apporté à mon travail et pour avoir accepté d'être co-rapporteur de cette thèse. Je tiens à remercier également toute l'équipe du CIRSEE pour le bon accueil qu'ils m'ont fait lors de mes visites au Pecq. Enfin, je remercie la Lyonnaise des Eaux pour avoir soutenu ce projet financièrement.

Ich danke Bernhard Wehrli, der meine Dissertation begleitet hat und das Referat übernommen hat, sowie W.H. Koppenol für die Übernahme des Korreferats.

Ich danke Jürg Hoigné für die Korrektur des 3. und 4. Kapitels sowie Adrian Ammann für die Korrektur des 2. Kapitels.

Die (sonst nirgends erhältlichen) Standards für die Iod-Trihalomethane wurden mir von F. Ventura, Societat General d'Aigües de Barcelona (AGBAR), zur Verfügung gestellt.

Meinen Eltern danke ich für die Unterstützung und Förderung während meiner ganzen Ausbildungszeit.

Schliesslich danke ich meiner Frau, die mich im nicht-wissenschaftlichen Teil der vergangenen vier Jahre begleitet und geliebt hat. Ich freue mich darauf, auch in Zukunft mit ihr durchs Leben zu gehen.

Table of Contents

Summary

Iodo-trihalomethanes (I-THMs) are by-products of the oxidative treatment of iodide-containing drinking waters. These compounds, especially iodoform (CHI_3), are undesired because they can be responsible for a bad taste and odor. Naturally occurring precursors of I-THMs are iodide (I^-) and natural organic matter (NOM). Several oxidants/disinfectants such as ozone, chlorine, or chloramine oxidize I^- to hypoiodous acid (HOI) in a fast reaction. Subsequently, HOI can react with NOM under formation of I-THMs. Alternative sinks for HOI are its oxidation to iodate (IO_3^-) or its disproportionation, which leads to the formation of I^- and IO_3^-.

To elucidate the potential of the formation of I-THMs during oxidative drinking water treatment, we investigated the reaction kinetics of iodine species, especially HOI, with respect to the formation of iodine-containing disinfection by-products.

Chapter 1 gives a general introduction into taste and odor problems, iodine chemistry, geochemistry, metabolism, toxicity, and its use for water disinfection.

Chapter 2 deals with two new analytical methods for the determination of the main inorganic iodine species, I^- and IO_3^-. The methods consist of an anion chromatography separation step followed by a postcolumn reaction and UV/vis detection. For the analysis of I^-, the interhalogen-compound IBr_2^- is formed by reaction of the analyte with hypobromite (OBr^-) and bromide (Br^-). IBr_2^- is detected at a wavelength of 249 nm. This allows a detection limit of 0.1 μg I^-/L (0.8 nM). For the analysis of IO_3^-, triiodide (I_3^-) is formed through reaction of the analyte with I^- and H^+. I_3^- is detected at a wavelength of 288 nm. This leads to a detection

limit of 0.1 µg IO_3^-/L (0.6 nM). The detection limits for I^- and IO_3^- allow their determination in natural waters without sample pretreatment.

Chapter 3 reports kinetic data of the disproportionation of HOI, according to:

$$3\ HOI \rightarrow IO_3^- + 2\ I^- + 3\ H^+$$

This reaction was found to be catalyzed by anions such as borate, phosphate, or carbonate. The half-life of HOI in natural waters due to the disproportionation lies between the two extremes of 4 days (50 µg/L HOI, pH = 9, 5 mM carbonate) and 3.5 years (1 µg/L HOI, pH = 6, no carbonate).

The oxidation kinetics of HOI and hypoiodite (OI^-) for the reaction with ozone, chlorine, and chloramine are described in chapter 4. Ozone oxidizes both HOI and OI^- in fast reactions ($k_{O3+HOI} = 3.6 \times 10^4\ M^{-1}s^{-1}$; $k_{O3+OI-} = 1.6 \times 10^6\ M^{-1}s^{-1}$). These high rate constants lead to a HOI half-life of ≤ 4 s for typical ozonation conditions (0.25-2 mg/L O_3, pH = 6-9). Chlorine species oxidize HOI by a combination of second- and third-order reactions ($k''_{HOCl+HOI} = 8.2\ M^{-1}s^{-1}$; $k'''_{HOCl+HOI} = 8.3 \times 10^4\ M^{-2}s^{-1}$; $k_{OCl-+HOI} = 52\ M^{-1}s^{-1}$). Typical HOI half-lifes in chlorination processes are between 8 min (2 mg/L Cl_2, pH = 9) and 10 h (0.2 mg/L Cl_2, pH = 6). The product of HOI oxidation by both ozone and chlorine is IO_3^-. Chloramine does not oxidize HOI.

Finally, kinetics of HOI consumption as well as formation of I-THMs and IO_3^- were investigated both in model and in natural waters (chapter 5). Phenols and in a smaller extent α-methyl carbonyl compounds were found to be reactive toward HOI and to yield CHI_3. For phenols, the rate constants for the consumption of HOI varied over almost 9 orders of magnitude from 1.5 $M^{-1}s^{-1}$ to 7 x 10^8 $M^{-1}s^{-1}$. For α-methyl carbonyl

compounds, kinetics were either first-order in [HOI] (0.05 - 12 $M^{-1}s^{-1}$) or zero-order in [HOI] (5×10^{-9} - 4×10^{-6} s^{-1}). The normalized yield and formation rate of CHI_3 per carbon decreased in the order resorcinol > α-methyl carbonyl compounds > phenol. The formation of I-THMs was significantly slower than the consumption of HOI. Therefore, it can be hypothesized that the addition reaction of HOI is not rate-determining in the formation of I-THMs but rather a final hydrolysis step.

In the ozonation of natural waters, no I-THMs were detected and more than 90% of I^- was transformed to IO_3^-. Chlorine led to the formation of both IO_3^- and I-THMs. With increasing chlorine doses, the CHI_3 formation decreased but the IO_3^- formation as well as the formation of mixed I-THMs such as $CHCl_2I$ and of classical THMs such as chloroform increased. In chloramination processes, I-THMs (especially CHI_3) were the main products. A comparison of reaction kinetics in model and in natural waters shows that the I-THM formation in natural waters can be explained by the presence of phenolic entities in the NOM.

In conclusion, the formation of CHI_3 in drinking waters is in competition with the oxidation of HOI to IO_3^- and the oxidation of THM-precursor sites in the NOM. The disproportionation is too slow to have an influence on the half-life of HOI. The oxidation of HOI to IO_3^- is dominant in ozonation processes but can also be important in chlorination processes. The oxidation of THM-precursors is only important in chlorine-based processes where it leads to the formation of mixed I-THMs rather than CHI_3. In chloramination processes however, the two competing reactions do not prevent the CHI_3-formation. The probability of CHI_3-formation in oxidative processes during drinking water disinfection therefore increases in the order ozone < chlorine < chloramine.

Seite Leer /
Blank leaf

Zusammenfassung

Iod-Trihalomethane (I-THM) können während der oxidativen Aufbereitung von iodidhaltigen Trinkwässern als Desinfektionsnebenprodukte gebildet werden. Unter diesen Verbindungen ist vor allem Iodoform (CHI_3) unerwünscht, da es dem Trinkwasser einen Geruch und Geschmack geben kann. Die natürlich vorkommenden Vorläufer der I-THM sind Iodid (I^-) und natürliches organisches Material (NOM). Verschiedene Oxidations- und Desinfektionsmittel der Trinkwasseraufbereitung wie z.B. Ozon, Chlor oder Chloramin oxidieren I^- in einer schnellen Reaktion zur unteriodigen Säure (HOI). HOI kann dann durch Reaktion mit dem NOM I-THM bilden. In Konkurrenz dazu kann HOI aber auch zu Iodat (IO_3^-) oxidiert werden oder in einer Disproportionierung zu I^- und IO_3^- reagieren.

Um die Bildung von I-THM charakterisieren zu können, haben wir die Kinetik von Reaktionen verschiedener Iod-Spezies, v.a. von HOI, in Bezug auf die Bildung iodhaltiger Nebenprodukte in der oxidativen Trinkwasseraufbereitung untersucht.

Kapitel 1 gibt eine Einführung in die Problematik von schlechtem Geruch und Geschmack, in die wässrige Chemie von Iod, dessen Geochemie, Metabolismus, Toxizität sowie Gebrauch als Desinfektionsmittel.

Im zweiten Kapitel werden zwei neue Analysenmethoden für die Quantifizierung von I^- und IO_3^- in natürlichen Wässern vorgestellt. Sie basieren auf einer ionenchromatographischen Trennung, der eine Nachsäulenreaktion und eine UV/Vis-Detektion folgen. Für die Bestimmung von I^- wird durch Reaktion mit Hypobromit (OBr^-) und Bromid (Br^-) die Interhalogenverbindung IBr_2^- erzeugt. Durch deren Detektion bei einer Wellenlänge von 249 nm kann eine Nachweisgrenze von 0.1 µg/L I^- (0.8 nM) erreicht werden. Für die Analyse von IO_3^- wird durch Reaktion mit I^- und

H^+ I_3^- gebildet. Die Detektion von I_3^- bei einer Wellenlänge von 288 nm führt zu einer Nachweisgrenze von 0.1 µg/L IO_3^- (0.6 nM).

Das dritte Kapitel dieser Arbeit geht auf die Kinetik der Disproportionierung von HOI ein:

$$3\,HOI \rightarrow IO_3^- + 2\,I^- + 3\,H^+$$

Diese Reaktion wird durch Anionen (z.B. Borat, Phosphat, Carbonat) katalysiert. Die Halbwertszeit von HOI liegt im Bereich von 4 Tagen (50 µg/L HOI, pH = 9, 5 mM Carbonat) bis 3.5 Jahren (1 µg/L HOI, pH = 6, ohne Carbonat).

Die Kinetik der Oxidation von HOI und Hypoiodit (OI^-) durch Ozon, Chlor und Chloramin wird im Kapitel 4 beschrieben. Die Oxidation von HOI und OI^- durch Ozon läuft sehr schnell ab ($k_{O3+HOI} = 3.6 \times 10^4\ M^{-1}s^{-1}$; $k_{O3+OI-} = 1.6 \times 10^6\ M^{-1}s^{-1}$). Die Halbwertszeit von HOI in einem typischen Ozonungsprozess (0.25-2 mg/L O_3, pH = 6-9) ist ≤ 4 s. Chlorspezies oxidieren HOI in einer Kombination von Reaktionen zweiter und dritter Ordnung ($k''_{HOCl+HOI} = 8.2\ M^{-1}s^{-1}$; $k'''_{HOCl+HOI} = 8.3 \times 10^4\ M^{-2}s^{-1}$; $k_{OCl-+HOI} = 52\ M^{-1}s^{-1}$). Die Halbwertszeit von HOI in Anwesenheit von Chlor bewegt sich zwischen 8 min (2 mg/L Cl_2, pH = 9) und 10 h (0.2 mg/L Cl_2, pH = 6). Das Produkt der Oxidation von HOI durch Ozon und Chlor ist IO_3^-. Chloramin reagiert nicht mit HOI.

Im letzten Teil dieser Arbeit wurden die Kinetiken des HOI-Abbaus sowie der Bildung von I-THM und von IO_3^- in Modell- und in natürlichen Wässern untersucht (Kapitel 5). Phenole und in kleinerem Ausmass α-Methylcarbonylverbindungen reagieren mit HOI und ergeben dabei CHI_3. Die gemessenen Geschwindigkeitskonstanten der Phenole mit HOI erstrecken sich über einen Bereich von fast 9 Grössenordnungen ($1.5\ M^{-1}s^{-1}$ bis $7 \times 10^8\ M^{-1}s^{-1}$). Die Kinetik der Reaktion mit α-Methylcarbonylverbindungen kann sowohl erster Ordnung in [HOI] (0.05-12 $M^{-1}s^{-1}$) als auch nullter Ordnung in [HOI] (5×10^{-9} - 4×10^{-6} s^{-1}) sein. Die pro Kohlenstoff normierte Ausbeute und Bildungsrate von CHI_3 nimmt in der Reihenfolge Resorcin > α-Methylcarbonyle > Phenol ab. Die Kinetik des HOI-Abbaus war signifikant schneller als die Kinetik der I-THM-Bildung. Dies deutet darauf hin, dass nicht die Addition von HOI der geschwindigkeitsbestimmende Schritt dieser Reaktion ist, sondern die abschliessende Hydrolyse.

In der Ozonung von natürlichen Wässern wurde der grösste Teil des HOI zu IO_3^- oxidiert. I-THM wurden keine nachgewiesen. In den Chlorungsexperimenten wurden verschiedene Mengen von IO_3^- und I-THM gefunden. Hohe Chlordosen führten zur vermehrten Bildung von IO_3^- und von klassischen Trihalomethanen wie z.B. Chloroform. Gleichzeitig wurde die Bildung von CHI_3 abgeschwächt. Die höchsten CHI_3-Konzentrationen wurden bei der Anwendung von Chloramin gefunden. Der Vergleich der Kinetiken in Modell- und in natürlichen Systemen zeigt, dass Phenolgruppen im NOM für die beobachteten Effekte verantwortlich sein können.

Abschliessend lässt sich sagen, dass die Bildung von CHI_3 in der Trinkwasseraufbereitung in Konkurrenz zur Oxidation von HOI zu IO_3^- und zur Oxidation von THM-Vorläufergruppen im NOM steht. Die Disproportionierung hat keinen Einfluss auf das Verhalten von HOI. Die Oxidation von HOI zu IO_3^- dominiert in Ozonungsprozessen, kann aber auch in Chlorungsprozessen von Bedeutung sein. Die Oxidation der THM-Vorläufergruppen ist in Anwesenheit von Chlor wichtig und führt zur Bildung von gemischten I-THM wie z.B. $CHCl_2I$ statt von CHI_3. In Chloraminprozessen können die zwei Konkurrenzreaktionen die Bildung von CHI_3 nicht verhindern. Die Wahrscheinlichkeit der Bildung von CHI_3 während der oxidativen Trinkwasseraufbereitung nimmt somit in der Reihenfolge Ozon < Chlor < Chloramin zu.

1. Introduction

1.1 Taste and Odor Problems in Drinking Water Treatment

Drinking water of a good quality has neither a taste nor an odor. However, this goal is not easy to achieve. Since taste and odor can be caused by minute amounts of impurities, it is often an analytical challenge to find the link between undesired organoleptic attributes and the responsible chemical compound. This is in general a prerequisite for the effective and reliable control of the water quality. Furthermore, the appearance of taste and odor problems is dependent on a large number of factors such as changing raw water quality, treatment, and post-treatment conditions.

It is not easy to find a precise and reproducible measure for the presence and the intensity of taste or odor. A tool which tries to meet these criteria is the flavor profile analysis (FPA; Bartels et al., 1986). According to this method, a number of panelists taste and smell the sample in a standardized procedure. They describe the sample with descriptors such as e.g. chlorinous, musty, or grassy and assign them an intensity. If they disagree on a specific aspect of a water, a consensus is developed by discussing the results.

The description of a taste can be reduced to the four fundamental sensations sweet, sour, salty, and bitter. Such a reduction is not possible for odors although a classification into 8 to 34 fundamental odors makes sense for practical reasons (Amoore, 1986). Another possibility for the classification of the odors is to define them by standard reference compounds. In such a way, earthy (geosmin), fruity (nonanal), musty (2-methylisoborneol), old grass (hexanal), almond (benzaldehyde), cucumber (nonenal), shoe polish (cumene) and other odors were standardized.

In a survey of the American Water Works Association in 1996, 40 % of the water utilities declared to be affected by taste and odor problems (Suffet et al., 1996). Especially utilities treating surface waters were concerned. They report customer complaints because of bad tastes and odors which are described as earthy, fishy, chlorine, medicinal, sour, metallic, and more. In average, water utilities spent 4.5 % of their total budget to cope with these problems.

Organoleptic problems in drinking waters result from natural, industrial, or treatment processes (Bartels et al., 1986). Compounds which originate from natural processes such as algal metabolites are frequently the reason for bad taste and odor. Examples are geosmin, methylisoborneol, or 2-isopropyl-3-methoxypyrazine. Geosmin is one of the compounds with the lowest taste and odor threshold ever determined (10 - 20 ng/L; Young et al., 1996). One case of geosmin occurrence was reported in a drinking water derived from a river water in Philadelphia where concentrations of up to 120 ng/L geosmin were detected in several episodes which lasted 10 to 30 days (Burlingame et al., 1986). The reason for the high geosmin concentrations was an unusual growth of algae as the result of a drought. The removal of natural compounds with taste and odor can occur by adsorption on activated carbon or by ozonation processes (Burlingame et al., 1986; Anselme et al., 1989).

Other sources of compounds which lead to bad taste and odor are chemical pollutants which are present in the raw water and not removed during treatment. Examples for such compounds are benzaldehyde, chlorobenzene, or benzothiazole (Bartels et al., 1986). Leaching of substances from pipes or tubes during storage and distribution of the finished drinking waters may also lead to taste and odor problems.

Finally, chemical reactions which occur during water treatment (e.g. disinfection) may lead to the formation of by-products with undesired organoleptical properties. In 1967, the drinking water in Zurich was contaminated by phenol which was deliberately introduced into the lake Zurich by a laundry company (Nägeli, 1969). Upon chlorination of this water, chlorophenol was formed which resulted in bad taste and odor. 60'000 people were affected by this incident. Subsequently, the disinfectant was changed to ozone. However, this incident had the positive side-effect that broad parts of the society became aware of the importance of the protection of water resources.

Another group of compounds which can be formed during drinking water treatment and which can result in taste and odor problems are the iodo-trihalomethanes (I-THMs). Their presence in oxidized drinking water has been discovered more than 20 years ago when developments in gas chromatography first allowed a screening for organic water contaminants. Several authors reported the presence of dichloroiodomethane ($CHCl_2I$) in chlorinated drinking water (Bunn et al., 1975; Giger et al., 1976). During a monitoring survey for organic micropollutants in the United States, $CHCl_2I$ was found in 85 of 111 finished drinking waters (Brass et al., 1977). Bunn et al. (1975) added halides to a raw water before chlorination. By this means, they could form all 10 chloro-, bromo-, iodo-, and mixed trihalomethanes and detect them by GC/MS. In the late 1980s, it was discovered that I-THMs can be responsible for taste and odor problems in the drinking water. Table 1.1 lists all THMs together with their taste and odor threshold concentrations. The taste and odor of CHI_3 was described as medicinal or pharmaceutical (Hansson et al., 1987; Suez Lyonnaise des Eaux, 1993). The taste of $CHCl_3$ was described as metallic and sweet, its odor as chemical and antiseptic (Young et al., 1996).

Table 1.1 Trihalomethanes and Their Taste and Odor Threshold Concentrations

		Taste and odor threshold in µg/L	ref.
Chloroform	$CHCl_3$	100 - 2000	a
Bromodichloromethane	$CHBrCl_2$	5	a
Dibromochloromethane	$CHBr_2Cl$		
Bromoform	$CHBr_3$	5	a
Dichloroiodomethane	$CHCl_2I$	6	b
Chlorodiiodomethane	$CHClI_2$	9	b
Dibromoiodomethane	$CHBr_2I$	3	b
Bromodiiodomethane	$CHBrI_2$	0.1	b
Bromochloroiodomethane	CHBrClI	5	b
Iodoform	CHI_3	0.03 - 1	b, c

a: Young et al., 1996; b: Khiari, 1999; c: Suez Lyonnaise des Eaux, 1993.

I-THMs can be formed through reaction of hypoiodous acid (HOI) with natural organic matter (NOM). HOI is usually not present in natural waters but it is produced from naturally occurring iodide (I^-) in oxidative treatment steps by ozone, chlorine, or chloramine. In competition to the addition to NOM, HOI can also disproportionate or be further oxidized by disinfectants and thus transformed to iodate (IO_3^-). Figure 1.1 shows a representation of these reactions which lead to the formation of IO_3^-, I-THMs, or other organic iodine-containing disinfection by-products.

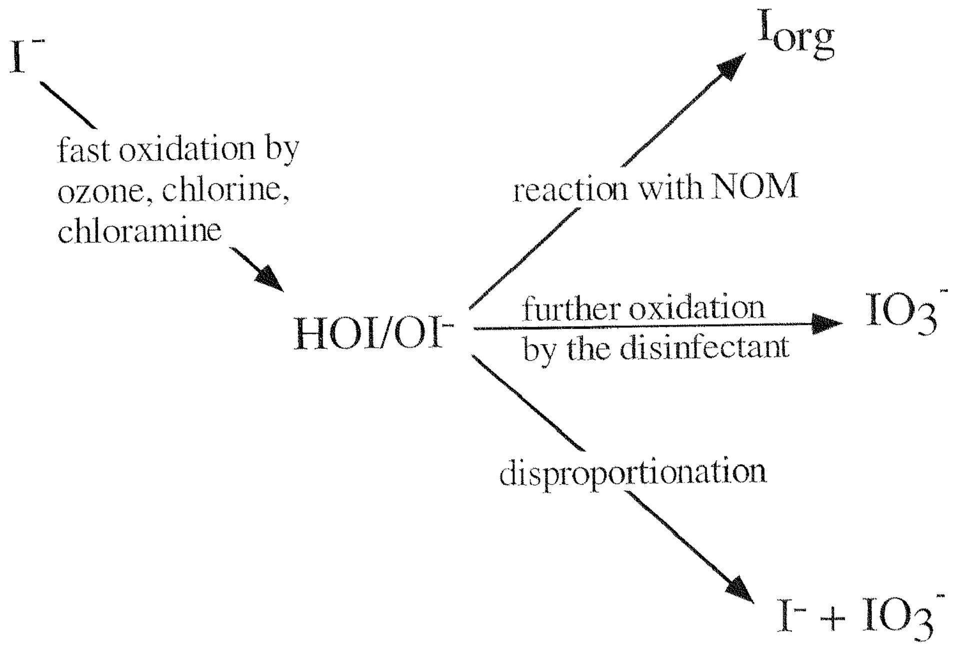

Figure 1.1: Fate of iodine during oxidative drinking water treatment processes: IO_3^- and iodoorganic compounds as possible sinks.

To be able to predict the significance of the above mentioned reactions, rate constants for different reactions of HOI which are relevant for drinking water practice were measured in laboratory systems. Chapter 3 gives an account of a study of the kinetics of the disproportionation of HOI. The oxidation of HOI by ozone, chlorine, and chloramine was investigated in chapter 4. Finally, chapter 5 reports rate constants of reactions of HOI with model organic compounds and kinetic data of the formation of I-THMs and IO_3^- in natural waters under varying oxidation conditions (ozone, chlorine, chloramine). Analytical methods for the monitoring of the inorganic species I^- and IO_3^- in natural waters were also developed (see chapter 2).

Cases of taste and odor problems in drinking water utilities related to I-THMs have been reported in Australia, France, and the United States. A strong medicinal taste appeared in the drinking water at Mundaring Weir

(Australia) after the disinfection of the distribution system was changed from chlorination to chloramination (Hansson et al., 1987). Several I-THMs (CHI_3, $CHClI_2$, $CHBr_2I$, $CHBrI_2$, CHBrClI) were detected in the chloraminated water. Due to the lack of analytical standards for the mixed I-THMs, only CHI_3 could be quantified. Levels of up to 8 µg/L CHI_3 were found after oxidation by 3 mg/L chloramine (pH = 8; I^- = 90 µg/L). However, CHI_3 was only formed when ammonia was added before chlorine. When ammonia was added 80 s after chlorine, the resulting CHI_3 concentration was < 1 µg/L. Hence, the taste and odor problems were resolved by reversing the order of addition of ammonia and chlorine.

In France, three cases of I-THM formation are reported by Bruchet et al. (1989). In a chlorinated well water from the Paris region, $CHCl_2I$, $CHBr_2I$, and CHI_3 were detected. This water exhibited a strong medicinal taste and odor. In another well water (90 µg/L I^-), formation of $CHBr_2I$, $CHBrI_2$, and CHI_3 in an ozone-based treatment train led to a strong medicinal taste. However, the appearance of the I-THMs was due to improper operation of the ozonation step. Chlorination of an ammonia-rich ground water yielded CHI_3 when chlorine was dosed below the breakpoint. After the chlorination was replaced by an ozonation, no similar episodes were reported any more.

In the United States, medicinal taste and odor due to I-THMs was reported in a chloraminated water for years (Gittelman & Yohe, 1989). All six I-THMs could be detected in that water. The taste and odor problems were significantly reduced by delaying the addition of ammonia by 5 min with respect to chlorine addition. A delay of 30 s did not improve the situation.

1.2 Aqueous Iodine Chemistry

Elemental iodine was discovered by Courtois in 1811 when he was preparing saltpeter from acidified seaweed ash to produce gunpowder for the Napoleonic wars (Courtois, 1813). Gay-Lussac (1814) subsequently studied some properties of the new element and named it 'ioeides' after the Greek word for 'violet', which is the color of iodine vapor. In the following section, the thermodynamics and kinetics of iodine in aqueous solutions are discussed.

1.2.1 Thermodynamics

The most common aqueous iodine species are listed in Table 1.2. Their main reactions are presented in Table 1.3.

The first reaction in Table 1.3 (eq. 1.1) is the hydrolysis of elemental iodine (I_2) to iodide (I^-) and hypoiodous acid (HOI). At high pH values, HOI dissociates to form hypoiodite (OI^-) with a pK_a of 10.4 (see chapter 3). At low pH, H_2OI^+ is formed through protonation of HOI ($pK_a = 1.4$; Bell & Gelles, 1951). The equilibrium concentrations of these species for a total I_2 concentration of 1 μM (250 μg/L) are shown in Fig. 1.2. At low pH, I_2 is the dominating species. At neutral and slightly basic pH, HOI and I^- become important and at pH > 10, OI^- is formed from HOI. The relative amount of HOI and OI^- increases with decreasing iodine concentration. For total $I_2 \leq 100$ nM (25 μg/L), $[HOI] + [OI^-] > [I_2]$ for any $pH \geq 5$.

Table 1.2: Aqueous Iodine Species[a]

chemical formula	customary name	IUPAC name (Leigh, 1990)	oxidation number
I^-	Iodide	Iodide(1-)	-I
I_2	Iodine	Diiodine	0
I_3^-	Triiodide	Triiodide(1-)	-1/3
H_2OI^+		Dihydrogen oxoiodate(1+)	+I
HOI	Hypoiodous acid	Hydrogen oxoiodate	+I
OI^-	Hypoiodite	Oxoiodate(1-)	+I
IO_2^-	Iodite	Dioxoiodate(1-)	+III
HIO_3	Iodic acid	Hydrogen trioxoiodate	+V
IO_3^-	Iodate	Trioxoiodate(1-)	+V
IO_4^-	Periodate	Tetroxoiodate(1-)	+VII

---

[a] Throughout this work, the customary names from the second column of Table 1.2 will be used

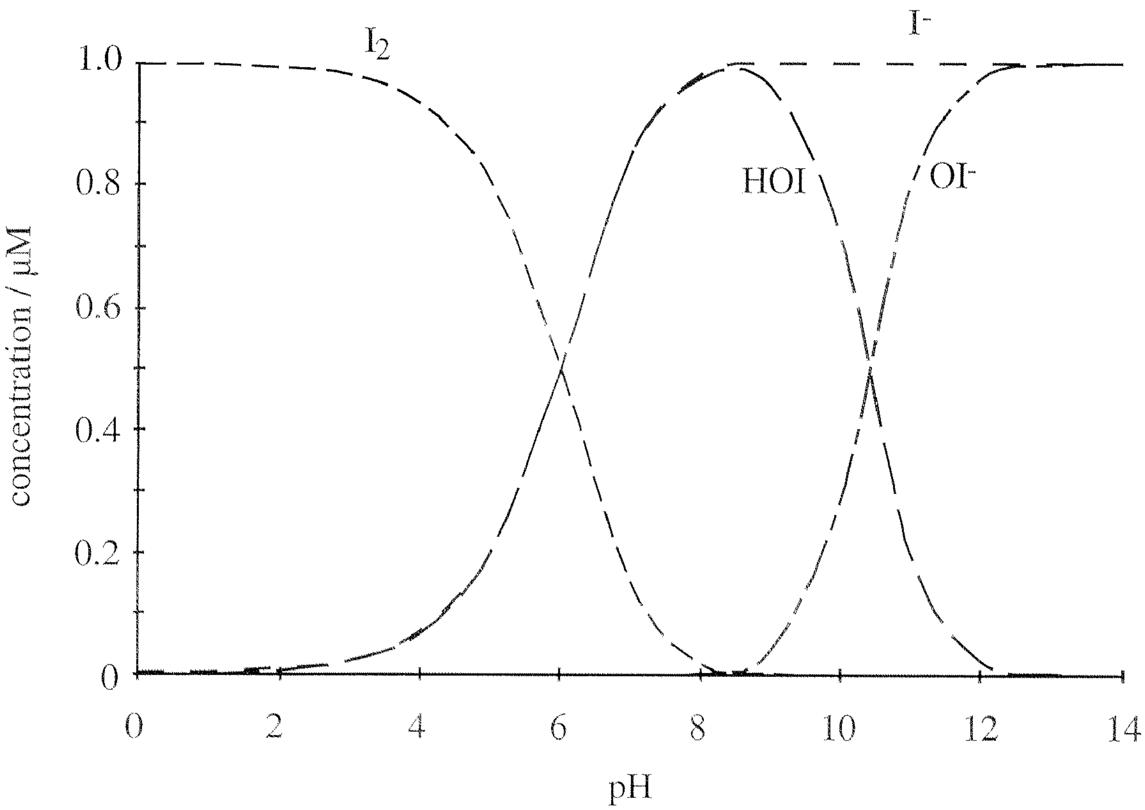

Figure 1.2: pH-dependent speciation of iodine (total concentration 1 µM I_2).

HOI can further react through a disproportionation to IO_3^- and I^- (eq. 1.2). The equilibrium of this reaction, which was not considered in Fig. 1.2, lies to more than 99 % on the right-hand side for environmental conditions (pH ≥ 6, total iodine < 2 µM (250 µg/L)). At low pH, IO_3^- can be protonated to iodic acid (HIO_3) which has a pK_a of 0.8 (Pethybridge & Prue, 1967). Periodate (IO_4^-) can be formed by an electrochemical oxidation of IO_3^- on a PbO_2 anode (Greenwood & Earnshaw, 1984).

Analytical methods for the determination of aqueous iodine species are reviewed and described in chapter 2 of this thesis.

Table 1.3: Reactions of Aqueous Iodine Species

equation	K	ref.	no.
$I_2 + H_2O = HOI + I^- + H^+$	5.44×10^{-13}	a	1.1
$3\ HOI = IO_3^- + 2\ I^- + 3\ H^+$	6×10^{-11}	b	1.2
$I_2 + I^- = I_3^-$	725	a	1.3

a: Burger & Liebhafsky, 1973; b: Sammet, 1905

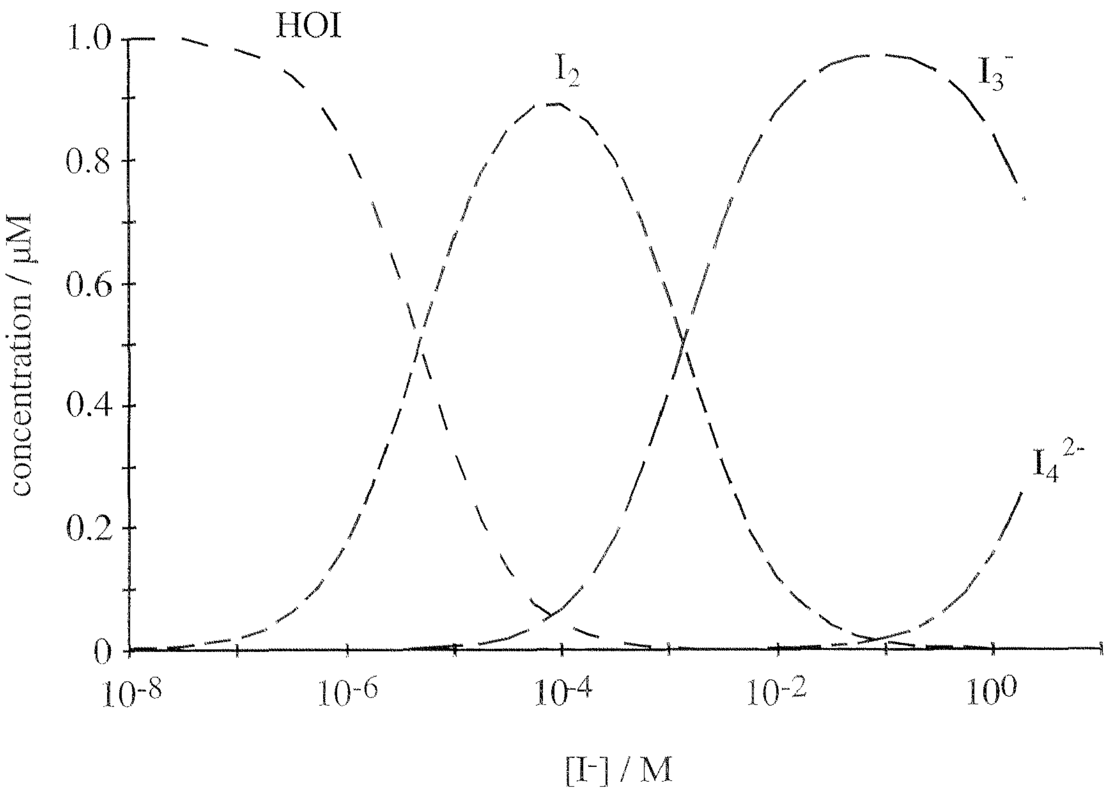

Figure 1.3: Speciation of 1 μM HOI at pH = 7 for varying free I^- concentrations.

I_2 is transformed to triiodide (I_3^-) in presence of I^- (eq. 1.3). I_2, HOI, and OI^- are all transformed to I_3^- for $[I^-] = 0.1$ M and $pH \leq 11$. For pH = 7, the speciation of HOI is shown at different free $[I^-]$ in Fig. 1.3. At $[I^-] < 10^{-6}$ M, HOI is the dominating species. With increasing $[I^-]$, the appearance of I_2, I_3^-, and finally I_4^{2-} can be observed. I_3^- has a strong UV/Vis absorption band with two maxima at 288 nm (ε = 38'200 $M^{-1}cm^{-1}$) and at 351 nm (ε = 25'700 $M^{-1}cm^{-1}$; see chapter 2).

In addition to I_3^- and I_4^{2-}, other polyiodide anions such as I_5^- or I_6^{2-} can be formed through reactions of I^-, I_2, and I_3^- (Ramette & Sandford, 1965; Genser & Connick, 1973; Sano et al., 1984). Mixed interhalogen compounds (e.g. ICl, ICl_2^-, I_2Cl^-, IBr, IBr_2^-, I_2Br^-) can be formed from HOI and I^- in the presence of Cl^- and Br^- (Margerum et al., 1986; Wang et al., 1989; Troy et al., 1991). Similarly to I_3^-, these compounds have high absorption coefficients. The equilibrium constants for the formation of all these species are shown in Table 1.4.

The standard reduction potentials for the aqueous iodine species at pH = 0 and pH = 14 are given in Fig. 1.4.

Appendix A gives an overview over all equilibrium constants which are mentioned and used in this work.

Table 1.4 Equilibrium Constants for the Formation of Polyiodide and Interhalogen Compounds at 25 °C.

equilibrium	K	ionic strength / M	ref.
$I_3^- + I^- = I_4^{2-}$	0.184	2	a
$I_3^- + I_2 = I_5^-$	9		b
$2\ I_3^- = I_6^{2-}$	0.41	0.023	c
$ICl_2^- = ICl + Cl^-$	0.013	0.5-1.0	d
$I_2 + Cl^- = I_2Cl^-$	1.7		e
$ICl + H_2O = HOI + Cl^- + H^+$	8.2×10^{-5}	0.5	d
$IBr_2^- = IBr + Br^-$	0.035	1.0	f
$IBr = I^- + I_2Br^-$	2×10^{-6}	1.0	f
$IBr + H_2O = HOI + H^+ + Br^-$	2.4×10^{-7}	0.5	f

a: Genser & Connick, 1973; b: Ramette & Sandford, 1965; c: Sano et al., 1984; d: Wang et al., 1989; e: Margerum et al., 1986; f: Troy et al., 1991.

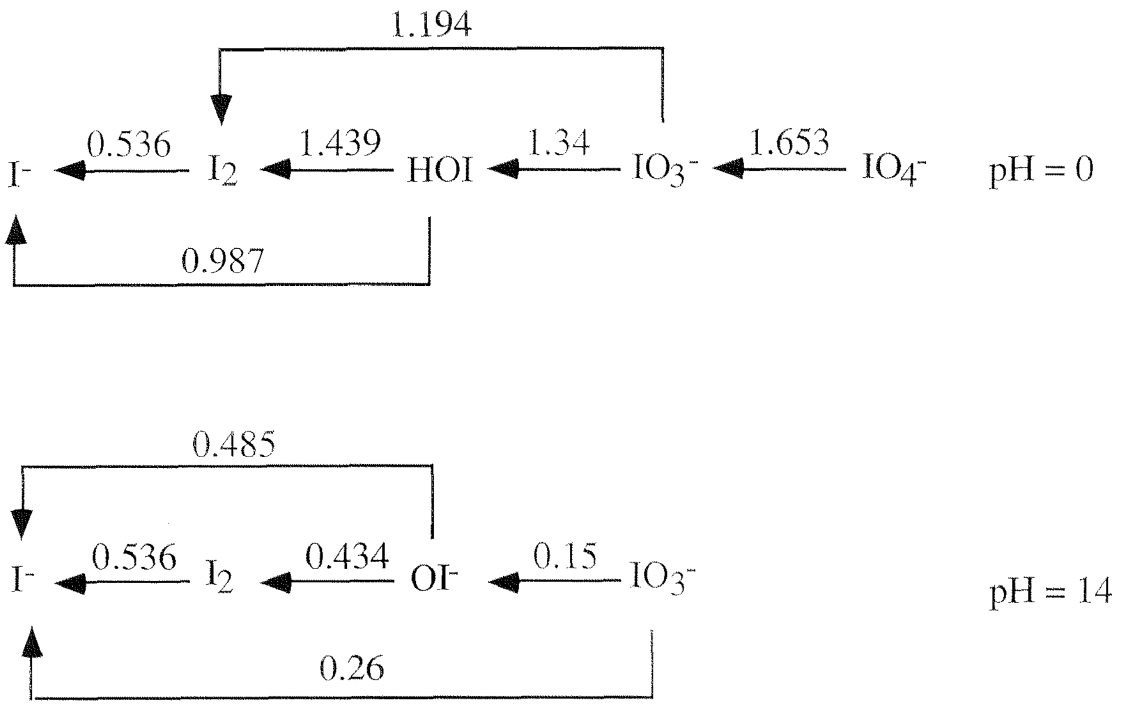

Figure 1.4: Standard reduction potentials in volts of various inorganic iodine species, adapted from Greenwood & Earnshaw (1984).

1.2.2 Kinetics

The kinetics of the equilibrium reaction 1.1 are very fast (see eq. 1.4). I_2 reacts with OH^- and forms the intermediate I_2OH^- (Lengyel et al., 1993). This decays rapidly to HOI and I^-. The back reaction of eq. 1.1 is very fast too. HOI reacts with I^- and yields I_2OH^- (Eigen & Kustin, 1962). This has two possibilities to be transformed to I_2. It can either decompose to I_2 and OH^- or react with H^+ and form I_2 and H_2O.

$$I_2 \begin{array}{c} \xrightarrow{8 \times 10^8\,M^{-1}s^{-1} \times [OH^-]} \\ \xleftarrow{6.9 \times 10^5\,s^{-1}} \\ \xleftarrow{2.2 \times 10^{10}\,M^{-1}s^{-1} \times [H^+]} \end{array} I_2OH^- \underset{5 \times 10^9\,M^{-1}s^{-1}}{\overset{1.3 \times 10^6\,s^{-1}}{\rightleftarrows}} HOI + I^- \quad (1.4)$$

The kinetics of reaction 1.2 are quite slow. Rate-determining steps are the reactions HOI+OI^- and HOI+HOI, the latter being catalyzed by anions such as carbonate, borate, or phosphate. Iodite (IO_2^-) is postulated to be a minor, unstable intermediate which is quickly further oxidized to IO_3^-. Chapter 3 of this thesis presents a detailed study of the kinetics of reaction 1.2 (disproportionation of HOI). The back reaction of eq. 1.2 is reported to be first-order in IO_3^-, second-order in I^-, and second-order in H^+ ($k = 3.0 \times 10^8\ M^{-4}s^{-1}$; Barton & Wright, 1968). Catalysis by anions such as carboxylate and phosphate was also observed for the back reaction. The kinetics of reaction 1.3 are very fast ($k_{I2+I-} = 6.2 \times 10^9\ M^{-1}s^{-1}$, $k_{I3-} = 8.5 \times 10^6\ s^{-1}$; Turner et al., 1972).

The above mentioned rate constants are also shown in the Appendix A together with all the rate constants which were measured in this work.

1.3 Geochemistry of Iodine

Iodine is a minor element in the natural environment (see Table 1.5). Its main geochemical reservoir is the sea. The dominant iodine species in deep seawater is IO_3^- which is the thermodynamically stable species. In the sea, transformation of I^- to IO_3^- may occur by bacterial processes but probably not by chemical oxidation (Luther et al., 1995). In the surface waters (< 100 m depth) however, IO_3^- concentrations are reduced by 10 - 30 % and corresponding amounts of I^- appear (McTaggart et al., 1994; Tian et al., 1996). The observed IO_3^- reduction in the surface waters is probably due to a biological process (Luther et al., 1995). Marine organisms such as phytoplankton and bacteria are known to take up IO_3^- and to release I^- (Moisan et al., 1994; Councell et al., 1997). The major part of ozone which is deposited onto the sea surface reacts with I^- (Garland & Curtis, 1981). The reaction between O_3 and I^- is very fast and leads to HOI which probably further reacts with natural organic matter.

Marine algae, which contain up to 2 mg I/g dry weight, or phytoplankton release iodoorganic compounds such as iodoform, bromodiiodomethane, dibromoiodomethane, bromochloroiodomethane, diiodomethane, chloroiodomethane, bromoiodomethane, methyl iodide, ethyl iodide, 1-bromo-2-iodoethane, 2-iodoethanol, 1-iodopropane, 2-iodopropane, iodoacetone, 1-iodobutane, 2-iodobutane, and 1-iodo-2-methylpropane to the seawater (Moore, 1977; Gschwend et al., 1985; Fuge & Johnson, 1986; Klick & Abrahamsson, 1992; Gribble, 1994; Moore et al., 1996; Giese et al., 1999). The compound which was found in the highest concentrations is CH_3I (0.1-10 ng/L in marine surface water; Lovelock, 1975; Moore & Tokarczyk, 1992; Reifenhäuser & Heumann, 1992).

Table 1.5: Iodine Concentrations in the Environment (Whitehead, 1984; Fuge & Johnson, 1986)

Seawater	45 - 60 µg/L
Rainwater	0.5 - 5 µg/L
River and lake water	0.5 - 20 µg/L
Groundwater	1 - 100 µg/L
Oilfield brine	20 - 300 µg/L
Atmosphere	10 - 20 ng/m^3
Igneous rocks	0.08 - 0.5 mg/kg
Sedimentary rocks	0.2 - 10 mg/kg
Marine sediments	3 - 400 mg/kg
Soils	0.5 - 20 mg/kg

CH_3I and many other iodoalkanes are volatile compounds. Hence, they may evaporate and be responsible for a transfer of iodine to the atmosphere. There, CH_3I has been found in concentrations of 0.05 - 5 ppt (Yokouchi et al., 1997). Other processes such as the reaction of I^- with O_3 or the light-induced oxidation of I^- might also contribute to the transfer of iodine to the atmosphere by formation of volatile species (Miyake & Tsunogai, 1963; Thompson & Zafiriou, 1983). All these processes lead to an enhanced volatilization of iodine when compared to other elements such as chlorine. The I:Cl ratio in sea-salt particles and in the atmosphere is a factor of 500 - 10'000 higher than in the seawater (Duce et al., 1963; Cicerone, 1981; Sturges & Barrie, 1988).

Volatilized iodoalkanes are not stable because of the weakness of the carbon-iodine bond. Their life-time in the sunlit atmosphere is less than 1 h (Mössinger et al., 1998). Photolysis leads to I radicals which react with O_3 to IO (Wayne et al., 1995). However, this reaction is not significant for the overall ozone destruction in the troposphere. The principal iodine reservoir species are HOI, $IONO_2$, and I_2O_2 (Wayne et al., 1995). In the stratosphere, iodine is present as IO during the day and as $IONO_2$ during the night. Recent articles report an IO concentration of < 0.5 pptv in the stratosphere. The authors conclude that iodine does not contribute to stratospheric ozone loss (Wennberg et al., 1997; Pundt et al., 1998).

Part of atmospheric iodine enters the cloud and rainwater. Iodine concentrations in rainwater are usually in the range 0.5 - 5 µg/L but sometimes concentrations of up to 20 µg/L were reported (Duce et al., 1963; Fuge & Johnson, 1986; Campos et al., 1996). The fact that the sea is the source of iodine is reflected by decreasing iodine concentrations in continental rain with increasing distance from the sea (Fig. 1.5). I^- and IO_3^- usually occur at similar concentrations in rainwater. In river waters however, the speciation is shifted toward I^- which accounts for about

90 % of total iodine. The total iodine concentration in surface waters is in the same range as in rainwater (Wong, 1991).

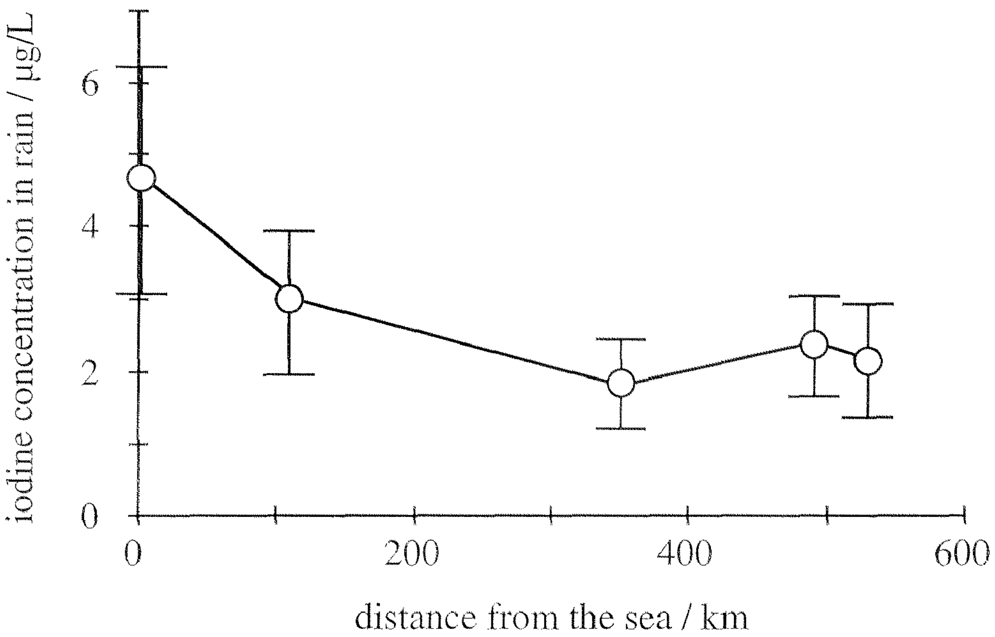

Figure 1.5: Iodine concentrations in the rain at different distances from the sea (Krupp & Aumann, 1999).

Iodine concentrations in soils and rocks are quite low. The average crustal abundance of 0.46 mg/kg is the lowest of the halogens with the obvious exception of astatine. For soil concentrations, the same gradient as for rainwater can be observed: Iodine is enriched in soils near the sea coast and depleted inside the continents (Fuge & Johnson, 1986). Soil iodine is not mobile. It is reported to be associated with humic material or with clay.

The geochemical cycle of iodine is hardly influenced by human activities. Anthropogenic iodine sources can be neglected compared to the natural sources. However, the release of radioactive iodine during accidents in nuclear power plants may be of high significance even if iodine concentrations are very low. The main iodine isotope which was discharged to the environment at the Chernobyl site was ^{131}I ($t_{1/2}$ = 8.02 d). Rainwater concentrations of ^{131}I were as high as 7240 Bq/L (1.5 x 10^{-12} g/L) in Wiesbaden, Germany (Hoffmann et al., 1987). The same authors found 300 Bq/L (6 x 10^{-14} g/L) in cow milk and 45.5 Bq/L (9.5 x 10^{-15} g/L) in mother's milk. In Switzerland, concentrations of up to 22 Bq/L (4.6 x 10^{-15} g/L) were found in a ground water (Waber et al., 1987). In the medicine, iodine-containing compounds are used as X-ray contrast agents. These compounds are not degraded neither in the human body nor in waste water treatment plants nor in the environment. They were found at concentrations of up to 8 µg/L (4 µg/L I) in run-offs of waste water treatment plants and up to 2.4 µg/L in ground water (Ternes et al., 1999). The iodine-containing X-ray contrast agents were also detected in several drinking waters.

1.4 Iodine Metabolism

Iodine supply through the nutrition is essential for humans, mammals, birds, reptiles, amphibians, and fish (Alexander, 1984). The dietary iodine requirement for adult human beings is 80 - 150 µg per day (WHO, 1996). Upon ingestion, iodine is absorbed in the gastrointestinal tract and actively transported into the thyroid. This 25-g gland is situated near the throat and contains more than 80 % of the total iodine (15-20 mg) in an adult (Hetzel & Maberly, 1986). This is enough for about three months supply. Two iodine-containing hormones, thyroxine (T_4) and triiodothyronine (T_3) are synthesized in the thyroid and released to the blood (see Fig. 1.6). Receptor sites for T_4 and T_3 are present in cell-nuclei of the hypophysis, the liver, the kidney, the heart, and the central nervous system.

In the fetus, neonate, and child, thyroid hormones exert a major influence on cellular differentiation, growth, and development.

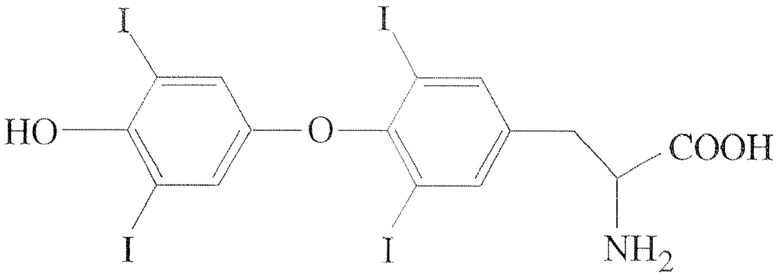

Thyroxine (T_4)

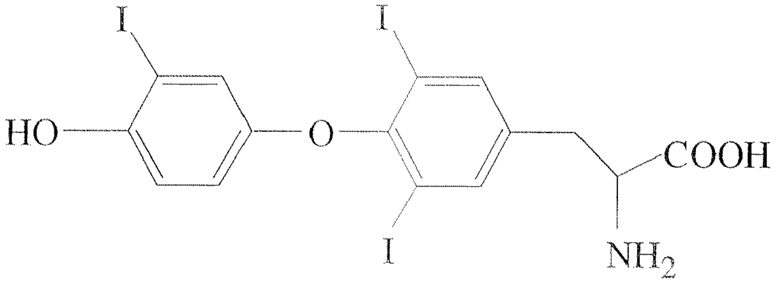

Triiodothyronine (T_3)

Figure 1.6: Chemical structures of two iodine-containing hormones.

Insufficient iodine supply can evoke serious health problems. Main iodine deficiency disorders in adults are goiter (swelling of the thyroid gland) and impaired mental function such as apathy and cretinism (Hetzel & Maberly, 1986; Delange et al., 1993). In children, iodine deficiency leads to retarded physical and mental development what results in lifelong disabilities. During pregnancy, iodine deficiency can lead to abortions and stillbirths. These disorders are endemic. Regions with a low natural iodine input from the sea such as central continental areas (e.g. central Asia, central Africa), mountainous regions (e.g. Himalayas, Andes, and Alps) and areas of high rainfall (e.g. India, Indonesia, Oceania) are especially affected (Fuge, 1987). The link between the above mentioned health problems and insufficient dietary iodine supply was already found in the 19th century (Langer, 1960).

In 1922, iodine addition to the table salt was introduced in Switzerland what led to a dramatic decrease of the goitre prevalence. Today, many countries apply this practice. The developed countries have been quite successful in the battle against iodine deficiency disorders although some problems still are present. Changing nutrition habits are a new challenge for the achievement of a sufficient iodine supply of the whole population. In developing countries, millions of people are still severely affected by iodine deficiency disorders. Addition of iodine to foodstuff requires a well-organized system. Furthermore, food supply is often based on subsistence agriculture what complicates the systematic addition of iodine. Other possibilities are the injection or ingestion of iodized oil. A single administration of iodized oil provides enough iodine for several years. Further hindrances of efficient iodine supply programs are social factors such as skepticism against governmental actions or strong influences of traditions. In Hotien (China) for example, people refused to use iodized salt because they feared that the supplements contained contraceptives (Xin-Min et al., 1997). In this case, iodine was added to the irrigation water. This resulted in a dramatically reduced children mortality by 50 % and in an increase in the number of sheep in the herds by 43 %. These positive effects lasted for at least 3 years after a unique addition of iodine to the irrigation water.

1.5 Toxicological Aspects

As mentioned above, IO_3^- is a possible by-product of disinfection of iodide-containing drinking waters. Since both chlorate (ClO_3^-) and bromate (BrO_3^-) are known to be toxic, the question of the toxicity of IO_3^- has to be raised (WHO, 1996). Ingested IO_3^- was quickly reduced to I^- in vivo by rats and rabbits as well as in vitro in whole blood and in glutathione solutions (Taurog et al., 1966). The in vivo reduction occurred within less than 3 min and took place whether IO_3^- was administered orally or intravenously. Rat whole blood reduced 150 mg/L IO_3^- to I^- within 2 min. This reaction also takes place in dogs. This is indicated by a study where elevated I^- levels in urine were found after the administration of 200 mg/kg of IO_3^- (Webster et al., 1966).

Acute toxicity data show similar results for both I^- and IO_3^-. Oral LD_{50} (lethal dose for 50 % of the population) in mice was 1000 mg/kg for IO_3^- and 1600 mg/kg for I^- (Webster et al., 1957). However, a considerable difference between the two species was observed for intravenous injection. LD_{50} was 100 mg/kg for IO_3^- and > 1200 mg/kg for I^-. Another study compared the mutagenic effects of the different halogenates (Eckhardt et al., 1981). While ClO_3^- and BrO_3^- showed mutagenic activity, IO_3^- had no such effect neither in the Ames test, nor in the micronucleus test on mouse bone marrow, nor in the recessive-lethal test in Drosophila. The absence of mutagenic activity for IO_3^- was also demonstrated in another study (Andersen, 1995).

For human consumption, an intake of 2 mg iodine per day is considered to be excessive by some authors (WHO, 1996). However, in some Japanese regions, daily iodine intakes of 50 - 80 mg through consumption of seafood do not lead to health effects. The FAO (Food and Agriculture Organization of the United Nations) and the WHO (World Health Organization) have set a provisional maximum tolerable daily intake of 1 mg/day based on data of the effects of I^-.

The toxicity of I^-, I_2, and IO_3^- to aquatic organisms (rainbow trout and *Daphnia magna*) was tested by Laverock et al. (1995). Rainbow trout were most sensitive to I_2 (LC_{50} (lethal concentration for 50 % of the population) ≥ 0.53 mg/L) and less sensitive to IO_3^- ($LC_{50} \geq 220$ mg/L) and I^- ($LC_{50} \geq 860$ mg/L). *Daphnia magna* were equally sensitive to I_2 ($LC_{50} \geq 0.17$ mg/L) and I^- ($LC_{50} \geq 0.16$ mg/L) and less sensitive to IO_3^- ($LC_{50} \geq 10.3$ mg/L).

1.6 Iodine as a Drinking Water Disinfectant

Elemental iodine (I_2) is an effective and economic water disinfectant (Gottardi, 1983). According to a manufacturer's instruction, a dose of 13 - 18 mg/L I_2 should be used during 20 min to ensure bacterial disinfection (Gerba et al., 1997). However, this was not sufficient for the complete inactivation of *Cryptosporidium parvum* oocysts. In practice, iodine is applied for drinking water disinfection during emergency situations such as earthquakes or floods, or in remote areas by travelers, campers, or soldiers. Another remote area is the space where NASA has used iodine as a drinking water disinfectant since the Apollo missions in 1969 and will continue to use it on the International Space Station (ISS; Atwater et al., 1996).

Iodine is released to the water by anionic resins which are loaded with polyiodide anions such as I_3^-. The possibility to store these resins during several months in a dry state has advantages over conventional drinking water disinfectants such as ozone or chlorine which require an in situ production or storage of aggressive chemicals. The drawbacks of iodine are its limited stability in water because of the disproportionation of HOI which leads to the inactive I^- and IO_3^-, its loss through volatilization, and the possible manifestation of bad taste and odor due to iodoform. Another drawback of iodine when compared to chlorine is its lower disinfection capacity which might be a result of a lower activity toward microbes or the lower stability in water (Table 1.6). However, the concentration of the disinfectants was only measured at the beginning in that study. A comparison of the effectiveness of iodine and chlorine is difficult when it is only based on initial concentrations and not on exposures.

Table 1.6: Comparison of Iodine and Chlorine as Water Disinfectants at pH = 7.9 - 8.3 (Ellis & van Vree, 1989).

disinfectant	dose / mg/L	reduction of fecal coliforms	reduction of fecal streptococci
chlorine	1.0	99.7 %	99 %
iodine	1.0	97 %	48 %
iodine	2.0	> 99.9 %	> 99 %

Seite Leer /
Blank leaf

2. Determination of Iodide and Iodate by Ion Chromatography with Postcolumn Reaction and UV/Visible Detection

Y. Bichsel and U. von Gunten, Analytical Chemistry **71**(1), 34-38 (1999).

Iodide and iodate can be determined by two new methods using anion-exchange chromatography with postcolumn reaction and UV/visible detection. Iodide is determined as IBr_2^- at 249 nm. Iodate is determined as I_3^- at 288 nm. The analyses can be run completely automatically and do not require any sample pre-treatment. The detection limits are 0.1 µg/L (0.8 nM) for iodide and 0.1 µg/L (0.6 nM) for iodate. The methods have been successfully applied to determine iodide and iodate in several mineral waters and in drinking water as well as for the determination of iodide in table salt.

2.1 Introduction

The need to determine iodide and iodate in environmental samples (≥ 0.5 µg/L) has arisen because iodine may play a role in taste and odor problems in drinking water (Whitehead, 1984; Hansson et al., 1987).

In the literature, many methods have been proposed for the determination of the different iodine species in water. One example is the iodide-catalyzed oxidation of leuco crystal violet by N-chlorosuccinimide (Lambert et al., 1975). This reaction is monitored spectrophotometrically, and its rate is dependent on the iodide concentration. The detection limit in distilled water is 2 µg/L. However, in natural waters, the solutions become turbid and make measurements impossible. Another possibility for the determination of iodide, iodine, and iodate is the formation of an iodinated phenol in a precolumn derivatization procedure and its detection with GC/MS (Shin et al., 1996). This method has a detection limit of 0.5 µg/L for all three species but it requires an extensive sample pretreatment.

There are numerous methods for determination of iodide and iodate with anion-exchange chromatography. Determination of iodide with anion-exchange chromatography and electrochemical detection yielded a detection limit of 10 µg/L (Han et al., 1987). However, after injection of environmental samples, the sensitivity decreased dramatically. This effect was probably due to matrix components which adsorbed to the electrode surface during the measurement. Iodide can be determined with anion chromatography and direct UV/visible detection after preconcentration of a 6 mL sample which leads to a detection limit of 0.1 µg/L (Ito, 1997). This method relies on a preconcentration step and may therefore be susceptible to undesired matrix effects, e.g., overloading of the preconcentration column with matrix anions such as Cl^-, SO_4^{2-}, and HCO_3^-. Iodate can be determined by anion-exchange chromatography and postcolumn reaction with UV/visible detection of Br_3^- (detection limit 0.1 µg/L; Weinberg & Yamada, 1998).

Our new methods are based on anion-exchange chromatography with postcolumn reactions and UV/visible detection as well. Iodide and iodate are determined under different chromatographic conditions:

(i) Iodide is determined as IBr_2^- which is formed after the ion chromatographic (IC) separation step in a bromide-containing eluent. The interhalogen compound is formed through addition of a basic hypobromite solution with subsequent acidification:

$$I^- + OBr^- + Br^- + 2\ H^+ = IBr_2^- + H_2O \qquad (2.1)$$

(ii) Iodate is determined as I_3^- which is formed after the IC separation step through addition of an iodide solution and subsequent acidification:

$$IO_3^- + 8\ I^- + 6\ H^+ = 3\ I_3^- + 3\ H_2O \qquad (2.2)$$

The postcolumn reactions are quantitative and selective and allow determination of low quantities with minimal interferences of other anions. The methods are not dependent on sophisticated or expensive laboratory equipment. They are simple, robust and well suited for routine analysis.

2.2 Experimental Section

2.2.1 Apparatus

Figure 2.1 shows the general outline of the ion chromatography system. The measurements were carried out on two systems, a Dionex DX-500 system (Dionex, Sunnyvale, CA) and a Sykam S1000 system (Gauting, Germany). The postcolumn reagent was added by a Dionex PC 10 reagent delivery module via a KEL-F mixing tee. The eluent was acidified by an ASRS-I membrane-exchange suppressor (Dionex) run in the chemical suppression mode. UV/visible detection was performed by a Spectroflow 773 absorbance detector (Kratos, Ramsey, NJ). The eluents and the postcolumn reagents were kept under a helium atmosphere. For further details of the apparatus see Table 2.1.

Table 2.1 General Conditions for the Analyses

sample loop volume	500 μL
reaction coil volume	750 μL (0.37 min)
regenerent	450 mM H_2SO_4
regenerent flow rate	3 mL/min
eluent flow rate	1.5 mL/min
postcolumn reagent flow rate	0.5 mL/min
iodide	
eluent	60 mM NaBr, 1 mM NaOH
guard column	Dionex AG 11, 4 mm i.d.
analytical column	Dionex AS 11, 4 mm i.d.
postcolumn reagent	5 μM Br_2, 2 mM NaOH
detector wavelength	249 nm
iodate	
eluent	40 mM $B(OH)_3$, 20 mM NaOH
guard column	Dionex AG 9, 4 mm i.d.
analytical column	Dionex AS 9, 4 mm i.d.
postcolumn reagent	250 mM KI
detector wavelength	288 nm

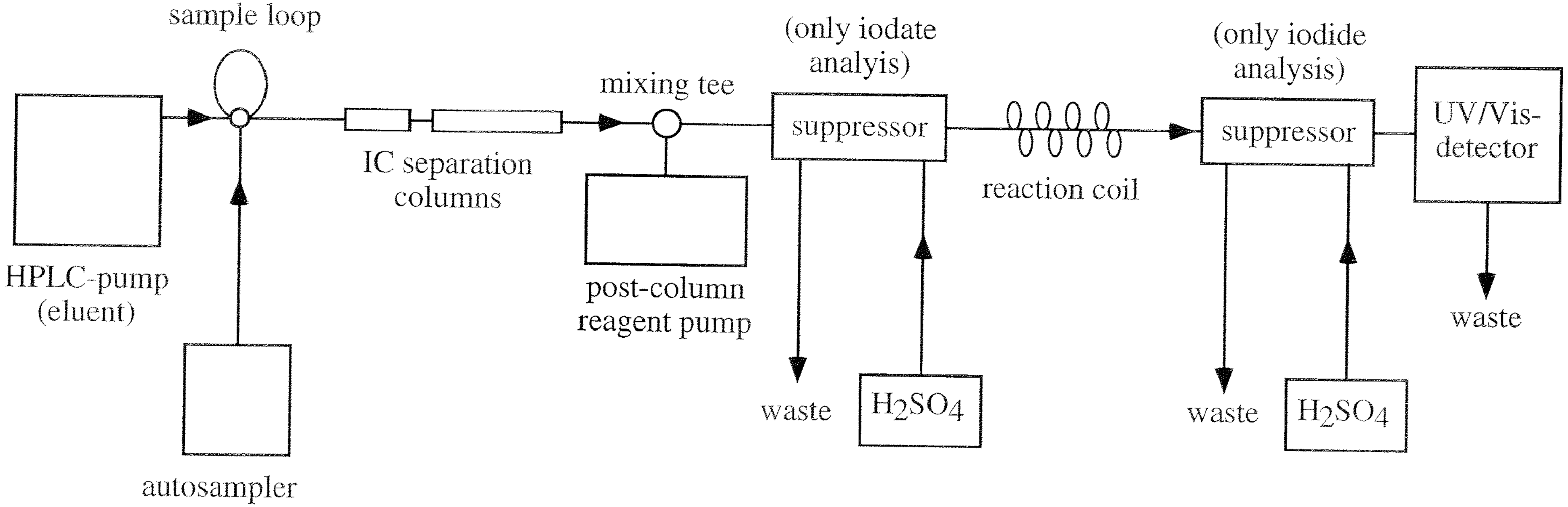

Figure 2.1: Outline of the components of the apparatus. The suppressor was placed between the reaction coil and the detector for the iodide analysis and between the mixing tee and the reaction coil for the iodate analysis.

2.2.2 Reagents

All reagents used were purchased from Fluka (Buchs, Switzerland) and were of the highest purity grade. Especially for the iodate determination it was very important to use the purest quality of KI (Fluka puriss. p.a.). When using other products, impurities led to a high threshold through reduction of I_3^- to iodide. Water was double-distilled in a quartz apparatus. Standard solutions of iodide were prepared daily, and standard solutions of iodate were prepared weekly. No special safety or toxicity considerations apply for any of the chemicals used under these conditions.

2.2.3 Procedure

The general conditions for the analytical methods are summarized in Table 2.1.

Iodide. For the separation of iodide from the matrix, a Dionex AG 11 guard column with an AS 11 analytical column was used. The eluent was basic and contained bromide as the eluting anion. The postcolumn reagent was a basic solution of Br_2 present as Br^- and the active species OBr^-. Between the reaction coil and the detector, the solution has been acidified by pumping it through a membrane-exchange suppressor. The suppressor was run in the chemical suppression mode with a sulfuric acid solution. The retention time of iodide was 3.2 min with a total running time for a chromatogram of 12 min. This additional time was important to allow a complete elution of all matrix anions. The absorbance was recorded at 249 nm.

As described above, the interhalogen species IBr_2^- is formed according to reaction 2.1 which can be expressed as a sequence of the following reactions.

$$I^- + OBr^- = Br^- + OI^- \tag{2.3}$$

$$OI^- + H^+ = HOI \tag{2.4}$$

$$HOI + H^+ + Br^- = IBr + H_2O \tag{2.5}$$

$$IBr + Br^- = IBr_2^- \tag{2.6}$$

According to Weast (1984), Chia (1958), and Troy et al. (1991), the equilibrium constants are $K_{2.3} = 2.1 \times 10^9$, $K_{2.4} = 4.3 \times 10^{10}$, $K_{2.5} = 4.17 \times 10^6$, and $K_{2.6} = 286$. Therefore, IBr_2^- is the dominant species for pH < 5, [HOI] < 10 µM and [Br^-] > 40 mM. The postcolumn reagent had to be basic to prevent the disproportionation of HOBr/OBr^- to bromide and bromate. Bromate does not oxidize iodide fast enough under these conditions. However, the equilibria of reactions 2.4 and 2.5 are on the right side at low pH values only. Therefore, the postcolumn reaction solution was basic to stabilize OBr^- and the solution was acidified after the reaction coil to shift the equilibria 2.4 and 2.5. Like many trihalogenide compounds, IBr_2^- has a strong UV absorption band (λ_{max} = 253 nm, ε = 57'200 M^{-1} cm^{-1}). Its UV/visible absorption spectrum is shown in Figure 2.2. A detection wavelength of 249 nm has been chosen because the difference of the absorption of IBr_2^- and the background component Br_3^- is maximal there. The postcolumn reagent component OBr^- forms Br_3^- in the suppressor. Br_3^- absorbs in the same wavelength range than IBr_2^-. The chosen detection wavelength of 249 nm has the largest difference between the background absorption of Br_3^- and the signal of IBr_2^-.

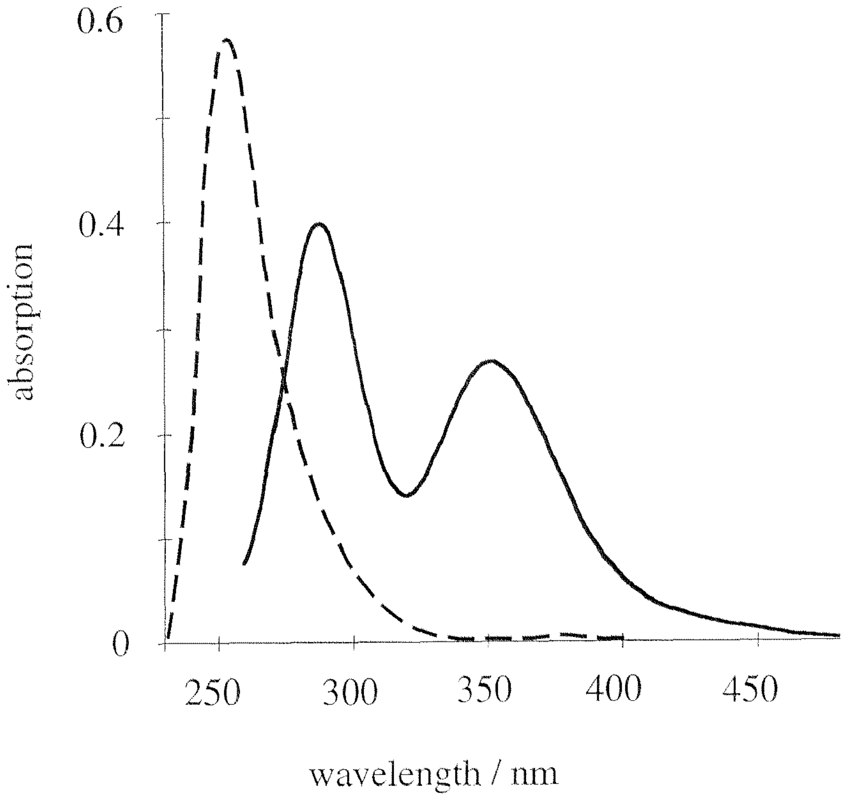

Figure 2.2: Absorption spectra of 10 μM I_3^- (solid line: λ_{max} = 288 nm, ε = 38'200 $M^{-1}cm^{-1}$; λ_{max} = 351 nm, ε = 25'700 $M^{-1}cm^{-1}$) and 10 μM IBr_2^- (dashed line: λ_{max} = 253 nm, ε = 57'200 M^{-1} cm^{-1}); cell path length 1 cm.

Iodate. For the separation of iodate from other anionic species, a Dionex AG 9 guard column and an AS 9 analytical column were used with a borate eluent. The postcolumn reagent was an iodide solution. Between the mixing tee and the reaction coil, a membrane-exchange suppressor was placed to acidify the eluent. The suppressor was run in the chemical suppression mode with a sulfuric acid solution. If acid is directly added to the iodide solution, I_3^- is formed due to oxidation with oxygen and the solution turns yellow. This leads to an increased background noise. The retention time of iodate was 2.4 min. At a running time of 4 min, the column was flushed with an eluent containing 250 mM $B(OH)_3$

and 100 mM NaOH during 5 min to elute anions with high affinity to the column. After this, a reequilibration with the weaker eluent was required during 8 min, yielding a total running time of 17 min for environmental samples and of 4 min for standards in distilled water (no flushing required). The absorbance was recorded at 288 nm where I_3^- has the maximal absorption (ε = 38'200 M^{-1} cm^{-1}). The UV/visible absorption spectrum of triiodide in Figure 2.2 shows a second absorption band at 351 nm with a molar absorption coefficient of 25'700 L mol^{-1} cm^{-1}. Quantification occurred via peak areas with an external calibration in double distilled water or with internal calibration.

I_3^- is formed according to reaction 2.2 which can be expressed as a sequence of the following reaction steps.

$$IO_3^- + 2\,I^- + 3\,H^+ = 3\,HOI \qquad (2.7)$$

$$HOI + I^- + H^+ = I_2 + H_2O \qquad (2.8)$$

$$I_2 + I^- = I_3^- \qquad (2.9)$$

The rate-limiting step for the formation of I_3^- is reaction 2.7. This reaction needs a low pH to allow a high reaction rate. Therefore, the suppressor was placed before the reaction coil for the iodate analysis. The stoichiometry of reaction 2.7 results in a chemical enhancement of a factor of 3. According to Palmer & Lietzke (1982), the equilibrium constants are $K_{2.6} = 9.01 \times 10^9$, $K_{2.7} = 2.07 \times 10^{12}$, and $K_{2.8} = 736$. Therefore, I_3^- is the dominant species for pH < 5, [HOI] < 1 mM and $[I^-] \approx 60$ mM.

2.3 Results and Discussion

2.3.1 Determination of Iodide

Optimization of the Postcolumn Reaction Conditions. The most delicate step in the formation of IBr_2^- is reaction 2.3, the oxidation of iodide to OI^-. Several oxidizing agents have been tested. According to reaction 2.7, *iodate* could be used for the oxidation of iodide. However, it did not react fast enough to ensure a quantitative reaction at $pH > 1$, since the rate of HOI formation is first-order in iodate and second-order in iodide (Barton & Wright, 1968). *Cerium (IV)* was tested as an oxidant that results in a high background absorption at 249 nm and therefore interferes with the measurement. *Hydrogen peroxide* oxidizes iodide to HOI: however, the reaction is only fast enough with heptamolybdate catalysis. Since molybdate absorbs at 249 nm, the background absorption was too high and yielded a high noise. *Hypobromite (OBr^-)* reacts with iodide in a quantitative and fast reaction and does not increase the background absorption significantly. Therefore, it has been chosen as the oxidizing agent for the iodide analysis.

In preliminary tests, chloride was used instead of bromide for the formation of the interhalogen species, ICl_2^-, which has its maximum absorbance at 230 nm ($\varepsilon = 42'000\ M^{-1}\ cm^{-1}$; Wang et al., 1989). However, the formation of ICl_2^- is thermodynamically less favorable than IBr_2^-. Therefore, a higher chloride concentration of 300 mM is required in the eluent. This leads to a shorter retention time of iodide and hinders a full separation of iodide from matrix components.

Calibration and Detection Limit. The calibration graph was linear between 0.2 µg/L and 100 µg/L iodide. The correlation coefficient (R^2) was 0.984 for the lowest measurable decade and 0.997 for the next higher decade. The detection limit ($S/N = 3$) was 0.1 µg/L. This value lies below the lower end of the concentration range of natural waters. The relative standard deviation (RSD) at 1 μg/L I^- was 12.8 % for 10 measurements.

Interferences. At concentrations of 10 g/L Cl^-, 1 g/L NO_3^-, 80 mg/L NO_2^-, 10 g/L SO_4^{2-}, or 5 g/L PO_4^{3-}, no interferences were observed. However, we found an increased sensitivity for iodide in a river water with > 4 mg/L DOC.

Iodide in Iodized Salt. To check for interferences with our method, the iodide content was measured in solutions of two different table salts and cross-checked with results of the leuco crystal violet (LCV) method (Lambert et al., 1975). We found good correspondences between the two methods. For the first salt (Jurasel, Switzerland), we found 20 ± 2 mg/kg with our method and 17 ± 1 mg/kg with the LCV method. For the other salt (Cérébos, France), we found 11 ± 2 mg/kg with our method and 14 ± 1 mg/kg with the LCV method. However, as discussed above, the leuco crystal violet method can only be used for relatively clean solutions where no interference with DOM is expected. Figure 2.3 shows a chromatogram of a sample of 500 mg/L table salt (300 mg/L Cl^-) with an iodide peak corresponding to a concentration of 10 μg/L. The chloride in the sample did not lead to any interference. Within certain limits, the iodide content determined in our study by two different methods corresponds well with the declaration of the producer (Jurasel: 15 mg/kg, Cérébos: 10-15 mg/kg).

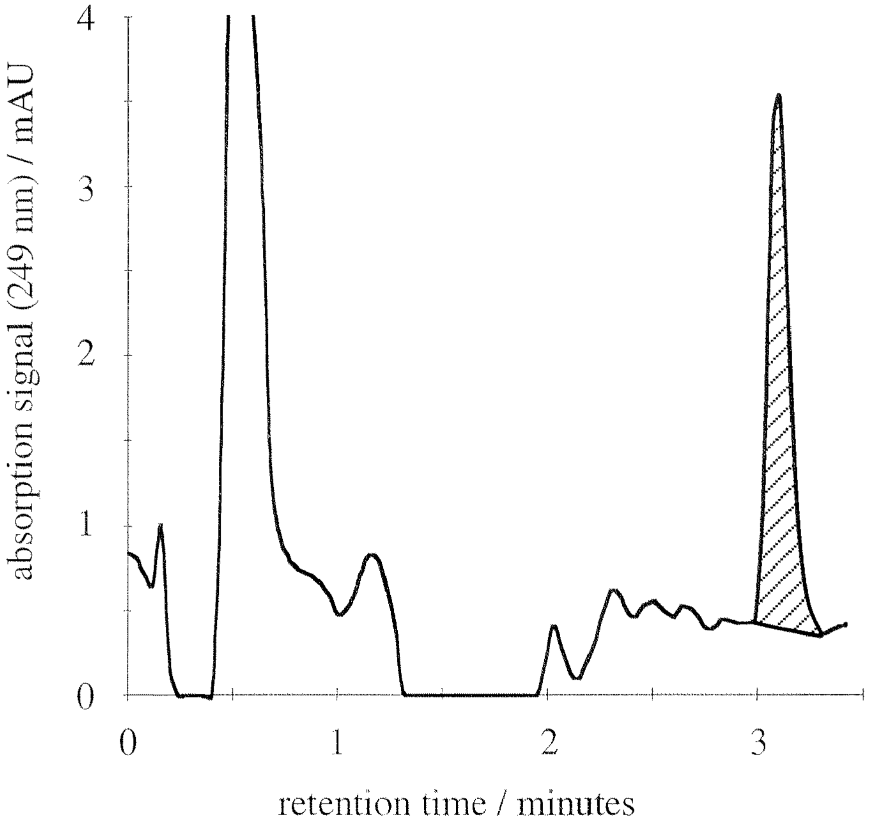

Figure 2.3: Determination of iodide in a solution of 500 mg/L table salt (Jurasel, Switzerland) containing 10 µg/L iodide.

2.3.2 Determination of Iodate

Optimization of the Reaction Conditions. The iodide concentration in the postcolumn reaction had to be optimized. At high concentrations (> 100 mM I^-), I_3^- is further transformed to I_4^{2-}, and at low concentrations (< 50 mM I^-), it dissociates to HOI or I_2 and I^- (see eqs 2.8 and 2.9; Genser & Connick, 1973). A low pH is important for the rate of the HOI formation reaction (Barton & Wright, 1968). However, oxygen readily oxidizes iodide at low pH. Therefore, the postcolumn reagent was a neutral iodide solution and the acid was added through a membrane-exchange suppressor before the reaction coil.

In testing the method for the determination of iodate, bromate, and chlorite of Weinberg & Yamada (1998), we found several differences. As a reducing agent, we have replaced the toxic nitrite by the unproblematic iodide. Due to this, the background absorption and therefore also the noise were significantly reduced. In general, the concentrations in the postcolumn reagent are much lower for this method. The setup of the apparatus is somewhat simpler because this method uses only one suppressor for the acidification of the postcolumn reagent.

Calibration Graph and Detection Limits. The linearity of the peak area versus analyte concentration holds for four orders of magnitude, from 0.2 µg/L to 2 mg/L. Correlation coefficients (R^2) for 0.2-2 µg/L are 0.987 and for 2-20 µg/L are 0.9998, respectively. The detection limit ($S/N = 3$) was 0.1 µg/L. This value is lower than the minimal iodate concentrations usually found in natural waters. Ten measurements at 1 µg/L IO_3^- gave a RSD of 6.0 %.

Interferences. At concentrations of 100 mg/L Cl^-, 100 mg/L NO_3^-, 2 mg/L NO_2^-, 500 mg/L SO_4^{2-}, or 500 mg/L PO_4^{3-}, no interferences were observed. Solutions of 1 mg/L chlorite, chlorate, bromide, or bromate gave no additional signal and did not alter the sensitivity to iodate. On principle, all species that can oxidize iodide and therefore form I_3^- could result in a signal. However, chlorate and bromate oxidize iodide only very slowly under the conditions used here ($pH = 1.2$).

2.3.3 The Speciation of Iodine in Natural Waters

Iodine Speciation during Drinking Water Ozonation. The speciation of iodine was analyzed in a water that has been oxidatively treated with 4 mg/L of ozone. Ozone oxidizes iodide in an instantaneous reaction to iodate. In a lake water (Lake Zürich, Switzerland; $pH = 7.8$, 1.42 mM hardness, 4 mg/L Cl^-, 15 mg/L SO_4^{2-}, 3.5 mg/L NO_3^-, 1.4 mg/L DOC), we found 3.7 µg/L I^- (29 nM) and 3.4 µg/L IO_3^- (19 nM). After oxidation, the iodate concentration was 9.2 µg/L (53 nM) and we did not find iodide any more. This corresponds well to the sum of iodide and iodate in the raw water. Iodide is therefore quantitatively oxidized to iodate in this water.

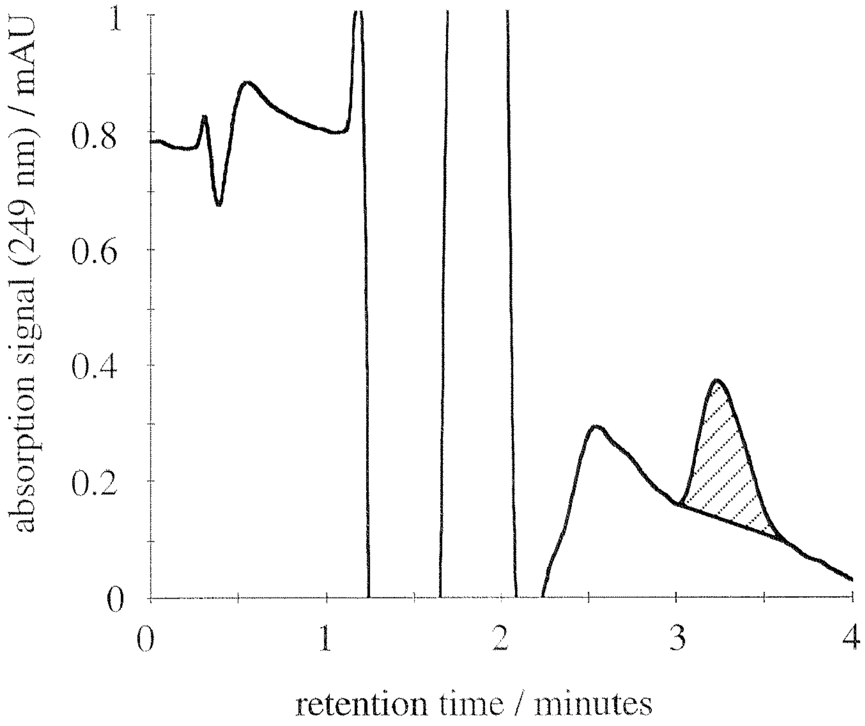

Figure 2.4: Determination of iodide in a mineral water (Henniez, Switzerland; 0.4 µg/L I^-, 10 mg/L Cl^-, 13 mg/L SO_4^{2-}, 18 mg/L NO_3^-, 394 mg/L HCO_3^-)

Iodine Speciation in Mineral Waters. Table 2.2 shows the iodide and iodate analyses of 16 mineral waters from central Europe. Most mineral waters contain less than 5 µg/L inorganic iodine. The highest concentration of 200 µg/L was found in Aqui which is an old water in the marine molasse containing high levels of bromide and chloride in addition to iodide. In this water, the iodine is present as iodide only. In contrast, it is remarkable that some mineral waters do not contain any iodide but 20 µg/L or even 100 µg/L iodate (Arkina, Cristalp). Such an

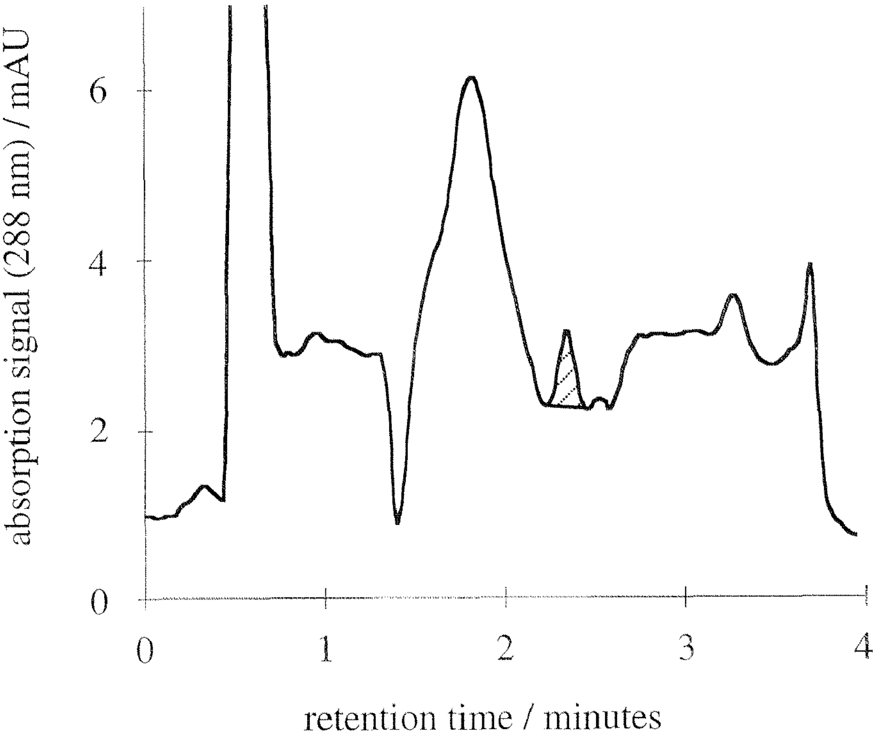

Figure 2.5: Determination of iodate in a mineral water (Henniez, Switzerland; 0.9 µg/L IO_3^- 10 mg/L Cl^-, 13 mg/L SO_4^{2-}, 18 mg/L NO_3^- 394 mg/L HCO_3^-)

iodine speciation would be expected for a water that has been oxidatively treated with ozone or another strong oxidant. Mineral waters are sometimes oxidized to eliminate manganese and iron. Figure 2.4 shows a chromatogram of the iodide determination in Henniez mineral water with a content of 0.4 µg/L iodide. The signals before and after the injection gap appear in the standards too.

Figure 2.5 shows a chromatogram of the same water but for the iodate determination with a content of 0.9 µg/L iodate. The retention time of iodate was 2.4 min. The other signals are method artifacts and appear in standards too. They could not be assigned to any anionic species. Due to the reproducibility of these signals, an iodate quantification based upon this chromatogram is still possible. The general background noise of the baseline is much smaller than the iodate peak in figure 2.5.

More results of analyses of iodide and iodate in natural waters and table salts can be found in appendix B.

Table 2.2 Determination of Iodide and Iodate in Several Mineral Waters

	content (µg/L)	
mineral water	iodide	iodate
Alpina (Rothenbrunnen, Switzerland)	37	2.1
Aqui (Zürich, Switzerland)	200	< 0.3
Juvina (Deutschkreutz, Austria)	43	3.4
Rhäzünser (Rhäzüns, Switzerland)	43	1.0
Valser (Vals, Switzerland)	7.2	< 0.3
Zurzacher (Zurzach, Switzerland)	4.0	2.1
Aproz (Aproz, Switzerland)	0.7	< 0.3
Arkina (Yverdon, Switzerland)	0.5	22
Cristalp (Saxon, Switzerland)	0.6	99
Eptinger (Sissach, Switzerland)	1.1	< 0.3
Evian (Evian, France)	0.8	1.8
Henniez (Henniez, Switzerland)	0.4	0.9
Rocchetta (Gualdo Tadino, Italy)	0.5	3.1
San Clemente (Monte Tamaro, Switzerland)	< 0.3	0.4
San Pellegrino (San Pellegrino Terme, Italy)	0.6	< 0.3
Vittel (Vittel, France)	0.4	2.4

3. Hypoiodous Acid: Kinetics of the Buffer-Catalyzed Disproportionation

Y. Bichsel and U. von Gunten, Water Research, in press.

The reactivity of hypoiodous acid (HOI) is an important factor for the fate of iodine in oxidative drinking water treatment. The possible reactions of HOI are its disproportionation, its oxidation to iodate (IO_3^-), or the reaction with natural organic matter. The latter reaction may result in the formation of iodoorganic compounds which are frequently responsible for taste and odor problems. The acid dissociation constant (pK_a) of HOI has been determined spectrophotometrically as 10.4±0.1 (T = 25°C; I = 50 mM). Kinetic constants and a new rate law for the disproportionation of HOI as catalyzed by hydrogencarbonate, carbonate, and borate are presented. In the pH range 7.6-11.1, the main uncatalyzed reactions are HOI + HOI ($k_{3.2} = 0.3\ M^{-1}s^{-1}$) and HOI + OI^- ($k_{3.3} = 15\ M^{-1}s^{-1}$). The buffer-catalyzed reaction step was found to be second-order in HOI and first-order in the buffer anion. The following rate constants were deduced: HOI + HOI + HCO_3^-: 50 $M^{-2}s^{-1}$; HOI + HOI + CO_3^{2-}: 5000 $M^{-2}s^{-1}$; HOI + HOI + $B(OH)_4^-$: 1700 $M^{-2}s^{-1}$. All these rate constants result in half-lifes for HOI of 10-1000 days under typical drinking water conditions.

3.1 Introduction

In the late eighties, it was observed that taste and odor problems in drinking waters were frequently linked to the presence of iodoorganic compounds (Hansson et al., 1987; Bruchet et al., 1989). The identified compounds were iodo-trihalomethanes (I-THMs) which can be formed in a reaction of hypoiodous acid (HOI) with natural organic matter (NOM). It has been estimated that I-THMs contribute to up to 25 % of the cases of bad taste and odor in drinking waters in France (Suez Lyonnaise des Eaux, 1993). The most problematic I-THM is iodoform (CHI_3) with an organoleptic threshold concentration of 0.03 - 1 µg/L (Bruchet et al., 1989; Khiari, 1999). This concentration has to be compared to the total iodine concentration in water resources which is usually in the range of 0.5 - 20 µg/L but which can exceed 50 µg/L in certain ground waters near the sea coast or under special geological circumstances (Fuge & Johnson, 1986; Wong, 1991). The most abundant iodine species in natural waters are iodide (I^-) and iodate (IO_3^-) (Fuge & Johnson, 1986).

In oxidative drinking water treatment, I^- is first oxidized to HOI in presence of ozone (Garland et al., 1980), chlorine (Nagy et al., 1988), and chloramine (Kumar et al., 1986) in a fast reaction. In a second step, some of these disinfectants oxidize HOI to IO_3^-. Ozone oxidizes I^- to IO_3^- within less than 4 s under typical drinking water treatment conditions (see chapter 4). In chlorination processes, the oxidation of HOI to IO_3^- is slower and occurs within minutes to hours. Chloramine does not oxidize HOI at all. Chlorine dioxide oxidizes I^- to I radicals which involves a different chemistry than the other disinfectants (Fabian & Gordon, 1997). The fate of I radicals in drinking water is unknown.

HOI can also disproportionate to IO_3^- and I^- or, as mentioned above, react with NOM what may lead to iodoorganic compounds. All these reactions of HOI - its oxidation to IO_3^-, its disproportionation to IO_3^- and I^-, and the reaction with NOM - are in kinetic competition. The relative reaction rates of these reactions determine the fraction of iodine found as IO_3^- and I_{org}. Whereas the oxidation of HOI is described in chapter 4 and reaction kinetics of HOI with organic compounds are shown in chapter 5, the present chapter focuses on the disproportionation.

The disproportionation of HOI can be described by the equilibrium:

$$3\ HOI = IO_3^- + 2\ I^- + 3\ H^+ \qquad (3.1)$$

The equilibrium constant of this reaction is 6×10^{-11} (Sammet, 1905). At pH > 5, HOI is therefore thermodynamically unstable since the equilibrium is forced to the right side of eq. 3.1. However, the formation of the reaction products IO_3^- and I^- is kinetically controlled. The kinetics of this reaction have been observed to be second-order in $[HOI]_{tot}$, the sum of [HOI] and $[OI^-]$ (Thomas et al., 1980; Wren et al., 1986; Truesdale, 1997; Urbansky et al., 1997). The reaction mechanism is generally described by a series of reactions (eqs 3.2-3.4) with the rate-limiting step being eq. 3.2 or eq. 3.3.

$$HOI + HOI \xrightarrow{k_{3.2}} IO_2^- + I^- + 2\ H^+ \qquad (3.2)$$

$$HOI + OI^- \xrightarrow{k_{3.3}} IO_2^- + I^- + H^+ \qquad (3.3)$$

$$IO_2^- + HOI \xrightarrow{fast} IO_3^- + I^- + H^+ \qquad (3.4)$$

The overall reaction 3.1 is catalyzed by buffers such as phosphate, borate, or acetate (Buxton & Sellers, 1985; Truesdale & Canosa-Mas, 1995; Urbansky et al., 1997). Because different interpretations for the catalysis are given in the literature, it has been difficult to find consistent rate constants for the catalyzed and uncatalyzed reaction steps. Therefore, the reported rate constants $k_{3.2}$ at buffer concentrations of 0-150 mM vary within a wide range of $< 2\ M^{-1}s^{-1}$ to $1000\ M^{-1}s^{-1}$ (Thomas et al., 1980; Truesdale, 1997; Urbansky et al., 1997). The rate constants $k_{3.3}$ were found to be between $40\ M^{-1}s^{-1}$ and $10^6\ M^{-1}s^{-1}$ (Wren et al., 1986; Truesdale & Canosa-Mas, 1995). A value of $2200\ M^{-2}s^{-1}$ was found for the catalysis of the reaction HOI + HOI by borate buffer (Buxton & Sellers, 1985).

Because the disproportionation can either occur through the reaction HOI + HOI (eq. 3.2) or HOI + OI^- (eq. 3.3), the dissociation constant of HOI is of particular importance. The pK_a of HOI has previously been indirectly determined as 10.6±0.8 (Chia, 1958).

To assess the fate of HOI in natural waters, we investigated the kinetics of the disproportionation of HOI as catalyzed by borate, hydrogencarbonate, and carbonate. Since the disproportionation strongly depends on the acid-base speciation of HOI, we also redetermined the pK_a of HOI.

3.2 Experimental Section

All experiments were performed in double-distilled water. pH measurements were carried out with a Ross electrode (ATI Orion, Boston, MA) and a Metrohm 632 pH-meter (Metrohm, Herisau, Switzerland) which was calibrated with standard buffer solutions (Merck; pH = 6.98, 8.95, 9.94, 11.88). Spectrophotometric measurements were performed on an Uvikon 940 spectrophotometer (Kontron Instruments, Eching, Germany). HOI is not a stable compound (disproportionation). It was freshly produced directly in the reaction vessel through hydrolysis of I_2 or through oxidation of I^- by HOCl.

3.2.1 Dissociation Constant of HOI

The pK_a of HOI was determined spectrophotometrically by measuring the pH-dependence of the UV-absorbance at 220-250 nm (pH = 8.7-11.5, 25±2°C) in a flow-through cell. It was not possible to perform the measurements in a static cell because of the depletion of HOI/OI^- due to fast disproportionation under the applied conditions. Buffered solutions of OCl^- (0.2-1 mM) and I^- solutions (0.023-0.46 mM) were delivered with two Dosimats (Metrohm, Herisau, Switzerland) and mixed in a mixing tee prior to the photometric cell. HOI was formed by oxidation of I^- with OCl^- ($k = 4.4 \times 10^{15}$ $M^{-1}s^{-1} \times [H^+]$; Kumar et al., 1986) within 80 μs - 250 ms (half-life of I^-). The residence times in the cell were 8 s (pathlength 50 mm) and 1.2 s (pathlength 5 mm). The concentration of the NaOCl stock solution (Aldrich) was determined as 5.6% with direct photometry of HOCl at 233 nm (ε = 100 $M^{-1}cm^{-1}$; Soulard et al., 1981). The buffer (phosphate) concentration varied from 14 to 17 mM to yield a constant ionic strength of 50 mM. $[OCl^-]$ was in excess relative to $[I^-]$ (molar ratio $[OCl^-]:[I^-]$ = 1.1-9) to ensure the instantaneous oxidation of I^- to HOI without transient I_2 formation. However, the excess of OCl^- did not lead to significant IO_3^- formation within the residence time of the solution in the flow-through cell (see chapter 4). The resulting pH was measured at the outlet of the flow-through cell.

3.2.2 Disproportionation Kinetics of HOI

The disproportionation of HOI was investigated at $[HOI]_{tot} = [HOI] + [OI^-]$ = 0.8-76 μM and at pH = 7.6-11.1 in 100 mL batch reactors at 25±2°C. The desired $[HOI]_{tot}(t{=}0)$ was achieved by adding an aqueous I_2 solution (≈ 1 mM, standardized by photometry: ε = 746 $M^{-1}cm^{-1}$ at 460 nm; Awtrey & Connick, 1951) to a buffered solution (2-30 mM of borate or carbonate/hydrogencarbonate). Under these conditions, I_2 hydrolyzes immediately to HOI/OI$^-$ and I$^-$ (reaction 3.5). Because of the lower [HOI], the disproportionation was, however, slower than for the conditions that we applied to determine the pK_a. During the reaction time of the disproportionation (10 h - 50 h), aliquots of the solutions were withdrawn and measured photometrically in excess of KI (0.15 M) where HOI and OI$^-$ are quantitatively transformed to I_3^-.

$$I^- + HOI + H^+ \rightleftharpoons I_2 + H_2O \qquad (3.5)$$

$$I_2 + I^- \rightleftharpoons I_3^- \qquad (3.6)$$

The equilibrium constants for reactions 3.5 and 3.6 are $K_{3.5} = 1.84 \times 10^{12}$ and $K_{3.6} = 725$, respectively (Burger & Liebhafsky, 1973). I_3^- was detected at 351 nm in a 4 cm cell with a molar absorption coefficient of 25'700 $M^{-1}cm^{-1}$ (see chapter 2) which allowed to measure $[HOI]_{tot} \geq 1$ µM.

To prevent the presence of CO_2 in the reaction solution we purged the solutions with N_2 prior to the beginning of the experiment and flushed the head-space of the reaction vessels when taking samples during the reaction time. Uptake of CO_2 leads to carbonate and hydrogencarbonate in the reaction solution which has a catalytic effect on the disproportionation.

In one experiment, the formation of IO_3^- was determined by quenching the disproportionation by H_2O_2 ($H_2O_2 + HOI = I^- + H^+ + H_2O + O_2$). IO_3^- was measured by ion chromatography and postcolumn reaction with a UV/vis-detection (see chapter 2). For the anion separation step, an AG-S 9 column (Dionex) was used. The postcolumn reaction yields I_3^- by reduction of IO_3^- to HOI followed by reactions 3.5 and 3.6. I_3^- can be measured by UV/vis-detection at 288 nm or 351 nm. The detection limit for IO_3^- in natural waters was 0.1 µg/L (0.6 nM).

3.3 Results and Discussion

3.3.1 Dissociation Constant of HOI

Figure 3.1 shows five of the recorded spectra of HOI/OI$^-$ between pH = 9.3 and pH = 11.5 which have been corrected for the background absorbance of phosphate and OCl$^-$. The molar absorption coefficients of HOI and OI$^-$ in the range of 250 to 220 nm increase from 150 to 1650 M^{-1}cm^{-1} for HOI and from 300 to 5100 M^{-1}cm^{-1} for OI$^-$. In our experiments, the wavelength region for best measurements was limited due to interferences by absorbance of HOCl and OCl$^-$ since it was added in excess of I$^-$ for the production of HOI. Both HOCl and OCl$^-$ absorb significantly at wavelengths > 250 nm. The lower wavelength region was limited by the absorbance of the buffer (phosphate) at $\lambda < 220$ nm. An accurate data evaluation was only possible at wavelengths with no interferences and maximum HOI/OI$^-$ absorption, i.e. in the range 220-225 nm.

The measured absorption $A_{obs}(\lambda)$ is the sum of the absorptions $A_{HOI}(\lambda)$ and $A_{OI^-}(\lambda)$ which can be attributed to the two species HOI and OI$^-$:

$$A_{obs}(\lambda) = A_{HOI}(\lambda) + A_{OI^-}(\lambda) = \varepsilon_{HOI}(\lambda) \cdot l \cdot [HOI] + \varepsilon_{OI^-}(\lambda) \cdot l \cdot [OI^-] \tag{3.7}$$

$$K_a = \frac{[OI^-][H^+]}{[HOI]} \tag{3.8}$$

Taking the acid-base equilibrium of HOI (eq. 3.8) into account, the following equation results:

$$\frac{A_{obs}(\lambda)}{l \cdot [HOI]_{tot}} = \varepsilon_{HOI}(\lambda) + K_a \frac{1}{[H^+]}(\varepsilon_{OI^-}(\lambda) - \frac{A_{obs}(\lambda)}{l \cdot [HOI]_{tot}}) \tag{3.9}$$

Equation 3.9 describes the relation between the dissociation constant K_a, the observed absorbance A_{obs} (at a particular wavelength λ), the total iodine concentration $[HOI]_{tot} = [HOI] + [OI^-]$, the cell pathlength l, and the molar absorption coefficients of the pure species ε_{HOI} and ε_{OI^-} (at a particular wavelength λ).

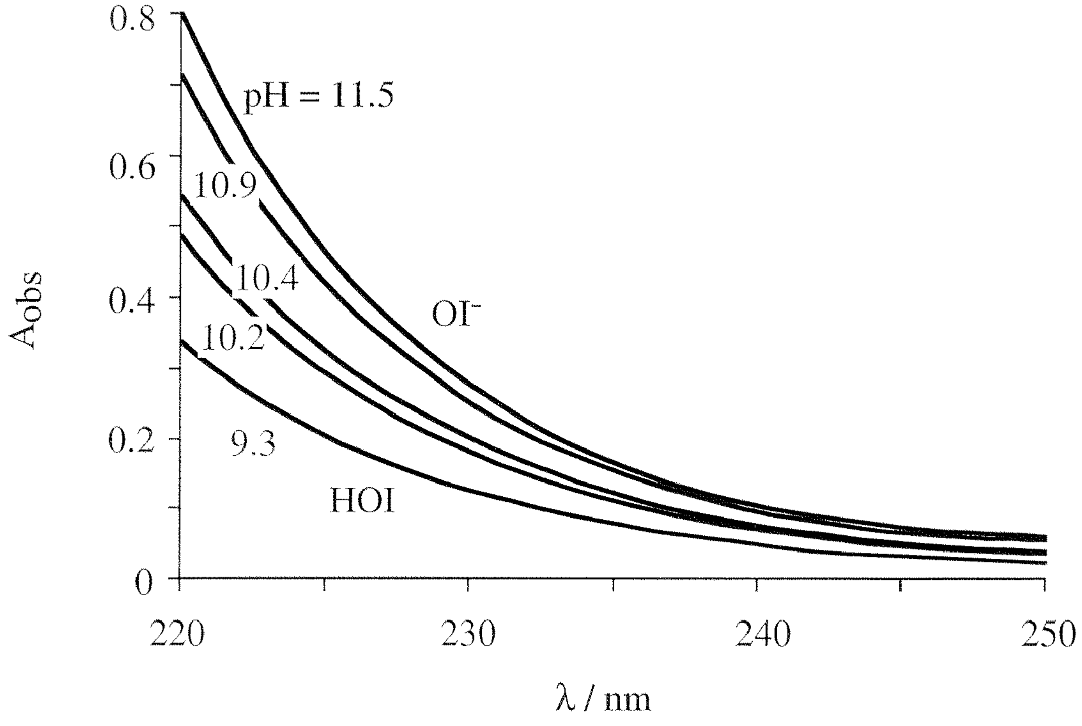

Figure 3.1: UV absorbance spectra (200-250 nm) of 345 μM HOI/OI⁻ at varying pH values (9.3 - 11.5); pathlength 5 mm; I = 50 mM (phosphate buffer); T = 25°C.

If the term on the left hand side of eq. 3.9 is plotted against the right hand side, a linear representation with K_a as slope results (see Fig. 3.2). According to Fig. 3.2 which shows the data measured at 220 nm, K_a can be calculated as $4.0 \pm 0.7 \times 10^{-11}$ ($pK_a = 10.4 \pm 0.1$). The intercept is the molar absorption coefficient of HOI at 220 nm, ε_{HOI} (λ = 220 nm). The ε_{HOI} (λ = 220 nm) determined by this procedure was 1650 $M^{-1}cm^{-1}$. However, eq. 3.9 has the restriction that the error increases with increasing pH when $\varepsilon_{OI^-}(\lambda) \approx \frac{A_{obs}(\lambda)}{l \cdot [HOI]_{tot}}$. Therefore, this equation was only applied for the range of pH < 10.4. A slightly different equation which was also derived from eq. 3.7 and 3.8 was used to interpret the data measured at pH > 10.4. For this pH range, ε_{OI^-} results as the intercept of the y-axis ($\varepsilon_{OI^-}(\lambda = 220\ \text{nm}) = 5100\ M^{-1}cm^{-1}$) while K_a^{-1} is the slope ($K_a = 4.2 \pm 0.8 \times 10^{-11}$ calculated from A_{obs} at 220 nm).

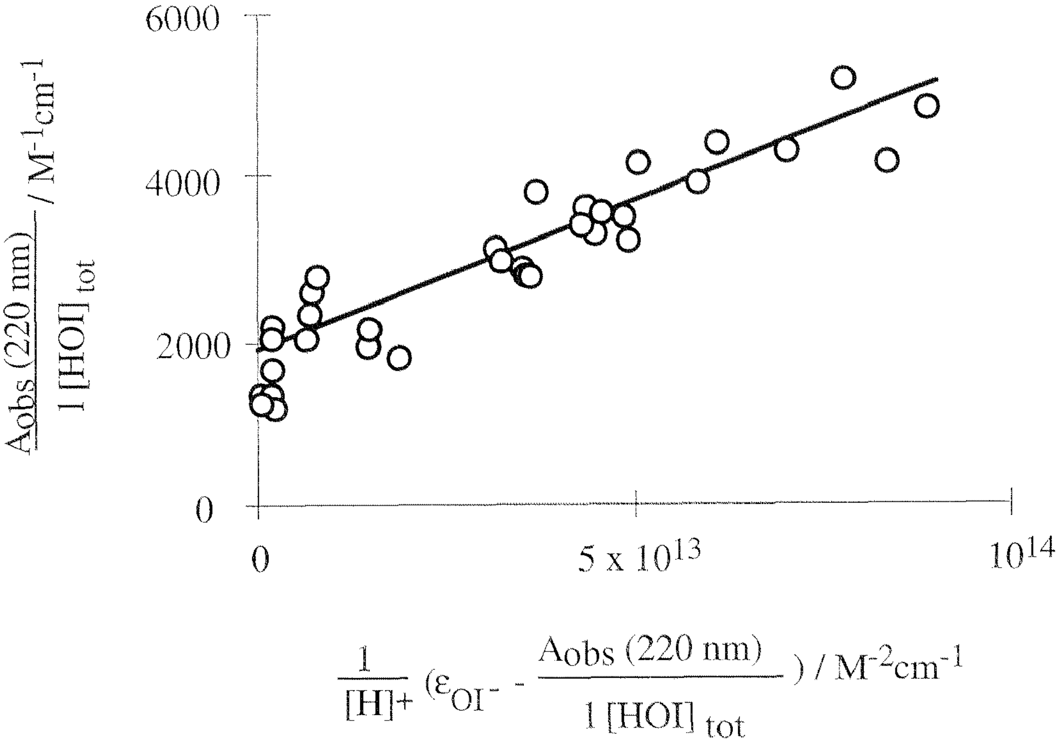

Figure 3.2: Determination of the pK_a of HOI (T = 25°C, ionic strength 50 mM): Linearisation of the absorbance data at 220 nm according to eq. 3.9 ($K_a = 4.0 \pm 0.7 \times 10^{-11}$; $r^2 = 0.868$, n=33).

K_a was calculated with both equations for A_{obs} at $\lambda = 220$ nm, $\lambda = 222$ nm, and $\lambda = 225$ nm and for $[HOI]_{tot} = 23\text{-}460\ \mu M$. The pK_a was 10.4±0.1 at 25°C with an ionic strength of 50 mM and did neither vary with the wavelength nor with $[HOI]_{tot}$. Within the errors given, both equations lead to the same pK_a. The indicated error of pK_a represents the 95% confidence interval.

Previously, Chia (1958) calculated a value of 10.6±0.8 with a combination of potentiometric and photometric methods. However, this value was based on indirect measurements including the two equilibrium constants of eq. 3.5 and 3.6 which are not very well known. In another study, a value of 10.0±0.3 was estimated from a limited spectrophotometric data set at pH = 4.0, 9.0, and 14.3 (Paquette & Ford, 1985). The pK_a determined in our study is within the range of the previous values. However, our direct measurements do not induce as many assumptions as the previous determinations.

3.3.2 Disproportionation Kinetics of HOI/OI⁻

The decrease of HOI/OI^- (initial concentration 0.8-76 μM) in buffered solutions (pH = 7.6-11.1) was measured spectrophotometrically (after reaction of HOI/OI^- to I_3^-). Figure 3.3 shows the measured (symbols) and calculated (line) decrease of $[HOI]_{tot}$ together with the IO_3^- formation in a typical experiment (10 μM HOI, 25 mM borate at pH = 8.0). IO_3^- which is formed according to eq. 3.1 cannot exceed 1/3 of the initial $[HOI]_{tot}$ (stoichiometric factor). The measured and calculated $[IO_3^-]$ (from HOI decrease according to eq. 3.1) are in almost perfect agreement (see Fig. 3.3). This is an independent confirmation of the assumed mechanism (eqs 3.2-3.4) in which the intermediate IO_2^- is rapidly oxidized to IO_3^-.

The disproportionation of HOI/OI^- was always found to be second-order in $[HOI]_{tot}$. Hence, linear plots ($r^2 > 0.99$) could be observed if 1 / $[HOI]_{tot}$ was plotted against the reaction time t according to:

$$\frac{1}{[HOI]_{tot}} = \frac{1}{[HOI]_{tot}(t=0)} + k_{obs}t \qquad (3.10)$$

The inset in Fig. 3.3 shows the linearisation of the experimental data according to equation 3.10 with the observed rate constant k_{obs} as the slope.

HOI was usually produced by hydrolysis of I_2. However, when HOI was produced by oxidation of I^- by HOCl, this had no influence on k_{obs}.

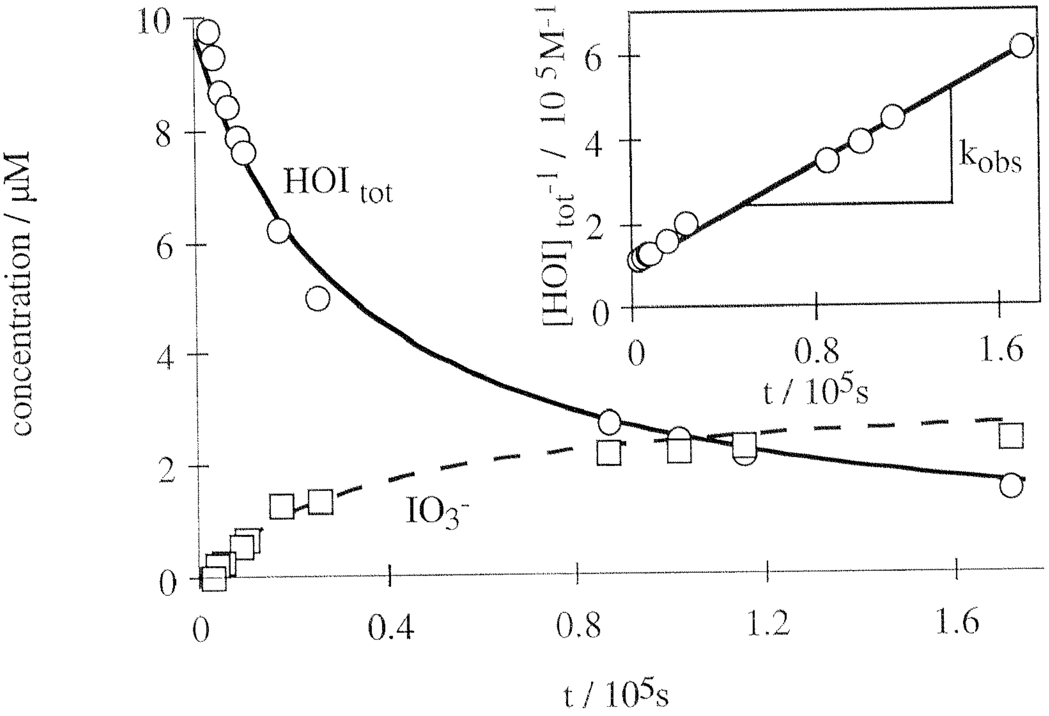

Figure 3.3: Decrease of $[HOI]_{tot}$ and formation of IO_3^- during the disproportionation of HOI/OI$^-$. Inset: Linearisation of the data according to eq. 3.10 (k_{obs} = 2.95 $M^{-1}s^{-1}$). Experimental conditions: $[HOI]_0$ = 10 µM; pH = 8.0, 25 mM borate; T = 25°C. Measured (symbols) and calculated (curves) data are shown.

All obtained k_{obs} values are listed in the Appendix C.

k_{obs} was dependent on the pH and the buffer concentration. High pH and high buffer concentrations accelerated the disproportionation of HOI. To elucidate the importance of the buffer catalysis on the disproportionation, we performed experiments under varying buffer concentrations and at varying pH.

A buffer catalysis can occur via the acidic or the basic form of the buffer or through both species. In principle, several reactions can be catalyzed: HOI + HOI, HOI + OI^-, and OI^- + OI^-. However, with the reaction OI^- + OI^-, we could not explain the pH-dependence of our experimental data. A reasonable fit of the data for borate and carbonate buffers was only achieved for two different mechanistic scenarios which cannot be distinguished from each other by our experiments. The first mechanism assumes that the basic form of the buffer is the active species and that two HOI molecules participate in the reaction. The second mechanism assumes that the protonated form of the buffer is the active species and that a HOI and an OI^- participate in the reaction. Chemical considerations led us to the assumption that the first mechanism is more likely than the second. We assume that the base interacts with the H-atom of HOI and thereby increases the nucleophile character of the I-atom. By this, the reactivity towards another HOI is enhanced.

As a result of this assumption, the following rate law for the base-catalyzed disproportionation can be postulated:

$$-\frac{1}{3}\frac{d[\mathrm{HOI}]_{tot}}{dt} = \frac{1}{3}k_{obs}[\mathrm{HOI}]_{tot}^{2} = k_{3.2}[\mathrm{HOI}]^{2} + k_{3.3}[\mathrm{HOI}][\mathrm{OI}^{-}] + \\ + k_{cat}[\mathrm{base}][\mathrm{HOI}]^{2} \qquad (3.11)$$

The factor of 1/3 corresponds to the stoichiometric factor of HOI in equation 3.1. Figure 3.4 shows a plot of $k_{obs}/3$ vs. $[\mathrm{base}][\mathrm{HOI}]^2 / [\mathrm{HOI}]_{tot}^2$ for experiments with varying buffer concentrations (borate) and varying pH values (squares, for circles see below). The linearity of the plot shows that the postulated eq. 3.11 is in agreement with experimental findings. The catalysis constant k_{cat} corresponds to the slope of the straight line.

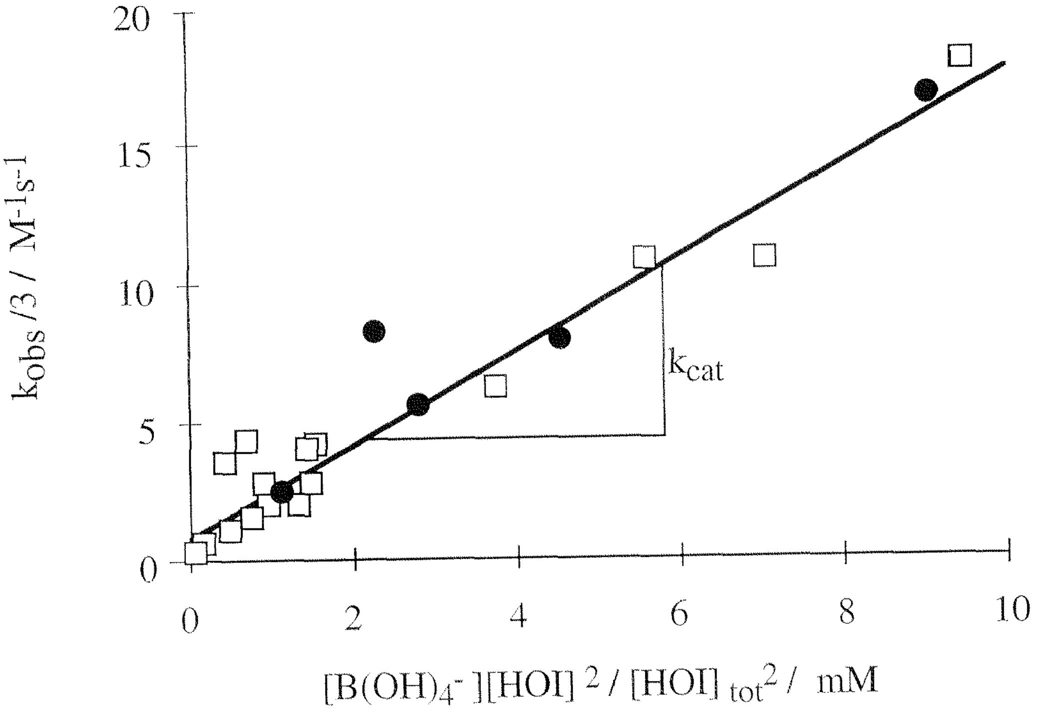

Figure 3.4: Experimental data and linear least-squares fit for the disproportionation of HOI in presence of borate according to eq. 3.11. The linearity of the plot shows that the postulated eq. 3.11 is in agreement with experimental findings. (□): data from this study; (•): data from Buxton & Sellers (1985); $k_{cat,borate} = 1.7\pm0.6 \times 10^3$ $M^{-2}s^{-1}$ with $r^2 = 0.992$ (n=29); Experimental conditions: pH = 7.6-10.6; total borate concentration = 2-25 mM; T = 25°C.

k_{cat} values for $B(OH)_4^-$, HCO_3^-, and CO_3^{2-} at 25°C are shown in Table 3.1. The k_{cat} values increase with increasing basicity of the buffer anions, $k_{CO_3^{2-}} > k_{B(OH)_4^-} > k_{HCO_3^-}$. An anion with a high basicity, such as CO_3^{2-}, can interact more strongly with the H-atom of HOI than an anion with a lower basicity, such as HCO_3^-. The interaction of the base with the proton in HOI leads to asymmetry (partial formation of OI^- like compound) which results in faster reaction.

Table 3.1 Rate Constants for the Disproportionation of HOI/OI$^-$ for Varying Reaction Conditions at 25 °C from This Study.

Eq. no	reaction	rate constant	[base] = 5 mM
(3.2)	HOI + HOI ($k_{3.2}$)	3±2 x 10^{-1} $M^{-1}s^{-1}$	
(3.3)	HOI + OI$^-$ ($k_{3.3}$)	15±1 $M^{-1}s^{-1}$	
(3.12)	HOI + HOI + HCO_3^-	5±2 x 10^1 $M^{-2}s^{-1}$	0.3±0.1 $M^{-1}s^{-1}$
(3.13)	HOI + HOI + CO_3^{2-}	5.0±0.5 x 10^3 $M^{-2}s^{-1}$	25±3 $M^{-1}s^{-1}$
(3.14)	HOI + HOI + $B(OH)_4^-$	1.7±0.6 x 10^3 $M^{-2}s^{-1}$	9±3 $M^{-1}s^{-1}$

Another compound which influenced the rate of the disproportionation was NH_4^+/NH_3. However, in contrast to borate and carbonate, ammonia did not catalyze the reaction but an inhibition was observed. At pH = 9.0, ammonia concentrations of 10-25 mM reduced k_{obs} by 50-80 %. This effect could be related to the fact that NH_3 is a nitrogen base and not an oxygen base like the other bases which were investigated in this study. According to the HSAB-concept (Hard and Soft Acids and Bases), nitrogen bases are softer than oxygen bases (Pearson, 1969). HOI has a hard part (H-atom) and a soft part (I-atom). Nitrogen bases might therefore rather interact with the I-atom of HOI whereas oxygen bases might rather interact with the H-atom. This difference could be a reason for the variation of the behavior with respect to the catalysis of the disproportionation.

The two rate constants for the uncatalyzed reactions HOI + HOI (eq. 3.2) and HOI + OI$^-$ (eq. 3.3), $k_{3.2}$ and $k_{3.3}$, were deduced from measurements at different pH-values and buffer concentrations by a regression analysis according to eq. 3.15. This equation was derived from equations 3.8 and 3.11 under the restriction that $[HOI]_{tot} = [HOI] + [OI^-]$.

$$\frac{k_{obs}[HOI]_{tot}^2}{3[HOI]^2} - k_{cat}[base] = k_{3.2} + k_{3.3}\frac{K_a}{[H^+]} \qquad (3.15)$$

Figure 3.5 shows a representation of eq. 3.15. The slope of the straight line corresponds to $k_{3.3}$, the y-axis intercept is $k_{3.2}$. For the determination of $k_{3.2}$, only the points at $pH < 9$ (low $K_a/[H^+]$) were used (see inset Fig. 3.5) since the reaction HOI + HOI only contributes significantly to the total reaction at $pH < 9$. The values of $k_{3.2}$ and $k_{3.3}$ are reported in Table 3.1. Because of the higher asymmetry between nucleophile and electrophile in the reaction $HOI + OI^-$, $k_{3.3}$ is larger than $k_{3.2}$. Therefore, a maximum rate for the uncatalyzed reaction can be expected at $pH = pK_a = 10.4$. A comparison of the rate constants for the catalyzed and the uncatalyzed reactions shows that at concentrations of 5 mM HCO_3^-/CO_3^{2-} or 4 mM $B(OH)_4^-$ at pH = 8, the rate of the catalyzed and of the uncatalyzed reaction are of the same order of magnitude (Table 3.1).

Compared to literature values, our $k_{3.2}$ and $k_{3.3}$ values are quite small. This is due to the fact that in some previous calculations the catalytic effect of the basic form of the buffer was not taken into consideration (Thomas et al., 1980; Truesdale et al., 1994). This led to high $k_{3.2}$ and $k_{3.3}$ values because the total disproportionation of both catalyzed and uncatalyzed reactions was attributed to $k_{3.2}$ and $k_{3.3}$. Buxton and Sellers (1985) however allowed for the catalytic effect of borate. Their raw data (pH = 9.1-9.7, 2-50 mM total borate) fit very well in our data set as is shown in Fig. 3.4 by the circles. We have evaluated their raw data according to eq. 3.11 and have found a k_{cat} value of $1.4 \pm 0.3 \times 10^3\ M^{-2}s^{-1}$ ($r^2 = 0.927$). This value is in agreement with our result (Table 3.1, eq. 3.14).

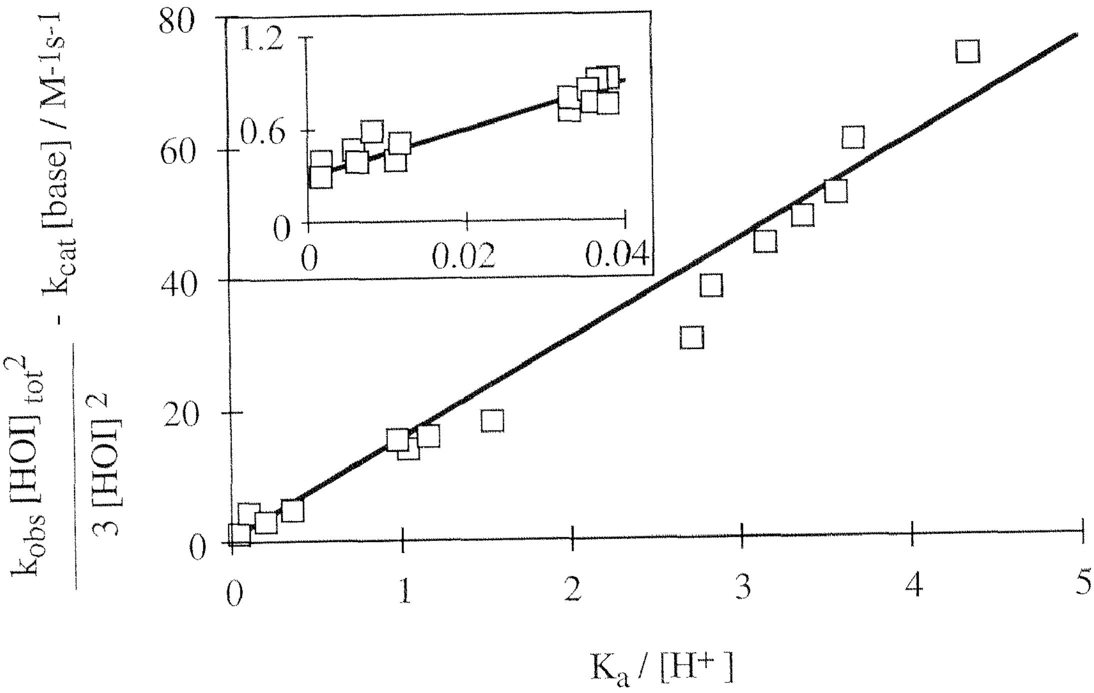

Figure 3.5: Determination of the rate constants $k_{3.2}$ and $k_{3.3}$ for the uncatalyzed reactions HOI + HOI and HOI + OI^- according to eq. 3.15. $k_{3.3}$ is the slope of the main linear curve (r^2 = 0.977, n=15). The inset shows the points which were used for the determination of $k_{3.2}$ (y-axis intercept), r^2 = 0.911 (n=14). Experimental conditions: pH = 7.6-11.1; $[HOI]_{tot}$ = 0.8-76 μM; carbonate and borate buffers (2 - 30 mM); T = 25°C.

3.3.3 Implications for Drinking Water Treatment

In oxidative drinking water treatment, HOI formed from the oxidation of I^- can have various fates which are kinetically determined. One possibility is the formation of undesired iodoorganic compounds such as CHI_3 which leads to a bad taste and odor of the drinking water. Our results allow to estimate the life-time of HOI/OI^- if disproportionation is the main reaction pathway.

Table 3.2 Initial Half-life of HOI at Varying HOI Concentrations, pH, and Carbonate Concentrations.

		$t_{1/2}$ / d			
[HOI] / µg/L	[carbonate] / mM	pH = 6	pH = 7	pH = 8	pH = 9
1	0	1300	1300	1100	500
10	0	130	130	110	50
100	0	13	13	11	5.0
1	5	700	680	540	190
10	5	70	68	54	19
100	5	7.0	6.8	5.4	1.9

The initial half-life of HOI has been calculated for different conditions (Table 3.2). Because the disproportionation is second-order in HOI/OI$^-$, the half-life of HOI depends strongly on its initial concentration. A ten-fold increase of [HOI](t=0) results in a ten-fold decrease of the initial half-life. An increase in the pH from 6 to 9 leads to an increase in the reaction rate because the speciation is shifted towards OI$^-$ which reacts faster than HOI. In presence of carbonate, the reaction rate is further increased because of the catalysis of HCO_3^- and CO_3^{2-}. According to Table 3.2, the initial half-life of HOI under drinking water relevant conditions (1-10 µg/L HOI, pH = 6-8, 0-5 mM carbonate) is on the order of 50-1300 d. The time for a 90 % removal of HOI is 9 times higher. Even under extreme conditions (100 µg/L HOI, pH = 9, 5 mM carbonate), the initial half-life is never lower than approximately 2 d. We can therefore conclude that the disproportionation of HOI/OI$^-$ is too slow under drinking water conditions to be of importance for the fate of HOI. The fate of HOI during drinking water treatment and distribution will therefore be determined by its reaction with NOM and its further oxidation to IO_3^-.

3.4 Conclusions

- The pK_a of HOI was determined to be 10.4±0.1. Therefore, under typical drinking water conditions, HOI is the major species, whereas OI$^-$ is only a minor species.

- The uncatalyzed disproportionation of HOI occurs through the reactions HOI + HOI and HOI + OI$^-$ at pH = 7.6 - 11.1. Bicarbonate, carbonate, and borate catalyze the disproportionation. We postulate that the catalysis is particularly important for the reaction HOI + HOI.

- Although catalyzed by carbonate, the disproportionation of HOI is slow under typical drinking water treatment conditions (pH = 6-8). The initial half-life of HOI lies in the order of a few days to years. Therefore, the life-time of HOI is not controlled by this reaction. During oxidative drinking water treatment, the fate of HOI is determined either by its further oxidation by an oxidant or by the reaction with NOM. The competition of these two reaction pathways determines the importance of the two final products which are IO_3^- or iodoorganic compounds.

4. Oxidation of Iodide and Hypoiodous Acid in the Disinfection of Natural Waters

Y. Bichsel and U. von Gunten, Environmental Science & Technology **33**(22), 4040-4045 (1999).

In aqueous oxidative processes with ozone (O_3), chlorine, or chloramine, naturally occurring iodide (I^-) can easily be oxidized to hypoiodous acid (HOI) which can react with natural organic matter (NOM) or be further oxidized to iodate (IO_3^-). Such processes can be of importance for the geochemistry of iodine and for the fate of iodine in industrial processes (drinking water treatment, aquacultures). Whereas IO_3^- is the desired sink for iodine in drinking waters, iodoorganic compounds (especially iodoform, CHI_3) are problematic due to their taste and odor.

To assess the sink for iodine during oxidation of natural waters, we determined the kinetics of several oxidation reactions of HOI. Ozone, chlorine, and chloramine have been tested as potential oxidants. Ozone oxidized both HOI and hypoiodite (OI^-) ($k_{O3+HOI} = 3.6 \times 10^4\ M^{-1}s^{-1}$; $k_{O3+OI-} = 1.6 \times 10^6\ M^{-1}s^{-1}$) in a fast reaction. Chlorine species oxidized HOI by a combination of second-order and third-order reactions ($k''_{HOCl+HOI} = 8.2\ M^{-1}s^{-1}$; $k'''_{HOCl+HOI} = 8.3 \times 10^4\ M^{-2}s^{-1}$; $k_{OCl-+HOI} = 52\ M^{-1}s^{-1}$). Monochloramine did not further oxidize HOI. The probability of the formation of iodoorganic compounds during drinking water disinfection therefore increases in the order $O_3 < Cl_2 < NH_2Cl$. In aquacultures, I^- is transformed to IO_3^- within seconds to minutes in the presence of chlorine or ozone. In the surface boundary layer of seawater, O_3 oxidizes I^- to HOI but not to IO_3^-.

4.1 Introduction

In seawater, iodine compounds can be found with typical surface concentrations of 45-60 μg/L (Fuge & Johnson, 1986; Wong, 1991). From there, biologically produced iodoorganic compounds (e.g. CH_2I_2; Klick & Abrahamsson, 1992) are transferred to the atmosphere. Another possibility for the release of iodine-containing compounds to the atmosphere is the evaporation of HOI, a species which can be formed by the reaction of I^- with O_3 (Thompson & Zafiriou, 1983). An alternative pathway for HOI is the reaction with NOM. Due to enhanced formation of volatile iodine-containing compounds at the sea surface, the [I]:[Cl] ratio increases by a factor of 500-10'000 from seawater to the atmosphere (Duce et al., 1963; Cicerone, 1981; Sturges & Barrie, 1988). From the atmosphere, the iodine species rain out which leads to a partial transfer into the continental water. The main species of iodine in freshwaters are I^- and IO_3^-. The total iodine concentration in water resources is usually in the range of 0.5-20 μg/L but it can exceed 50 μg/L in certain groundwaters near the sea coast or under special geological circumstances (Fuge & Johnson, 1986; Wong, 1991).

During oxidation and disinfection processes, I^- is rapidly oxidized. The oxidation kinetics of I^- with several oxidants/disinfectants and the product formation have been investigated earlier (Table 4.1). For typical concentrations of disinfectants applied in drinking water treatment, the half-life of I^- is in the order of milliseconds for ozonation and chlorination and in the minute range in the presence of chloramine or ClO_2. With exception of ClO_2 (formation of I-radicals), HOI is the first oxidation product and determines the further fate of iodine compounds in oxidative drinking water treatment. The fate of I-radicals which are formed in the presence of chlorine dioxide is not known.

Table 4.1 Rate Constants for the Oxidation of I$^-$ with Several Oxidants / Disinfectants

	rate constant	product	reference
O_3	2×10^9 $M^{-1}s^{-1}$	HOI	Garland et al., 1980
HOCl	4.3×10^8 $M^{-1}s^{-1}$	HOI	Nagy et al., 1988
NH_2Cl	$2.4 \times 10^{10} \times [H^+]$ $M^{-2}s^{-1}$	HOI	Kumar et al., 1986
ClO_2	1.87×10^3 $M^{-1}s^{-1}$	I$^\bullet$	Fabian & Gordon, 1997

In the late 1980s, it was observed that taste and odor problems in drinking waters were frequently linked to the presence of iodoorganic compounds (Hansson et al., 1987; Bruchet et al., 1989). The identified compounds were iodo-trihalomethanes (I-THMs; in particular iodoform CHI_3) which can be formed via a reaction of HOI with NOM, the iodoform reaction (Vollhardt & Schore, 1994). CHI_3 has an organoleptic threshold concentration of 0.03 - 1 μg/L (Bruchet et al., 1989; Khiari, 1999). It has been estimated that I-THMs may be partly responsible for up to 25 % of the cases of bad taste and odor in drinking waters in France (Suez Lyonnaise des Eaux, 1993).

The formation of undesired iodoorganic compounds is in kinetic competition with the disproportionation of HOI/OI$^-$ (see eqs 4.1 - 4.3) or its further oxidation to IO_3^- by NH_2Cl, Cl_2, or O_3. The sinks for these reactions are iodoorganic compounds or IO_3^- which both are so far not included in the guidelines for drinking water of the World Health Organization (WHO, 1993). In contrast to bromate (BrO_3^-), IO_3^- can probably be considered as nontoxic because ingested IO_3^- is quickly reduced to I$^-$ in vivo and in vitro by glutathione (Taurog et al., 1966). I$^-$ is then taken up by the thyroid gland which produces iodine-containing hormones (thyroxine and triiodothyronine).

The disproportionation of HOI is a reaction in which HOI (oxidation state +I) reacts with itself leading to a reduced species (I^-, oxidation state -I) and to an oxidized species (IO_3^-, oxidation state +V). It can be described by a sequence of the two reactions 4.1 and 4.2 whereas reaction 4.1 is rate-determining:

$$HOI + HOI \rightarrow IO_2^- + I^- + 2\ H^+ \qquad (4.1)$$

$$HOI + IO_2^- \rightarrow IO_3^- + I^- + H^+ \qquad (4.2)$$

The overall reaction can be described by reaction 4.3:

$$3\ HOI \rightarrow IO_3^- + 2\ I^- + 3\ H^+ \qquad (4.3)$$

The kinetics of this reaction are described in chapter 3. A catalysis by anions such as borate, phosphate, or carbonate was observed. However, the overall reaction was very slow under typical drinking water conditions. The half-life of HOI according to the disproportionation lies in the range of 4 days (50 μg/L HOI, pH 9, 5 mM carbonate) to 3.5 years (1 μg/L HOI, pH 6, no carbonate). Hence, IO_3^- formation by this pathway is of minor importance during drinking water treatment. The main sinks for HOI are its addition to functional groups of the NOM or its further oxidation by a disinfectant.

Black et al. (1968) suggested that the product of the oxidation of HOI/OI^- by O_3 or HOCl is IO_3^-. In contrast, they did not find IO_3^- as a product of the reaction of HOI with NH_2Cl. The rate constant of the reaction of HOCl with HOI has been reported to be < 20 $M^{-1}s^{-1}$ (Lengyel et al., 1996).

In the present study, we investigated the kinetics of the oxidation of HOI by O_3, $HOCl/OCl^-$, and NH_2Cl to assess the fate of HOI with respect to further oxidation to IO_3^-. This reaction is in competition to the formation of iodoorganic compounds. HOI is quickly produced from naturally occurring I^- with all of these oxidants.

4.2 Experimental Section

All experiments were performed in double-distilled water. pH measurements were carried out with a Ross electrode (ATI Orion, Boston, MA) and a Metrohm 632 pH-meter (Metrohm, Herisau, Switzerland) which was calibrated with standard buffer solutions (Merck). Spectrophotometrical measurements were performed on an Uvikon 940 spectrophotometer (Kontron Instruments, Eching, Germany).

Because HOI is not stable in water, it has to be freshly produced directly in the reaction vessel. Prior to each investigation, HOI was produced by oxidation of I^- with O_3, HOCl, or NH_2Cl (for kinetics see Table 4.1). The concentration of the NaOCl stock solution (Aldrich) was determined as 5.6% with direct photometry of HOCl at 230 nm ($\varepsilon = 100$ $M^{-1}cm^{-1}$; Soulard et al., 1981). According to eqs 4.1 - 4.3, HOI disproportionates to form I^- and IO_3^-. Under the conditions applied in this study however, the disproportionation was negligible relative to the other processes. This was confirmed by blank experiments.

IO_3^- was analyzed with ion chromatography and postcolumn reaction with UV/Vis-detection as described in chapter 2. The method consists of an anion chromatograph with a AG/S 9 column (Dionex) with postcolumn reaction to form I_3^- and the UV/Vis-detection of this species at 288 nm. The detection limit (S/N = 3) in natural waters was 0.1 µg/L (0.6 nM). IO_3^- solutions were stable for at least 7 days.

4.2.1 Ozonation Kinetics

Ozone stock solutions were produced by continuously bubbling ozone-containing oxygen through distilled water at 0 °C (Bader & Hoigné, 1981). The resulting O_3 concentration was typically around 1 mM. The kinetics of the oxidation of HOI/OI$^-$ by O_3 were investigated in a continuous flow-through system at 25±2 °C. An O_3 solution (17-73 μM, pH = 3.5) and a buffered I$^-$ solution (4-18 μM, pH = 3.0-9.7) were pumped by two mechanically driven glass syringes (Dosimat 665, Metrohm, Herisau, Switzerland) and mixed in a first mixing tee to pass a capillary tube. The buffer concentration (phosphate) was 50 mM. At the end of the capillary (observation point), a solution of indigo trisulfonate (70 μM), malonic acid (5 mM), and phosphoric acid (0.1 M) was added through a second mixing tee to stop the reaction and at the same time detect the residual O_3 by decoloration of indigo (Bader & Hoigné, 1981). Indigo reacts quantitatively and very quickly with O_3. HOI also reacts with indigo but this reaction was quenched by addition of malonic acid. The reaction time for the reaction O_3 + HOI/OI$^-$ was defined by the volume of the capillary tube and the flux of the mixed solution and varied from 0.15 to 2.4 s. From the decrease of [O_3], an observed rate constant was calculated according to second-order kinetics. The pH was measured at the observation point. The experimental setup was similar to the one applied by Hunt & Mariñas (1997).

4.2.2 Chlorination Kinetics

The kinetics of the oxidation of HOI by HOCl/OCl$^-$ were investigated in 20-50 mL batch reactors under pseudo-first-order conditions ([HOCl/OCl$^-$] >> [HOI]) at 10±2 °C and at 25±2 °C. Chlorine (5-450 μM) was added to I$^-$ solutions (0.5-33 μM) at a molar ratio [HOCl/OCl$^-$]:[I$^-$] of 10:1 to 20:1. HOI was formed immediately after chlorine addition. The pH was varied from 5.3 to 8.9. The buffer concentration (phosphate) was 3-33 mM but at least 1000 times higher than [HOI]. Aliquots of the reaction solution were withdrawn after 10 s - 10 h and added to an acidic phenol solution ([phenol] = 3 x [HOCl]) to quench the reaction. Both HOI and HOCl react quantitatively and quickly with phenol. The formation of IO_3^- was measured by ion chromatography (see chapter 2).

4.2.3 Oxidation by NH_2Cl

The kinetics of the oxidation of HOI by NH_2Cl were investigated in 20 mL batch reactors under pseudo-first-order conditions ($NH_2Cl \gg HOI$) at 25±2 °C. I^- (0.1 μM) was added to solutions containing chlorine (5-1000 μM) and ammonia (5-1000 μM) at a molar ratio $[HOCl]:[NH_4^+] = 1$. HOI was formed immediately after the addition of I^- (kinetics see Table 4.1). The pH was 7.2-8.5. The buffer concentration (phosphate) was 3-33 mM and was at least 1000 times higher than the [HOI]. Aliquots of the reaction solution were withdrawn after 1 - 50 h and added to an acidic sulfite solution ($[HSO_3^-]:[NH_2Cl]$ = 1.2-1.5) which quenched the reaction. The acidification of the sulfite solution was needed to prevent the reduction of IO_3^- by sulfite (Rabai & Beck, 1988). The formation of IO_3^- was measured by ion chromatography (see chapter 2). Blank experiments to test the importance of the disproportionation were run under exactly the same conditions but without adding ammonia and by adding just 0.1 μM of chlorine to form HOI.

4.3 Results and Discussion

4.3.1 Stoichiometry and Kinetics of the Oxidation of HOI and OI⁻ by O_3

HOI is formed very quickly by oxidation of I^- in ozonation processes (see Table 4.1). It was previously shown and confirmed by us that the reaction of O_3 with I^- did not produce free radicals that initiated a radical-type chain reaction for accelerating the decomposition of aqueous O_3 (Hoigné et al., 1985). This means that no O_3^- is formed by an electron transfer from I^- to O_3. That the oxidation of I^- occurs through an O-atom transfer reaction is also indicated in the present study.

The stoichiometry of the reaction of O_3 with I^- was determined at different ratios of $[O_3]:[I^-]$ by measuring IO_3^- formation. For ratios $[O_3]:[I^-] \geq 3:1$, we found a complete oxidation of I^- to IO_3^- (pH 4 and 8.5). The overall reaction of O_3 with I^- can therefore be formulated as:

$$3\,O_3 + I^- = IO_3^- + 3\,O_2 \qquad (4.4)$$

A formation of periodate (IO_4^-) which would result in a higher O_3 consumption has not been observed. This is in agreement with previous studies (Black et al., 1968; Hoigné et al., 1985).

A straightforward formation of the halogenate ion as for iodine cannot be observed for all halogens. In current drinking water treatment, BrO_3^- is of particular interest due to its potential carcinogenicity. In this case, Br^- is oxidized to OBr^- which is partly reduced to Br^-. This leads to a catalytic cycling between Br^- and OBr^-, during which O_3 is consumed (Haag & Hoigné, 1983; von Gunten & Hoigné, 1994). Part of the OBr^- is oxidized by O_3 which leads to BrO_3^- formation in analogy to the behavior of HOI/OI⁻. In contrast to HOI/OI⁻ which are both oxidized by O_3, only OBr^- further reacts with O_3. Because of the slower kinetics, O_3 is not the only oxidant which is involved in BrO_3^- formation during ozonation. A significant part of the BrO_3^- formation occurs by oxidation with hydroxyl radicals (von Gunten & Hoigné, 1994).

The kinetics of the oxidation of HOI/OI⁻ by O_3 have been determined in the pH range 6.0 - 9.7 and for ratios $[O_3]:[I^-]$ of 3.0 - 6.5 by measuring the O_3 depletion in a flow-through apparatus. Blank experiments in absence of I^- showed that O_3 was stable during the reaction time ($t_{1/2} \geq 18$ s). Observed rate constants $k_{obs,O3}$ were determined by a second-order kinetics approach ($r^2 > 0.9$). Between pH 6.0 and pH 8.0, the $k_{obs,O3}$ remained constant, whereas at pH > 8.0, a pH-dependent increase was observed (Fig. 4.1). This can be explained by assuming that the oxidation of HOI dominates the reaction at pH < 8.0 and that the oxidation of OI^- becomes important at higher pH-values. From $k_{obs,O3}$ at pH < 8.0, the rate constant k_{O3+HOI} of the oxidation of HOI by O_3 can be calculated as $3.6 \pm 1.0 \times 10^4$ $M^{-1}s^{-1}$. The error indicates the standard deviation (n = 18). The rate constant k_{O3+OI^-} for the reaction of OI^- with O_3 can be calculated from the pH-dependence of $k_{obs,O3}$ for pH > 8.0 if the $pK_a = 10.4$ of HOI is considered (chapter 3):

$$k_{obs,O3} = k_{O3+HOI} + k_{O3+OI^-} / (1+10^{pKa-pH}) \qquad (4.5)$$

The inset of Fig. 4.1 shows the linearization of the data according to eq. 4.5. The slope of the resulting line is $k_{O3+OI^-} = 1.6 \pm 0.5 \times 10^6$ $M^{-1}s^{-1}$. The error indicates the standard deviation of the linear regression ($r^2 = 0.937$, n = 16). The line in Fig. 4.1 shows the fit according to eq 4.5 for the observed data of $k_{obs,O3}$. Table 4.2 shows both rate constants for the reaction of O_3 with HOI and OI^-. Compared to OBr^- ($k_{O3+OBr^-} = 430$ $M^{-1}s^{-1}$; Haag & Hoigné, 1983) and OCl^- ($k_{O3+OCl^-} = 120$ $M^{-1}s^{-1}$; Hoigné et al., 1985), the oxidation of OI^- by O_3 is about four orders of magnitude faster. In contrast to HOI, both HOCl and HOBr cannot be oxidized by O_3 (Haag & Hoigné, 1983; Hoigné et al., 1985).

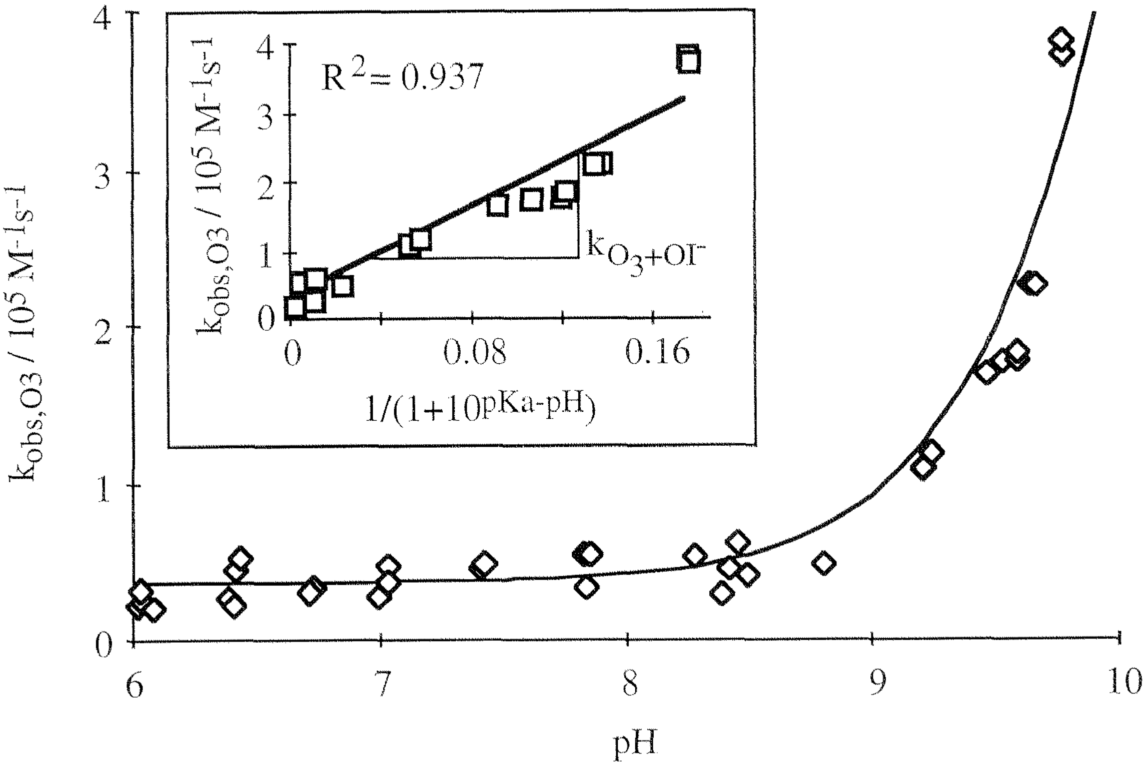

Figure 4.1: pH-dependence of the observed second-order rate constant $k_{obs,O3}$ of the oxidation of HOI and OI^- by O_3. The inset shows the linearization with linear regression according to eq 4.5.

The reactivity of O_3 toward different iodine species is important for iodometric O_3 gas-phase determination (Bablon et al., 1991). Usually, the O_3-containing gas is bubbled through a solution of 60-300 mM I^- at neutral pH. From Table 4.1, we can assume that the first oxidation step of I^- leads immediately to HOI. The further consumption of O_3 by HOI is in competition with the reaction of O_3 with I^-. Since the reaction of O_3 with I^- is 5 orders of magnitude faster than with HOI and since $[I^-] >> [HOI]$, no further oxidation of HOI has to be expected. In addition, under these conditions HOI quickly reacts with I^- to form I_2 (4.4 x 10^{12} $M^{-2}s^{-1}$ x $[H^+]$; Eigen & Kustin, 1962) which again hinders the further oxidation of HOI by O_3.

Table 4.2 Rate Constants and Products for Oxidation of HOI and OI^- with O_3, HOCl, OCl^-, and NH_2Cl from This Study

reaction	10 °C	25 °C		product
HOI + O_3 (k_{O3+HOI})		$3.6\pm1.0 \times 10^4$	$M^{-1}s^{-1}$	IO_3^-
OI^- + O_3 (k_{O3+OI^-})		$1.6\pm0.5 \times 10^6$	$M^{-1}s^{-1}$	IO_3^-
HOI + HOCl + HOCl ($k'''_{HOCl+HOI}$)	$8.3\pm0.8 \times 10^4$	$8.3\pm0.8 \times 10^4$	$M^{-2}s^{-1}$	IO_3^-
HOI + HOCl ($k''_{HOCl+HOI}$)	5.6 ± 1.0	8.2 ± 0.8	$M^{-1}s^{-1}$	IO_3^-
HOI + OCl^- ($k_{OCl-+HOI}$)	33 ± 4	52 ± 5	$M^{-1}s^{-1}$	IO_3^-
HOI + NH_2Cl ($k_{NH2Cl+HOI}$)		$< 2 \times 10^{-3}$	$M^{-1}s^{-1}$	unknown
OI^- + NH_2Cl ($k_{NH2Cl+OI-}$)		< 3	$M^{-1}s^{-1}$	unknown

4.3.2 Stoichiometry and Kinetics of the Oxidation of HOI by HOCl and OCl^-.

The stoichiometry of the reaction of HOCl/OCl^- with I^- was investigated at pH 5.3 - 8.7 and at a molar ratio of [HOCl]:[I^-] = 4:1. As mentioned earlier, the first oxidation step from I^- to HOI occurs immediately. For the further reaction, the formation of IO_3^- was measured together with the sum of [HOCl] + [OCl^-] + [HOI] which was measured as I_3^- (in excess of I^-) by spectrophotometry. HOCl/OCl^- (3.0±0.1 mol) was consumed for every mol of I^- and yielded 0.99±0.02 mol of IO_3^- according to reactions 4.6 and 4.7.

$$2\,HOCl + HOI \rightarrow IO_3^- + 2\,Cl^- + 3\,H^+ \quad (4.6)$$

$$2\,OCl^- + HOI \rightarrow IO_3^- + 2\,Cl^- + H^+ \quad (4.7)$$

Therefore, it can be assumed that no stable intermediate and no IO_4^- are formed. IO_3^- formation was already observed in an earlier investigation (Black et al., 1968).

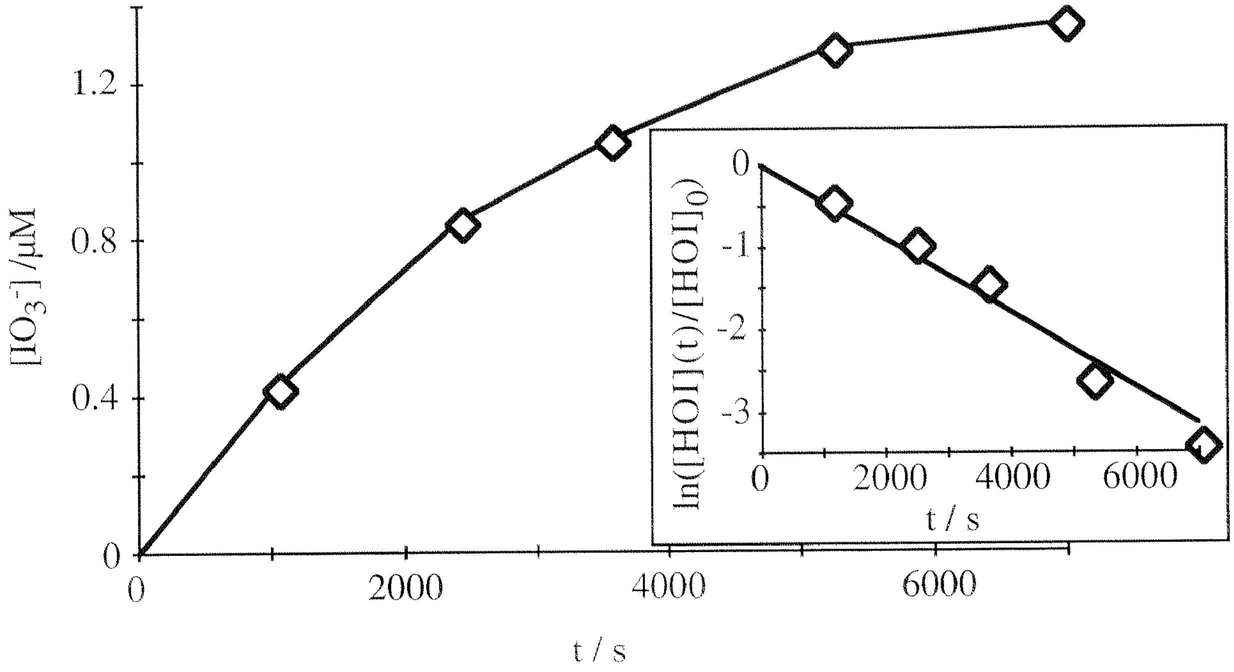

Figure 4.2: IO_3^- formation from the oxidation of HOI by HOCl/OCl⁻. Error bars show the standard deviation of the IO_3^- determination. The inset shows the linearization with linear regression according to pseudo-first-order kinetics. $k_{obs,HOCltot}$ can be calculated from the slope to be $5.3 \times 10^{-4}\ s^{-1}$. Experimental conditions: $[HOCl]_{tot} = 15.3\ \mu M$; pH = 7.2; $[HOI]_0 = 1.4\ \mu M$; T = 24 °C.

The kinetics of the reaction of hypochlorous acid (HOCl) and hypochlorite (OCl^-) with HOI/OI^- was investigated under pseudo-first-order conditions in the pH range 5.3 - 8.9, at 10 °C as well as at 25 °C, and at chlorine concentrations of 5 - 450 μM by measuring the rate of formation of IO_3^-. The IO_3^- formation in a typical experiment is shown in Fig. 4.2. The observed rate constant $k_{obs,HOCltot}$ for the oxidation of HOI by $[HOCl]_{tot} = [HOCl] + [OCl^-]$ was calculated as a pseudo-first-order rate constant from the decrease of [HOI](t) (see inset Fig. 4.2). [HOI](t) was calculated by subtracting the formed $[IO_3^-](t)$ from the initial $[HOI]_0$. Under our reaction conditions, the disproportionation of HOI did not interfere and the buffer concentration did not alter the reaction rate. The pK_a of HOCl was taken as 7.53 (Weast, 1984).

Figure 4.3 shows the dependence of $k_{obs,HOCltot}$ on the HOCl concentration in the pH range 5.3-6.4. Because the observed rate constants did not depend on the pH in this pH range, we concluded that OCl^- did not play a role and HOCl was the kinetically dominant species. The reaction is first-order in HOCl at low concentrations (5-20 μM; Fig. 4.4). At higher HOCl concentrations (100-450 μM), a term that is second-order in HOCl must be considered. The oxidation kinetics of HOI by HOCl are, therefore, a result of two pathways, which both contribute to the overall reaction:

$$\frac{d[IO_3^-]}{dt} = k_{obs,Cl}[HOI] = k''_{HOCl+HOI}[HOCl][HOI] + $$
$$+k'''_{HOCl+HOI}[HOCl]^2[HOI] \qquad (4.8)$$

The rate constant $k''_{HOCl+HOI}$ of the second-order reaction was determined by a linear regression in the concentration range of [HOCl] = 5-20 μM ($k_{obs,HOCltot}$ vs. [HOCl]) which yields $k''_{HOCl+HOI} = 8.2\pm0.8\ M^{-1}s^{-1}$ (25 °C). The error indicates the standard deviation of the linear regression (r^2 =

0.964, n = 14). This value is in agreement with an earlier study (Lengyel et al., 1996). At this low [HOCl], the third-order reaction can be neglected. For the calculation of the third-order rate constant $k'''_{HOCl+HOI}$, only experimental data for the range of 100-450 μM HOCl was used. According to eq 4.8, $k'''_{HOCl+HOI}$ was found as the slope of a plot of $k_{obs,HOCltot}$ - $k''_{HOCl+HOI}$ [HOCl] vs. $[HOCl]^2$ to be 8.3±0.8 x 10^4 $M^{-2}s^{-1}$ (25 °C; standard deviation; r^2 = 0.939, n = 13).

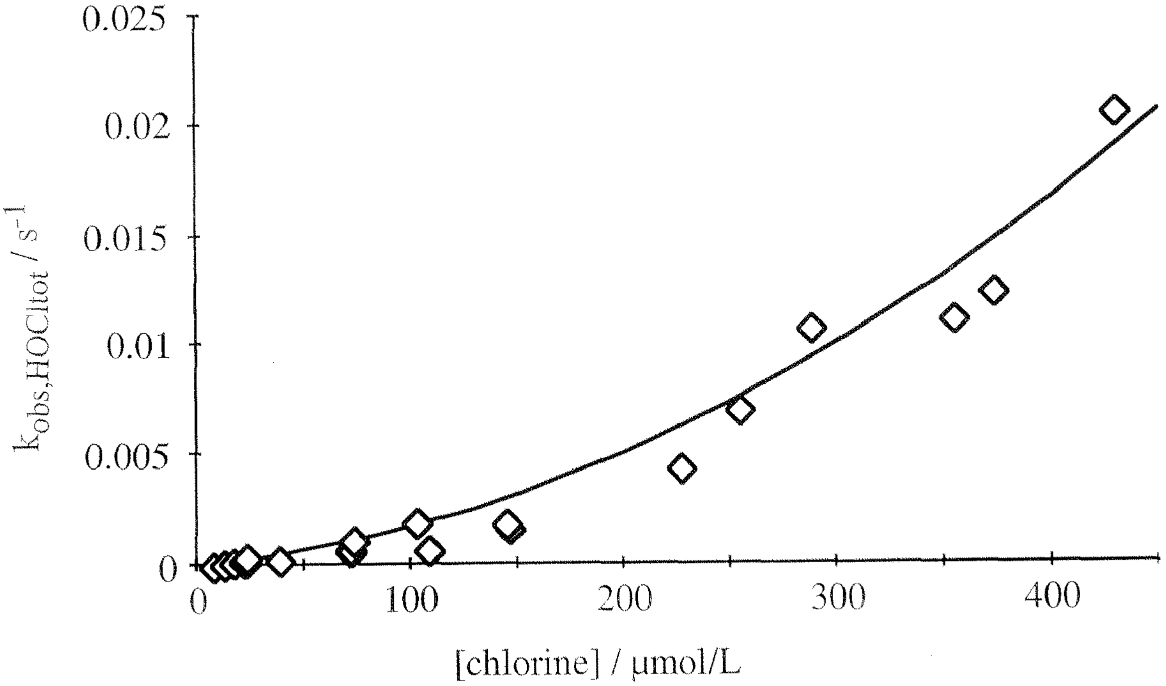

Figure 4.3: Dependence of the observed pseudo-first-order rate constants $k_{obs,HOCltot}$ for the oxidation of HOI by HOCl on the concentration of chlorine (pH = 5.3-6.4; 25 °C).

The mixed order of the reaction kinetics of the oxidation of HOI by HOCl can be explained by two hypothetical pathways. The differences result from an addition of HOI to the O-atom or the Cl-atom of HOCl. The first case results in a new iodine-oxygen bond which leads to iodite (IO_2^-). IO_2^- is quickly further oxidized to IO_3^- by HOCl. Such a reaction mechanism would result in a first-order behavior in [HOCl]. The second

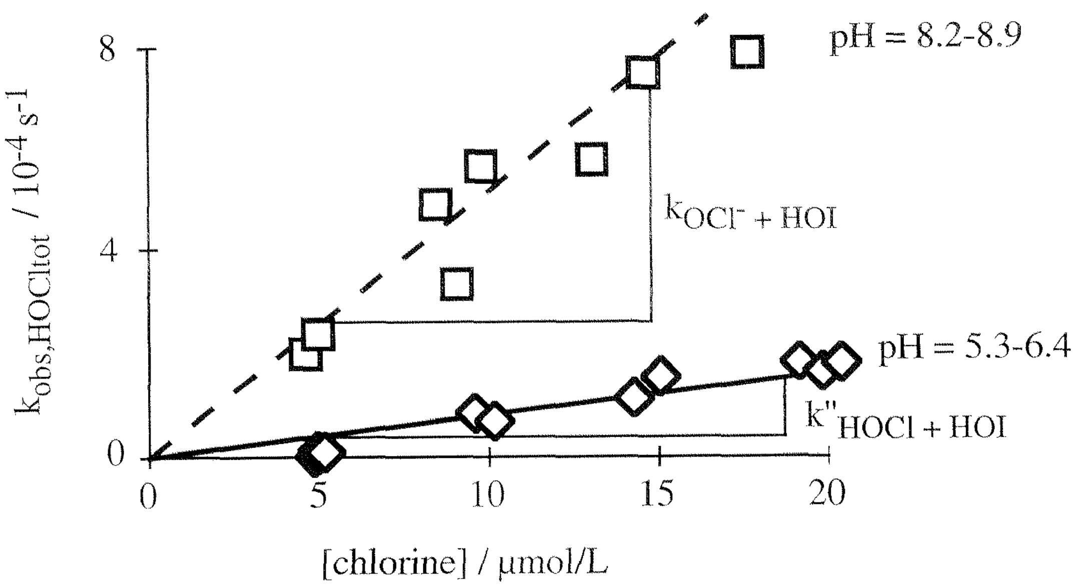

Figure 4.4: Dependence of the observed pseudo-first-order rate constants $k_{obs,HOCltot}$ for the oxidation of HOI by HOCl and OCl^- on the concentration of chlorine in the low concentration range (25 °C). Lines show the best linear fit.

pathway leads to the fast formation of an intermediate with an iodine-chlorine bond (e.g. HOI-ClOH). This intermediate can either quickly re-dissociate to the initial compounds (HOCl, HOI) or alternatively react with a second HOCl. This would lead to a compound such as e.g. HOI-$(ClOH)_2$ which would quickly hydrolyze to IO_3^-. If the rate-determining step is the reaction of the second HOCl with the interhalogen compound (HOI-ClOH), a second-order kinetics with respect to HOCl results. The rate constants for the reactions of HOI with HOCl are compiled in Table 4.2. It can be calculated that for [HOCl] = 100 μM, the second-order pathway and the third-order pathway have a comparable reaction rate. In oxidative drinking water treatment, HOCl concentrations are usually considerably lower. At [HOCl] = 3 μM (0.2 mg/L Cl_2), the second-order pathway contributes 99.9 % to the reaction of HOI with HOCl whereas this value decreases to 80 % for [HOCl] = 30 μM (2 mg/L Cl_2).

In the pH range 8.2 to 8.9, the reaction of HOCl/OCl$^-$ with HOI was investigated in an OCl$^-$ concentration range of 5-20 μM. Since the observed pseudo-first-order rate constants did not depend on the pH in this pH range, we concluded that OCl$^-$ and HOI were the kinetically dominating species. The reaction of HOI with OCl$^-$ was first-order in OCl$^-$ (see Fig. 4.4). Table 4.2 shows the corresponding rate constants. At 25 °C, we found $k_{OCl^-+HOI} = 52 \pm 5\ M^{-1}s^{-1}$. The error indicates the standard deviation of the linear regression ($r^2 = 0.920$, $n = 9$). The rate constants for the first-order reactions of OCl$^-$ are significantly higher than the rate constants for HOCl. Under typical drinking water treatment conditions (3 - 30 μM or 0.2-2 mg/L Cl_2), the reaction OCl$^-$ + HOI is therefore dominant and contributes 60 % (pH = 7) to 99.5 % (pH = 9) to the overall HOI oxidation by chlorine.

All observed rate constants which were determined for the oxidation of HOI/OI$^-$ by O_3 and chlorine are shown in the Appendix C.

4.3.3 Reaction of Ammonia and Monochloramine with HOI

In the presence of ammonia, the formation of haloamines during disinfection is an important part of the aqueous chemistry of chlorine and bromine (Johnson & Overby, 1971; Wolfe et al., 1985). However, the formation of iodamines in water has not been observed so far. To test the formation of iodamines, we measured the UV-absorbance spectra between 200 nm and 250 nm of solutions containing an excess of ammonia (0.01 - 3 M) relative to HOI (0.1-0.5 mM) at pH = 7.0 - 8.5 in a flow-through apparatus (to avoid disproportionation). The residence time in the photometry cell was 8 s. Because HOI absorbs in the observed range, we expected a change in the absorbance spectra if iodamine is formed. However, the observed spectra did not differ from the sum of the absorbance spectra of the single components. These results are an indication that iodamines (NH_xI_{3-x}; x = 0-2) are not formed in water under these conditions.

Monochloramine (NH_2Cl) is known to oxidize I^- to HOI in a relatively fast, pH-dependent reaction (Table 4.1). To determine the rate constant for further oxidation of HOI by NH_2Cl, we measured the corresponding IO_3^- formation in the pH range 7.2-8.5 in the presence of 0.005-1.0 mM of NH_2Cl and 0.1 μM of HOI. Within the first 77 h of the reaction, we detected $[IO_3^-]$ which was less than 25% of the initial [HOI]. This observation is in agreement with an earlier report (Black et al., 1968) and allows estimation of a maximum rate constant $k_{NH2Cl+HOI}$ for the reaction NH_2Cl + HOI of 2×10^{-3} $M^{-1}s^{-1}$. This constant applies if HOI was the reactive species. However, OI^- could as well be the reactive species. In this case, the corresponding maximum rate constant $k_{NH2Cl+OI-}$ for the reaction NH_2Cl + OI^- would be 3 $M^{-1}s^{-1}$.

4.3.4 Implications for Drinking Water Production

Ozonation. In a typical ozonation process, the half-life of HOI is very short and varies between the extremes 0.19 s (2 mg/L O_3, pH 9) and 3.7 s (0.25 mg/L O_3, pH 6). During ozonation, formation of iodoorganic compounds can therefore only occur if it is an extremely fast reaction. CHI_3 was reported to form within hours in a natural water (TOC 2.5 mg/L; Karpel Vel Leitner et al., 1998). In this water, an ozonation would oxidize HOI much faster than CHI_3 was formed. In addition, since O_3 is present in high excess, HOI would have to react very specifically with NOM functional groups. Therefore, the formation of iodoorganic compounds in ozonation processes is rather unlikely.

Chlorination. In chlorination processes, the half-life of HOI is higher than in ozonation processes. At a concentration of 2 mg/L Cl_2 and a pH of 9, the half-life of HOI is 8 min. At a concentration of 0.2 mg/L

Cl_2 and a pH of 6, the half-life of HOI is 10 h. Therefore, the formation of iodoorganic compounds, which has been observed to occur in a similar time-range, seems to be possible especially at low pH and at low chlorine concentrations (Karpel Vel Leitner et al., 1998). However, the NOM-sites which are reactive toward HOI may also be oxidized by HOCl in a competing reaction. Because HOCl is present in large excess relative to HOI (2-4 orders of magnitude), a rate constant for HOI of 10^2-10^4 fold the corresponding HOCl rate constant would be required to have a 1:1 distribution of chlorinated and iodinated organic products. This restriction considerably reduces the probability of the production of iodoorganic compounds.

Chloramination. Chloramine is often the disinfectant of choice for distribution systems because of its long-term stability and, on the contrary to chlorine, its small production of disinfection by-products such as trihalomethanes. With regard to the formation of iodoorganic compounds, the long half-life of HOI in chloramination processes is a new constraint which has to be accounted for when selecting a disinfectant for I^--containing waters. In chloramination processes, the conditions for the formation of undesired iodoorganic compounds are very favorable. According to Fig. 4.5, I^- is first oxidized to HOI by NH_2Cl which then can further react with NOM in two different ways: In a reaction with NOM_1, it can add to the NOM with the formation of iodoorganic compounds. The other possibility is a reduction of HOI back to I^- (NOM_2). Since NH_2Cl is in high excess relative to I^-, the latter can be oxidized to HOI again and undergo the two reactions according to Fig. 4.5. The cyclic character of this reaction pathway with iodoorganic compounds as a final sink may lead to elevated levels of these undesired by-products.

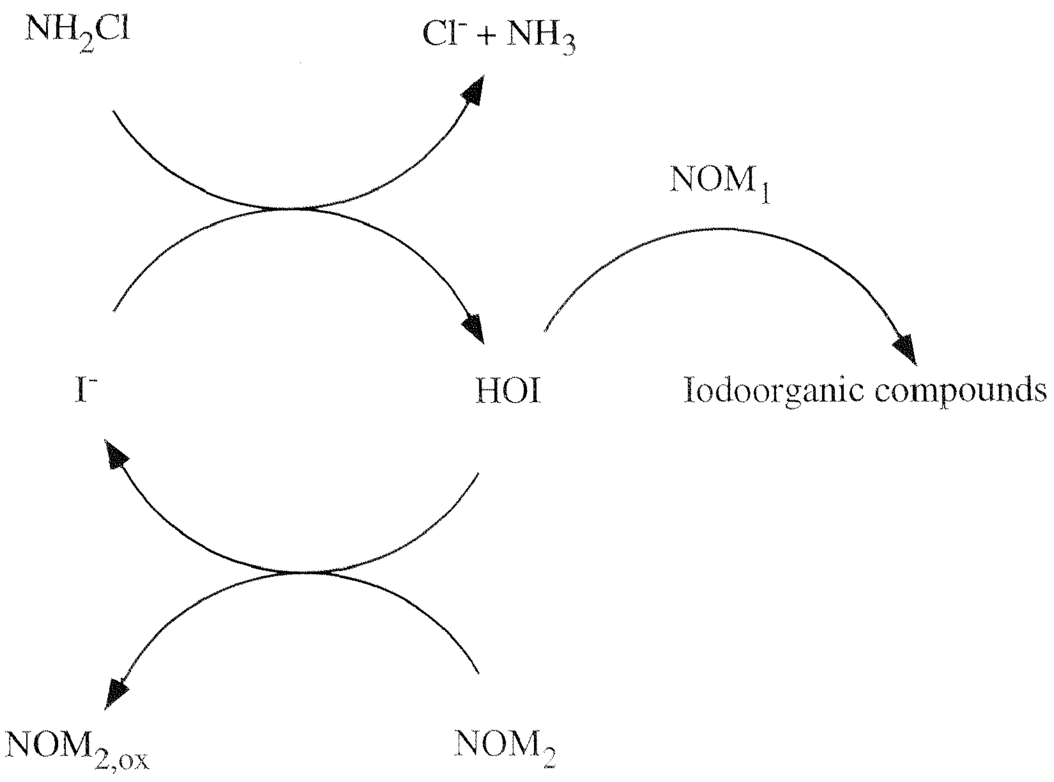

Figure 4.5: Schematic representation of the formation of iodoorganic compounds in chloramination processes.

In the literature, the formation of iodoorganic compounds has been mainly observed during chloraminations (Hansson et al., 1987; Karpel Vel Leitner et al., 1998). When chloramine was utilized, mainly CHI_3 was formed whereas only low concentrations of the bromo- and chloro-trihalomethanes ($CHCl_3$, $CHCl_2Br$, $CHClBr_2$, $CHBr_3$) were observed. When chlorine was used to treat the same waters, only bromo- and chloro-trihalomethanes were observed but no CHI_3. These findings can be understood by our kinetic measurements. Elsewhere, it has been reported that the formation of iodoorganic compounds is strongly dependent on the order of addition of chlorine and ammonia in disinfection processes for the distribution system (Hansson et al, 1987). When chlorine was added first, no formation of iodoform was observed. The lag-time between the addition of chlorine and the addition of ammonia was 80 s. HOI cannot be completely oxidized to IO_3^- within this short time. The formation of I-THMs might be hindered due to reaction of HOCl with THM-precursor sites in the NOM. If ammonia was added before HOCl, a formation of iodoorganic compounds has been observed. In this case, HOCl reacted immediately with ammonia to NH_2Cl which then can be treated as the chloramination case.

Figure 4.6 schematically summarizes the fates of iodine during oxidative drinking water treatment. Whereas IO_3^- is a desired sink for HOI, iodoorganic compounds have to be avoided due to possible taste and odor problems. From our study we conclude that IO_3^- is only a major sink in ozonation and part of chlorination processes. Oxidation of HOI by NH_2Cl is certainly too slow to compete with HOI reactions with NOM. Disproportionation of HOI which is discussed in chapter 3 is so slow under drinking water treatment conditions that it does not lead to significant IO_3^- formation. Even at high ammonia concentrations, the formation of iodamines was not observed. A summary of the half-life of HOI in the presence of O_3, Cl_2, or NH_2Cl as well as the half-life of HOI with respect to the disproportionation is shown in Fig. 4.7. The half-life of HOI has to be related to the kinetics of formation of iodoorganic compounds which occur in the order of hours (Karpel Vel Leitner et al., 1998).

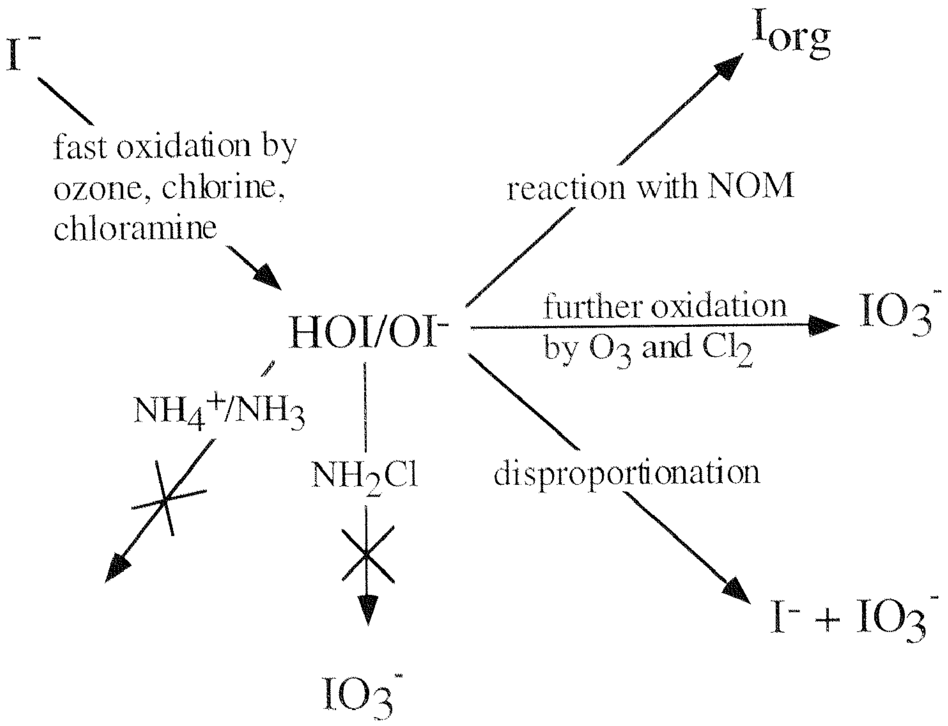

Figure 4.6: Fate of iodine during oxidative drinking water treatment processes: IO_3^- and iodoorganic compounds as possible sinks.

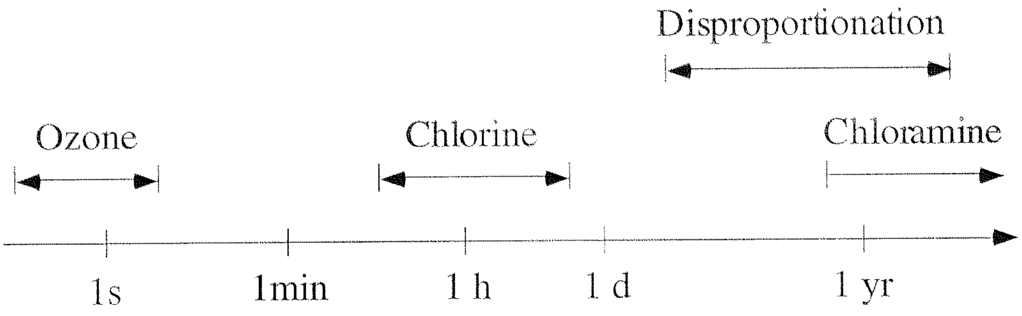

Figure 4.7: Typical half-lives for HOI for different disinfectants and the disproportionation under typical drinking water treatment conditions. Ozonation: 0.25-2 mg/L O_3, pH 6-9; chlorination: 0.2-2 mg/L Cl_2, pH 6-9; chloramination: $\leq$ 2 mg/L Cl_2; disproportionation: 1-50 μg/L HOI, 0-5 mM carbonate, pH 6-9 (chapter 3). The oxidation processes transform I^- into HOI/OI^- within a typical time of less than 1 ms for O_3 and Cl_2 and less than 15 min for NH_2Cl.

4.3.5 Implications for Seawater Chemistry.

O_3 Deposition and IO_3^- Formation. Our kinetic data of the reaction O_3 + HOI/OI$^-$ may be significant for the iodine chemistry in the surface boundary layer of seawater or for the dry deposition of O_3 to the sea. Estimated concentrations in the surface boundary layer are 2 nM for HOI and 200 nM for I$^-$ (Thompson & Zafiriou, 1983). Under these conditions and at pH = 8.1, the apparent first-order rate constant for the consumption of O_3 by HOI/OI$^-$ is 10^{-4} s^{-1}, which has to be compared to the rate constant for the consumption of O_3 by I$^-$, which is 4×10^2 s^{-1} (Garland et al., 1980). The reaction of O_3 with HOI/OI$^-$ accounts therefore to less than 10^{-4} % of O_3 consumption. The depletion of O_3 and the formation of HOI by the reaction O_3 + I$^-$ is reported to be 6×10^9 $cm^{-2}s^{-1}$ (Thompson & Zafiriou, 1983). This is the number of molecules which react per cm^2 of sea surface and per second. From this, by the reaction O_3 + HOI/OI$^-$, a depletion of O_3 of 3000 $cm^{-2}s^{-1}$ and a IO_3^- formation of 1500 $cm^{-2}s^{-1}$ can be calculated. Accounting for diffusion from the surface layer (D = 2×10^{-5} cm^2s^{-1}) and setting the size of this layer to 30 µm, this results in a steady-state concentration of IO_3^- of 4×10^{-16} M. The influence of the reaction O_3 + HOI/OI$^-$ on the chemistry of the surface boundary layer or on the dry deposition of O_3 to the sea can therefore be neglected. The formation of iodoorganic compounds is therefore possible through this mechanism.

Aquacultures. Oxidation of seawater by O_3 or Cl_2 is sometimes applied for disease control in aquacultures (Chang et al., 1998; Douillet & Pickering, 1999). Suggested oxidation conditions are a residual concentration of 0.5 mg/L O_3 after 10 min. Under these conditions, the half-life of HOI is ≤ 1.5 s. For the use of chlorine, a dose of 5 mg/L is suggested. In a chlorination, the half-life of HOI depends on the stability of chlorine in the particular water. For hypothetical half-lifes of chlorine of 1 min, 10 min, or 60 min IO_3^- formation from HOI oxidation may be 23 %, 92%, or 100 %, respectively. IO_3^- is therefore formed in ozonation and in chlorination processes. The extent of IO_3^- formation depends on the stability of the disinfectant in a particular water. If chlorine is quickly consumed by other water constituents such as NOM or Br^-, the formation of IO_3^- is not complete and iodoorganic compounds may form. The high concentration of I^- in the seawater (45-60 μg/L) compared to freshwaters (0.5-20 μg/L) has no influence on the oxidation as long as a sufficient excess of the disinfectant is used.

Seite Leer /
Blank leaf

5. Formation of Iodo-Trihalomethanes in Natural and Model Waters

Y. Bichsel and U. von Gunten, to be submitted to Environmental Science & Technology.

The formation of iodo-trihalomethanes (I-THMs) such as iodoform (CHI_3) during oxidative treatment of iodide-containing drinking waters can be responsible for taste and odor problems. I-THMs are formed by reactions of hypoiodous acid (HOI) with natural organic matter. HOI is quickly formed from naturally occurring iodide (I^-) by oxidation with ozone, chlorine, and chloramine. The kinetics of reactions of HOI with organic model compounds as well as the resulting CHI_3 formation were measured. Phenols and in a smaller extent α-methyl carbonyl compounds were found to be reactive toward HOI and also to yield CHI_3. For phenols, the rate constants for the consumption of HOI varied over almost 9 orders of magnitude from 1.5 $M^{-1}s^{-1}$ to 7 x 10^8 $M^{-1}s^{-1}$. Resorcinol yielded much more CHI_3 than phenol or α-methyl carbonyl compounds. The kinetics of the formation of I-THMs were also measured in natural waters which were oxidatively treated with ozone, chlorine, or chloramine. When using ozone, no I-THMs were detected and most I^- was transformed to IO_3^-. Chlorine led to the formation of both IO_3^- and I-THMs. With increasing chlorine doses, the CHI_3 formation decreased but the IO_3^- formation as well as the formation of classical THMs such as chloroform increased. In chloramination processes, I-THMs (especially CHI_3) were the main products. The formation of I-THMs was significantly slower than

the consumption of HOI. Therefore, it can be hypothesized that the addition reaction of HOI is not rate-determining but rather a final hydrolysis step. A comparison of kinetic results of model compounds with natural waters shows that the CHI_3 formation in natural waters can be explained by activated phenolic groups.

5.1 Introduction

About 25 years ago, the formation of trihalomethanes (THMs) during drinking water chlorination was discovered (Kleopfer & Fairless, 1972; Bellar et al., 1974; Rook, 1974). The four THMs which usually are found and studied are chloroform ($CHCl_3$), bromodichloromethane ($CHBrCl_2$), dibromochloromethane ($CHBr_2Cl$), and bromoform ($CHBr_3$). These compounds will be referred to as 'classical THMs' in this chapter. The discovery of these compounds had many consequences for drinking water treatment. The potentially carcinogenic activity of these compounds led to stringent drinking water standards of 100 μg/L for total THMs in the E.U. and 80 μg/L for total THMs in the U.S. (EU, 1998; USEPA, 1998). Guideline values of the World Health Organization (WHO) are 100 μg/L for $CHBr_3$ and $CHBr_2Cl$, 60 μg/L for $CHBrCl_2$, and 200 μg/L for $CHCl_3$ (WHO, 1993).

In iodide-containing waters, the formation of six additional THMs, the iodo-trihalomethanes (I-THMs), can occur through incorporation of one or more iodine atom into a THM. The resulting compounds are iodoform (CHI_3), chlorodiiodomethane ($CHClI_2$), bromodiiodomethane ($CHBrI_2$), dichloroiodomethane ($CHCl_2I$), dibromoiodomethane ($CHBr_2I$), and bromochloroiodomethane ($CHBrClI$). In contrast to the classical THMs, no adverse health effects have been attributed to I-THMs. However, these compounds and especially CHI_3 were found to be responsible for the occurrence of bad taste and odor in drinking waters in the late 1980s (Hansson et al., 1987; Bruchet et al., 1989; Gittelman & Yohe, 1989). The organoleptic threshold concentration of CHI_3 lies between 0.03 and 1 μg/L which is the lowest value of all I-THMs (Suez Lyonnaise des Eaux, 1993; Khiari, 1999). Total iodine concentrations in water resources are usually in the range of 0.5-20 μg/L but can exceed 50 μg/L in certain ground waters near the sea coast or under special geological circumstances (Fuge & Johnson, 1986). Therefore, the formation of CHI_3 above its organoleptic threshold concentration from naturally occurring iodide (I^-) is possible during oxidative drinking water treatment.

In oxidative drinking water treatment, I^- is first oxidized to HOI in presence of ozone (Garland et al., 1980), chlorine (Nagy et al., 1988), or chloramine (Kumar et al., 1986) in a fast reaction. In a second step, some of these oxidants/disinfectants oxidize HOI to iodate (IO_3^-). The kinetics of these reactions have been determined for ozone, chlorine, and chloramine in an earlier study (chapter 4). In a typical ozonation (0.25-2.0 mg/L O_3), IO_3^- is formed within less than 4 s. The oxidation of HOI by chlorine is slower. The half-life of HOI in a typical chlorination process (0.2-2 mg/L Cl_2, pH = 6-9) is 8 - 600 min. Chloramine does not oxidize HOI to IO_3^-. Chlorine dioxide (ClO_2) oxidizes I^- to I-radicals. This involves a completely different chemistry than the other disinfectants (Fabian & Gordon, 1997). The fate of I-radicals in drinking water is unknown.

An alternative sink for HOI is its disproportionation. Thereby, HOI (oxidation state +I) reacts with itself leading to a reduced species (I^-, oxidation state -I) and to an oxidized species (IO_3^-, oxidation state +V). The disproportionation can be described by reaction 5.1.

$$3\ HOI \rightarrow IO_3^- + 2\ I^- + 3\ H^+ \qquad (5.1)$$

In an earlier study, we showed that this reaction is only of minor importance in drinking waters (chapter 3).

To describe the reactivity of HOI, its pH-dependent speciation has to be considered. The pK_a of HOI is 10.4 (chapter 3). In the oxidation of HOI by O_3, the reactivity of hypoiodite (OI^-) contributes more than 63 % to the oxidation rate at pH = 9.0 although this species represents only 4 % of the total HOI (chapter 4). At low pH, H_2OI^+ can be formed by protonation of HOI ($pK_a = 1.4 \pm 0.3$; Bell & Gelles, 1951; Burger & Liebhafsky, 1973).

The formation of I-THMs from the reaction of HOI with natural organic matter (NOM) is in kinetic competition with the oxidation of HOI to IO_3^- and the disproportionation of HOI. The present study focuses on the kinetics of the reaction of HOI with organic compounds and on the formation kinetics of I-THMs both in natural and model waters. The relative reaction rates of the oxidation of HOI, the disproportionation, and the addition to organic compounds determine the product distribution between IO_3^- and iodoorganic compounds such as I-THMs.

I-THMs were detected in several drinking waters. In one case, a change from chlorination to chloramination led to the formation of 5 μg/L CHI_3 from an I^- concentration of 50 μg/L (Hansson et al., 1987). In another water, up to 30 μg/L CHI_3 and only low concentrations of the classical THMs were formed from 200 μg/L I^- when chloramine was utilized (Karpel Vel Leitner et al., 1998). When chlorine was used to treat the same water, only classical THMs were observed but no CHI_3. Another study reports the appearance of CHI_3 after the chlorination of a water with a high I^- concentration (150-200 μg/L; Bruchet et al., 1989). The same study describes the formation of I-THMs in an ozonation during failure of the ozonation step (90 μg/L I^-).

5.2 Experimental Section

All chemicals were of the highest purity grade. With exception of pinacolone which was redistilled, all chemicals were used without further purification. HOI is not stable in water (disproportionation). Prior to experiments, it was freshly produced through oxidation of I^- by HOCl from a NaOCl stock solution (Aldrich) of approximately 0.68 M. The exact concentration could be determined in excess of I^- as I_3^- ($\varepsilon_{288\ nm}$ = 38'200 $M^{-1}cm^{-1}$; chapter 2). pH measurements were carried out with a Ross electrode (ATI Orion, Boston, MA) and a Metrohm 632 pH-meter (Metrohm, Herisau, Switzerland) which was calibrated with standard buffer solutions (Merck). Spectrophotometric measurements were performed on an Uvikon 940 spectrophotometer (Kontron Instruments, Eching, Germany).

5.2.1 Consumption of HOI by Organic Model Compounds

The kinetics of the consumption of HOI by organic model compounds was measured in double-distilled water in 250 mL batch reactors and in a continuous-flow apparatus under pseudo-first-order conditions ([model compound] >> [HOI]) at 25±2 °C. HOI was prepared by mixing I^- and OCl^- in a volumetric flask and diluting it to a concentration of 1-4 μM. Between pH 3 and 11, pH was controlled by 0.5 - 5 mM of phosphate buffer. For pH < 3, only sulfuric acid was used to control the pH, whereas for pH > 11, only NaOH was used for this purpose. More experimental details can be seen in Tables 5.1-5.3.

The continuous-flow apparatus consisted of three mechanically driven glass syringes (Dosimat 665, Metrohm, Herisau, Switzerland) which pumped a solution of HOI and phosphate, a solution of the model compound, and an iodide solution (0.45 M KI). All three solutions were pumped with the same flux of 5 mL/min. The HOI solution and the model compound solution were mixed in a first mixing tee. Thereafter, they passed a capillary tube of well defined volume. The I^- solution was added through a second mixing tee at the end of the capillary (observation point). This experimental set-up was similar to the one applied by Hunt & Mariñas (1997). I^- stopped the reaction and allowed at the same time to detect the residual HOI in a 5 cm flow-through photometric cell by formation of I_3^- (k_{HOI+I^-} = 5 x 10^9 $M^{-1}s^{-1}$ (Eigen & Kustin, 1962), $k_{I_2+I^-}$ = 6.2 x 10^9 $M^{-1}s^{-1}$ (Turner et al., 1972); $\varepsilon_{351\ nm}$= 25'700 $M^{-1}cm^{-1}$; chapter 2) as shown in eq. 5.2.

$$HOI + 2\ I^- + H^+ = I_3^- + H_2O \tag{5.2}$$

In drinking water systems with an excess of oxidant, reaction 5.2 is not important because I^- is immediately oxidized to HOI or to IO_3^-. The reaction time for the reaction of the model compound with HOI was defined by the volume of the capillary tube and the flux of the mixed solution. It varied from 0.8 to 2.7 s. The pH was measured at the observation point.

The decrease of HOI in the batch experiments was measured by placing 25 mL aliquots of the reaction solution into a 10 cm photometric cell together with 5 mL of 1 M KI. I^- stopped the reaction immediately by quantitatively transforming HOI to I_3^- which was measured as described above (eq. 5.2). This resulted in a detection limit for HOI of 0.4 µM.

5.2.2 Formation of CHI_3 in Model Solutions

The kinetics of the formation of CHI_3 in model solutions were investigated in nanopure water (Barnstead B-pure system) in batch reactors at 25±2 °C. The pH was controlled by 1 mM phosphate buffers (pH = 7.0) and 1 mM borate buffers (pH = 9.0). The initial concentration was 1 µM model compound and 6 µM HOI. This excess of HOI allowed iodine-addition over several steps which eventually led to CHI_3. In addition, a residual HOI concentration could be guaranteed for the duration of the experiment. The following parameters were analyzed during the reaction time (32 h): HOI, CHI_3, and IO_3^-. HOI was analyzed by photometry as described above.

The analysis of the I-THMs was performed with liquid-liquid extraction into methyl tert-butyl ether (Fluka 'for residue analysis' ≥ 99.8 %, Buchs, Switzerland) and GC/ECD according to Cancho et al. (1999). Chromatographic separation was performed on a DB-5 column (J&W). The following compounds were detected by this method: $CHCl_2I$ (limit of detection (LOD) 1.3 μg/L (S/N = 3)), CHBrClI (LOD 0.9 μg/L), $CHBr_2I$ (LOD 0.6 μg/L), $CHClI_2$ (LOD 0.3 μg/L), $CHBrI_2$ (LOD 0.07 μg/L), and CHI_3 (LOD 0.1 μg/L). With exception of CHI_3, I-THM standards are not commercially available. For this study, standards were supplied by F. Ventura, Societat General d'Aigües de Barcelona (AGBAR).

IO_3^- was analyzed with ion chromatography and postcolumn reaction with UV/Vis-detection as described earlier (chapter 2). The method consists of an anion chromatographic separation with a Dionex AG/S 9 column with postcolumn reaction to form I_3^- and the UV/Vis-detection of this species at 288 nm. The detection limit (S/N = 3) in natural waters was 0.1 μg/L (0.6 nM). The analysis of IO_3^- allowed to quantify the amount of HOI which had disproportionated by assuming that only this reaction formed IO_3^-. Thus, the consumption of HOI by the model compounds could be calculated.

5.2.3 Formation of I-THMs and IO_3^- in Natural Waters

Two natural waters (from Seine river, France and lake Zurich, Switzerland) were spiked with varying amounts of I^- and oxidatively treated with chloramine, chlorine, or ozone at 25±2 °C. DOC was 1.3 mg/L in the lake water and 3.5 mg/L in the river water. The concentration of Br^- was

30 μg/L in the river water and 15 μg/L in the lake water. Ammonia was below 6 μg N/L. The pH was controlled by addition of 10 mM $B(OH)_3$ and adjusted to 6.2 or 8.0 by NaOH (1 M, 10.8 M). The solution was transferred to head-space free bottles immediately after the addition of the oxidant. The following parameters were analyzed during the reaction time (24 - 35 h): HOI, I-THMs, IO_3^-, classical THMs, oxidant concentration, pH. The I-THMs and IO_3^- were analyzed as described above.

In these systems, it was not possible to analyze HOI by the photometric method as described above. Oxidants such as chloramine, chlorine, or ozone severely interfere in that method because they also oxidize I^- to I_3^-. Therefore, HOI was analyzed as iodophenol by HPLC. 20 μM of phenol were added to an aliquot of the reaction solution to transform HOI to iodophenol. Phenol reacts quickly and quantitatively with HOI (see below). Both p-iodophenol and o-iodophenol are formed in this reaction. The two compounds were quantified relative to a p-iodophenol standard solution by assuming that both iodophenols had the same sensitivity. The sum of them was calculated to determine the HOI concentration. The chromatographic separation was done on a Nucleosil 103-5 C_{18} column (Macherey-Nagel, Düren, Germany) with an eluent consisting of 65 % methanol, 34.9 % water, and 0.1 % acetic acid (retention times 5.5 min for o-iodophenol and 6.5 min for p-iodophenol). UV detection at 231 nm yielded a detection limit of 2 nM I.

The four classical THMs ($CHCl_3$, $CHBrCl_2$, $CHBr_2Cl$, $CHBr_3$) were analyzed by head-space GC/ECD. 5 mL of the reaction solution were placed into 10 mL vials together with a double excess of sulfite to quench the reactive chlorine and iodine species. The vials were sealed with PTFE seals. After heating the sample to 60 °C during 15 min, 1000 μl of the head-space were injected on a DB-5 column. Detection limits (S/N = 3) were 0.06 μg/L ($CHBrCl_2$), 0.1 μg/L ($CHBr_2Cl$), 0.3 μg/L ($CHCl_3$), and 0.5 μg/L ($CHBr_3$).

Oxidant concentrations were determined with the indigo method (ozone; Bader & Hoigné, 1981) or with the ABTS method (chlorine, chloramine; Pinkernell et al., 1999).

5.3 Results and Discussion

5.3.1 Consumption of HOI and Formation of CHI_3 by Model Compounds

A series of organic model compounds have been tested for their reactivity toward HOI and the formation of CHI_3 in these reactions. The two main classes which have been investigated are phenols and α-methyl carbonyl compounds. These compounds which are known to react with halogens are present in substructures of NOM (Vollhardt & Schore, 1994).

Consumption of HOI by Phenols. The reaction kinetics of HOI with six para-substituted phenols were investigated under pseudo-first-order conditions ([phenol]>>[HOI]) in a batch and in a continuous-flow system. Experimental details (pH, buffer concentrations, concentrations of phenols, initial HOI concentrations, number of experiments) and the calculated rate constants are shown in Table 5.1. The kinetics were always first-order in phenol and first-order in HOI. The rate constants were determined by a least squares fit for eq. 5.3-5.5.

Table 5.1 Rate Constants for the Reaction of Phenols with HOI

compound	pK_a	pH range	mM buffer	[phenol] / µM	[HOI](t=0) / µM	n^c	observed rate constants / $M^{-1}s^{-1}$		
							k_3	k_4	k_5
p-Methoxy-phenol	10.20^a	3.1-4.7	1	10-20	1.1-3.5	11	$5 \pm 1 \times 10^4$	< 100	$7 \pm 2 \times 10^8$
p-Cresol	10.26^a	2.5-4.9	0-1	10	0.8-2.6	8	$4.0 \pm 1.5 \times 10^4$	$3 \pm 1 \times 10^2$	$7 \pm 3 \times 10^8$
Phenol	9.99^a	3.1-8.6	2.5-5	10-500	1.7-5	27	$5 \pm 2 \times 10^4$	$1.0 \pm 0.3 \times 10^2$	$2 \pm 1 \times 10^6$
p-Chloro-phenol	9.43^a	1.5-7.7	0-1	10-200	1.2-2.3	14	$3 \pm 1 \times 10^3$	< 5	$1.6 \pm 0.5 \times 10^5$
p-Iodo-phenol	9.20^a	0.5-8.2	0-1	10-200	0.8-5.0	16	$4 \pm 1 \times 10^3$	20±8	$1.5 \pm 0.8 \times 10^5$
p-Cyano-phenol	7.86^b	1.9-8.4	0-1	10-1000	1.1-2.3	18	$2 \pm 1 \times 10^2$	1.5±0.5	$4 \pm 2 \times 10^2$

a: Dean, 1985; b: this work; c: n = number of kinetic experiments ([HOI] vs. t)

$$H_2OI^+ + \text{(substituted)phenol} \xrightarrow{k_3} \text{products} \quad (5.3)$$

$$HOI + \text{(substituted)phenol} \xrightarrow{k_4} \text{products} \quad (5.4)$$

$$HOI + \text{(substituted)phenolate} \xrightarrow{k_5} \text{products} \quad (5.5)$$

Figure 5.1 depicts the pH-dependence of the observed second-order rate constants for a highly reactive phenol (p-methoxyphenol), a moderately reactive phenol (p-iodophenol), and a less reactive phenol (p-cyanophenol). At low pH values, the reaction H_2OI^+ + phenol is dominant (eq. 5.3). The results for p-iodophenol confirm the pK_a value of 1.4±0.3 for H_2OI^+ (see Fig. 5.1). At pH < 3.5, the observed second-order rate constant increases with decreasing pH due to the shift of HOI to H_2OI^+. H_2OI^+ is expected to have a higher reactivity as a result of its higher electrophilic character. This increase stops at pH < 1, where the concentration of H_2OI^+ does not further increase. However, the rate constant continues to increase at pH < 1 for p-cyanophenol. Other unknown reactions might be responsible for this behavior. At higher pH values (3.5 < pH < 5), the observed second-order rate constants go through a minimum. In this pH range, reaction 5.4 involving HOI and the phenol becomes important for p-cresol, phenol, p-iodophenol, and p-cyanophenol. For p-chlorophenol and p-methoxyphenol, k_4 could not be determined because reaction 5.4 is always negligible compared to reactions 5.3 and 5.5. In these cases, it is only possible to indicate a maximum value for k_4. At high pH values (pH > 5), the overall reaction is dominated by the phenolate (reaction 5.5). This results in a ten-fold increase of the overall rate constant with every pH unit until the pK_a of the phenol is reached. All determined rate constants k_3, k_4, and k_5 are shown in Table 5.1. They cover a range of almost 9 orders of magnitude (1.5 to 7×10^8 $M^{-1}s^{-1}$).

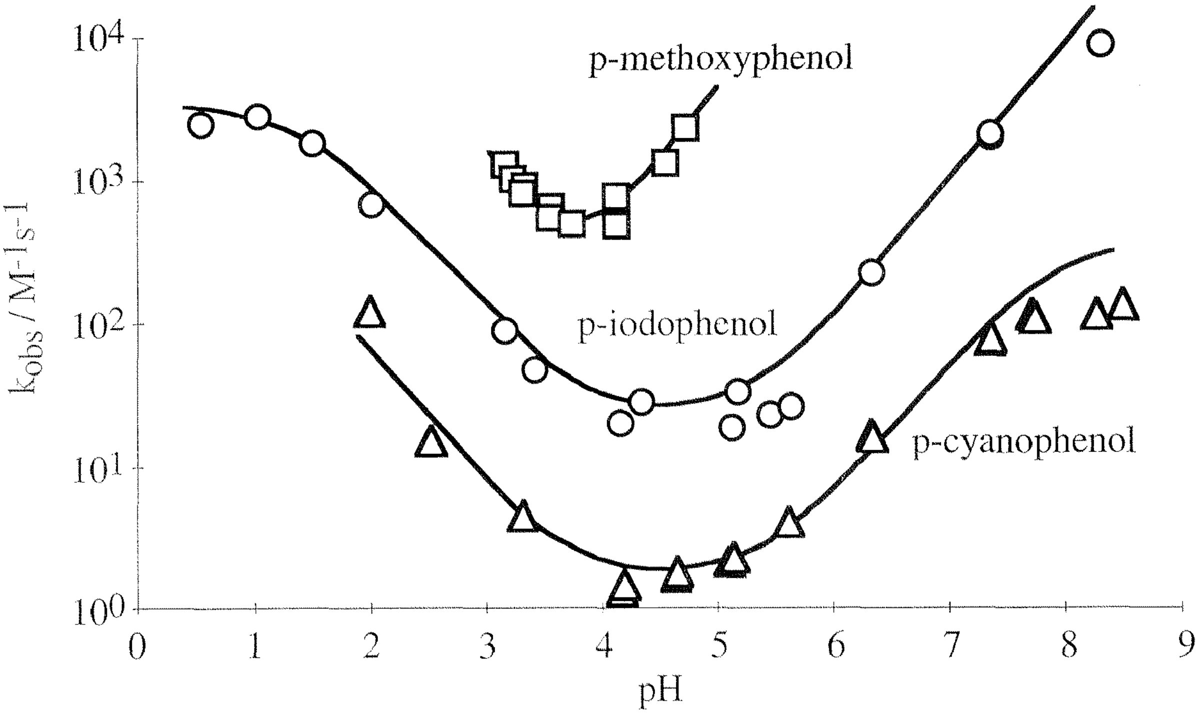

Figure 5.1: pH-dependence of the observed second-order rate constant of the reaction of HOI with some phenols. Symbols: experimental results, lines: calculated according to eq. 5.3-5.5.

A comparison of the rate constants for different phenols is shown in Fig. 5.2. All determined rate constants are displayed against the Hammett coefficients σ_p of the substituents of the phenols (Johnson, 1980). These coefficients describe the electron-withdrawing or donating effect of functional groups as substituents of aromatic systems at a certain position (ortho, meta, or para). High σ_p values can be found for electron-withdrawing substituents such as the -CN group whereas low σ_p values are found for electron-donating substituents such as the $-OCH_3$ group. For all three rate constants k_3, k_4, and k_5, linearity can be observed with a negative slope (Fig. 5.2). A negative slope is typical for reactions in which the aromatic compound reacts as the nucleophile (Johnson, 1980). The steepest line was found for reaction 5.5 what means that this reaction is most susceptible to the influence of substituents. k_5 varied between 400 $M^{-1}s^{-1}$ (p-cyanophenol) and 7 x 10^8 $M^{-1}s^{-1}$ (p-cresol and p-methoxyphenol).

For reaction 5.3, the rate constant increased only for the compounds with $\sigma_p > 0$ and remained constant for the two other compounds (see Fig. 5.2). This effect might be the result of the change of the rate-determining step in the reaction H_2OI^+ + phenol. For compounds with $\sigma_p > 0$, the electron density of the aromatic system influences the rate-determining step. For the compounds with $\sigma_p < 0$, the rate-determining step is probably not affected by the electron density of the aromatic system. For all compounds, we found $k_5 > k_3 > k_4$. The observation that $k_5 > k_4$ can be explained by the increased nucleophilicity of the phenolate compared to the phenol. The fact that $k_3 > k_4$ can be explained by the increased electrophilicity of H_2OI^+ compared to HOI.

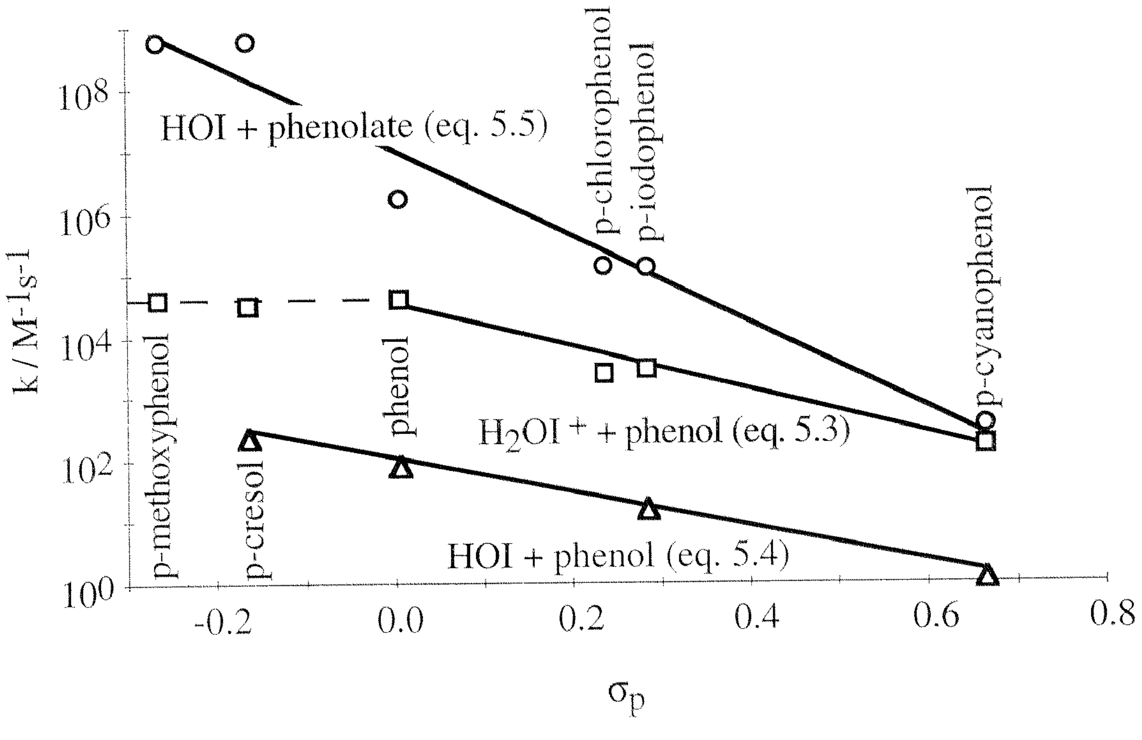

Figure 5.2: Dependence of the calculated rate constants for the reaction of HOI and H_2OI^+ with p-substituted phenols on the Hammett coefficient σ_p (Johnson, 1980). $r^2 = 0.966$ (eq. 5.3), $r^2 = 0.965$ (eq. 5.4), $r^2 = 0.966$ (eq. 5.5)

The reactions of HOI with substituted phenols are significantly faster than the corresponding reactions of HOCl. p-Cresol reacts 2’000-20’000 times faster with HOI than with HOCl (k_4^{HOCl} = 0.14 $M^{-1}s^{-1}$; k_5^{HOCl} = 30’000 $M^{-1}s^{-1}$; Gallard, 1999). The difference between HOCl and HOI is smaller for the more electrophilic phenols such as p-cyanophenol (factor 4-60: k_4^{HOCl} = 0.025 $M^{-1}s^{-1}$; k_5^{HOCl} = 90 $M^{-1}s^{-1}$; Gallard, 1999). HOI can therefore compete with HOCl for the reaction with phenols even if HOCl is present in high excess relative to HOI.

Formation of CHI_3 from Phenols. The formation of CHI_3 was measured at pH = 7.0 and 9.0 with an initial concentration of 6 μM HOI and 1 μM phenol or resorcinol. Both compounds resulted in CHI_3 formation but resorcinol yielded much more CHI_3 (normalized to HOI exposure) than phenol. For resorcinol, 4 to 7 % of the C atoms were incorporated into CHI_3 after 6 h. This corresponds to 0.25 to 0.4 mol CHI_3 per mol resorcinol. The HOI consumption of both compounds occurred mainly in the first 2 h and amounted to 2 mol HOI per mol phenol and 5 mol HOI per mol resorcinol.

To be able to compare the results of the model solutions with natural waters (see below), the CHI_3 yield q with respect to the exposure to HOI ($\int[HOI]dt$) and the initial DOC concentration (in mol/L C) was calculated according to eq. 5.6. This yield is a measure for the concentration of CHI_3 which was formed as a result of a certain HOI exposure on a certain DOC concentration during the time t.

$$q = \frac{[CHI_3]}{\int[HOI]dt[DOC]} \qquad \text{or} \qquad \frac{[CHI_3]}{[DOC]} = q\int[HOI]dt \qquad (5.6)$$

Figure 5.3 shows a representation of the experimental data expressed in terms of eq. 5.6 where $[CHI_3]/[DOC]$ is the iodoform formation normalized to carbon. q can be read as the slope of a linear fit of the data. For

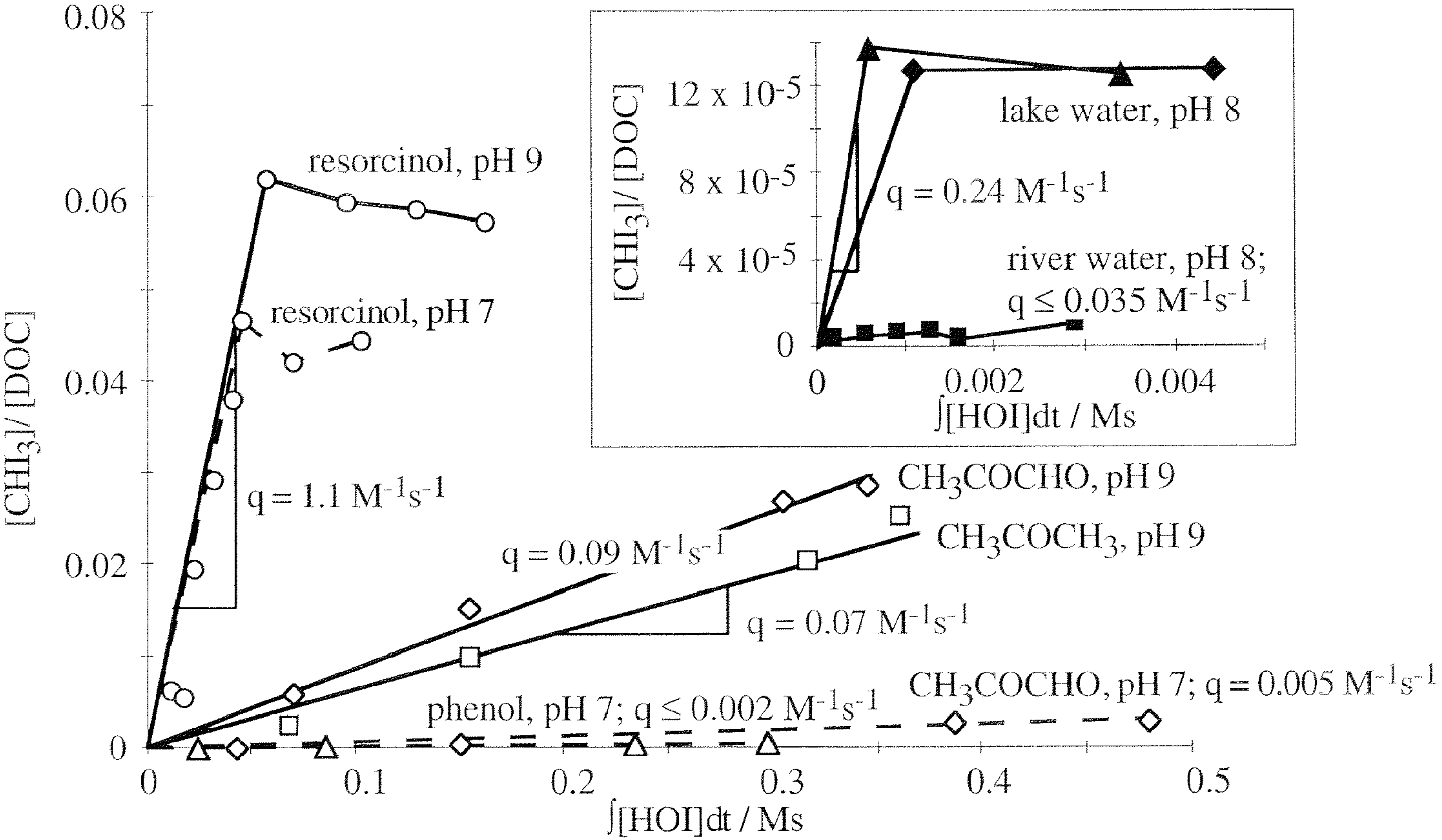

Figure 5.3: Formation of CHI$_3$ in model and in natural waters (data transformed according to eq. 5.6). Model compounds: resorcinol (open circles), acetone (open squares), methylglyoxal (open diamonds), and phenol (open triangles) at pH = 7 (dashed lines) and pH = 9 (solid lines). Inset: Natural waters; Lake Zurich, 1 mg/L NH$_2$Cl (full triangles) and 0.5 mg/L NH$_2$Cl (full diamonds); Seine river, 0.5 mg/L NH$_2$Cl (full squares); pH = 8.

phenol (triangles), this value is lower than 0.002 $M^{-1}s^{-1}$ at pH = 7. At pH = 9, no CHI_3 formation could be detected. For resorcinol (circles), it reaches a maximum value of 1.1 $M^{-1}s^{-1}$ during the first 6 h ($\int[HOI]dt < 0.05$ Ms). This steep increase corresponds to a CHI_3 formation of e.g. 15 nM/h or 6 µg/L/h in a solution of 10 µg/L HOI and 1 mg/L resorcinol.

Consumption of HOI by α-Methyl Carbonyl Compounds. The consumption of HOI by α-methyl carbonyl compounds was investigated in batch reactors under pseudo-first-order conditions. Since 1822, the reaction of iodine with these compounds is known as the 'iodoform reaction' (Fuson & Bull, 1934). A reaction scheme for this is presented in eq. 5.7:

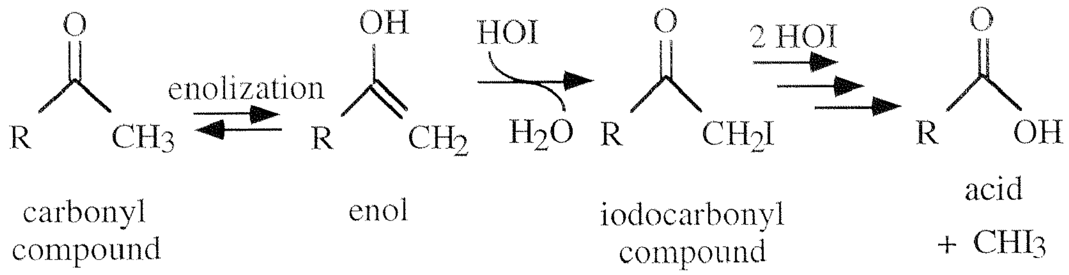

(5.7)

According to eq. 5.7, HOI does not react directly with the carbonyl compound but only with the enol. The formation of the enol (enolization) can be catalyzed by several species: H^+, H_2O, and OH^-. The halogenation of an α-methyl carbonyl compound proceeds three times until the methyl group is transformed into a triiodomethyl group. The triiodocarbonyl compound then hydrolyzes with the formation of CHI_3 and the corresponding acid (RCOOH).

For the iodination reaction, either the enolization or the addition of HOI to the enol are rate-determining. If the enolization is rate-determining, the overall reaction rate depends only on the carbonyl compound concentration and the pH, but not on [HOI] and the rate law becomes zero-order in HOI (eq. 5.8). In this case, the HOI concentration decreases linearly with time. This can be seen in Fig. 5.4 (squares) which shows two possibilities for the HOI decrease by reaction with acetone. The other case (circles) will be discussed below. It was demonstrated previously that under certain conditions the enolization is the rate-determining step of the halogenation of carbonyl compounds because the rate constants of iodination and bromination reactions were equal. This shows that the halogen does not participate in the rate-determining step under the used conditions (Dubois & Toullec, 1971).

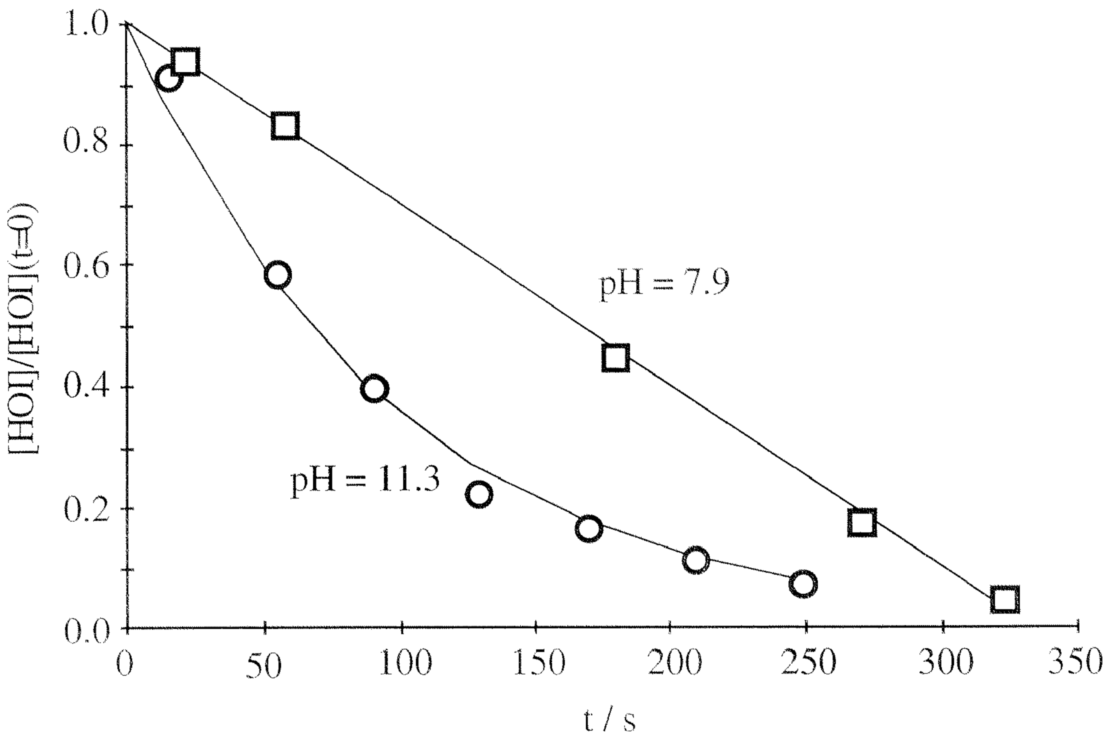

Figure 5.4: Decrease of HOI through reaction with acetone. Squares: pH = 7.9, 50 mM acetone, [HOI](t = 0) = 3.9 μM; Circles: pH = 11.3, 2 mM acetone, [HOI](t = 0) = 2.2 μM; Lines are least-squares fits.

At the pH values investigated in this study, OH^- and H_2O are the main catalysts for the enolization.

$$-\frac{d[HOI]}{dt} = k_{H_2O}[\text{ketone}] + k_{OH^-}[OH^-][\text{ketone}] \qquad (5.8)$$

Experimental results for the reaction of HOI with acetaldehyde, pinacolone, and acetone (at pH < 8.3) could be modeled with eq. 5.8. Acetate ($R = O^-$) was also investigated but no reaction could be detected. The calculated rate constants are presented in Table 5.2. In Fig. 5.5, the experimental data (symbols) is shown together with the fitted pH-dependence of the observed first-order rate constant (lines). Acetaldehyde is the most reactive of these compounds, pinacolone the least reactive. The electron-withdrawing character of R determines the rate of reaction.

The observed rate constants for the experiments HOI + phenols and α-methyl carbonyl compounds are presented in the Appendix C.

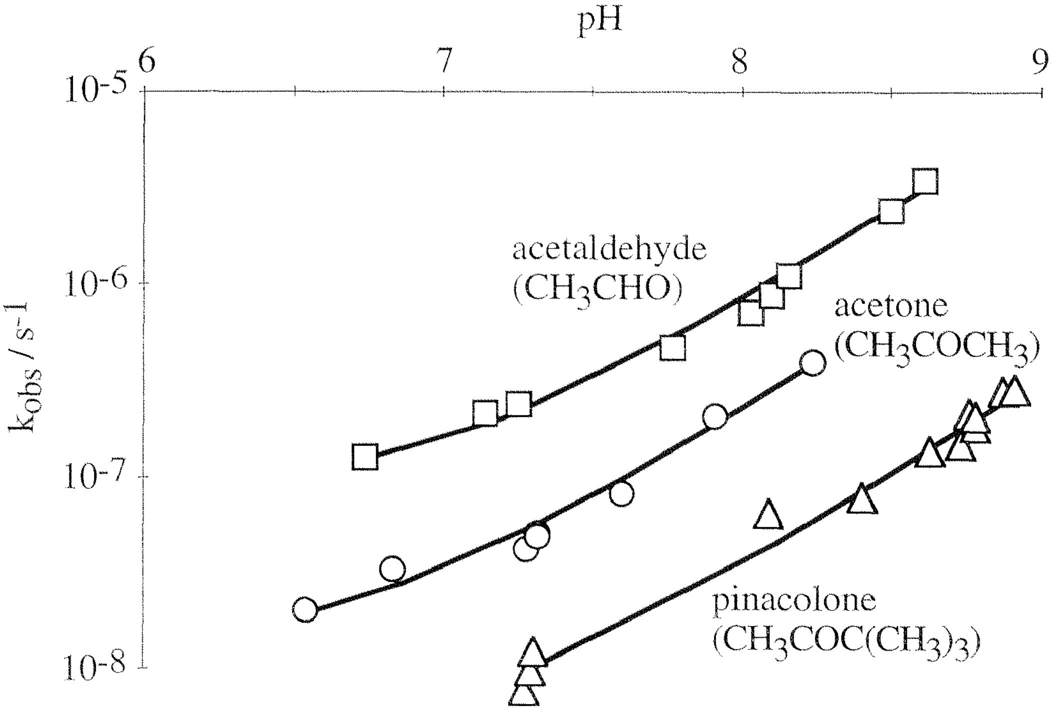

Figure 5.5: Observed first-order rate constants for the iodination of three α-methyl carbonyl compounds. Symbols are experimental data, lines are fits according to eq. 5.8.

Table 5.2 Rate Constants for the Reaction of α-Methyl Carbonyl Compounds with HOI

compound CH_3COR	R	pH range	mM buffer	[comp.] / mM	[HOI](t=0) / μM	n^a	observed rate constants
Acetaldehyde	H	6.8-8.6	1-2	0.3-10	2.2-2.9	10	$k_{H_2O} = 9\pm1 x10^{-8}\ s^{-1}$ $k_{OH^-} = 0.90\pm0.04\ M^{-1}s^{-1}$
Pinacolone	t-butyl	4.8-8.9	1-2	1-100	2-4	14	$k_{H_2O}= 4\pm2x10^{-9}\ s^{-1}$ $k_{OH^-} = 0.037\pm0.002\ M^{-1}s^{-1}$
Acetate	O^-	8.3-9.9	1	100-1000	2.0-2.3	5	$k_{H_2O}< 2x10^{-10}\ s^{-1}$ $k_{OH^-} < 3x10^{-6}\ M^{-1}s^{-1}$
Acetone	CH_3	6.0-8.3	1	31-64	1.7-5.5	9	$k_{H_2O} = 1.3\pm0.4x10^{-8}\ s^{-1}$ $k_{OH^-} = 0.25\pm0.03\ M^{-1}s^{-1}$
Acetone	CH_3	9.1-11.6	0-1	2.0-8.4	1.3-3.8	9	$k_6 = 2.5\pm1.0\ M^{-1}s^{-1}$ $k_7 = 3\pm1x10^3\ M^{-2}s^{-1}$
Methylglyoxal	CHO	3.9-9.1	1-2	0.03-2	0.9-4.5	19	$k_8 = 6\pm2\ x\ 10^2\ M^{-1.4}s^{-1}$; $a = 0.4\pm0.1$

a: n = number of kinetic experiments ([HOI] vs. t)

From the ratio of $k_{OH^-}:k_{H_2O}$, it can be calculated that at pH = 7, H_2O and OH^- have the same catalytic effect on the iodination of the three compounds acetaldehyde, pinacolone, and acetone. At higher pH values, OH^- is dominant. At lower pH values, H_2O is responsible for the major part of the catalysis which means that the observed rate constant does not depend on the pH. At even lower pH values, H^+ influences the reaction rate. However, this pH range was not investigated in the present study.

In the literature, a value of 0.52 $M^{-1}s^{-1}$ (k_{OH^-}) is given for the hydroxide-catalyzed enolization of acetone (Bell & Longuet-Higgins, 1946). This compares quite well with our findings ($k_{OH^-} = 0.25\ M^{-1}s^{-1}$).

When the pH increases, the rate of the iodination increases because of enhanced OH^- catalysis. At a certain pH however, the enolization becomes fast enough to be comparable to the addition of HOI to the enol. In this case, both the enolization and the addition of HOI influence the overall reaction rate. At even higher pH, the addition of HOI to the enol becomes the rate-determining step and the reaction rate is first-order in HOI. In this case, the keto-enol equilibrium can be kinetically treated as a fast pre-equilibrium. This has been observed for acetone at pH > 9.1. Figure 5.4 shows an example for the iodination of acetone at pH = 11.3 where the first-order kinetics in HOI result in an exponential [HOI] decrease. From the dependence of the observed second-order rate constant of HOI + acetone on the pH (9.1 < pH < 11.6), it can be concluded that two reactions significantly contribute to the overall decrease of HOI, HOI + enol and OI^-+ enolate (eq. 5.9).

$$-\frac{d[HOI]}{dt} = k_6[HOI][acetone] + k_7[OI^-][OH^-][acetone] \qquad (5.9)$$

Inclusion of either of the two reactions HOI + enolate or OI^- + enol did not reflect the pH-dependence of the observed second-order rate constant correctly.

The pH ranges for the two kinetic regimes which are given in this study are not absolute. They depend on the ratio of [acetone] to [HOI]. At high ratios [acetone]:[HOI], the HOI addition is more likely the rate-determining step whereas at low [acetone]:[HOI] ratios, the enolization tends to be rate-determining.

The kinetics of the reaction of HOI with methylglyoxal were also investigated. However, the results could not be fitted with either of the two equations 5.8 or 5.9. The reaction was first-order in HOI and in methylglyoxal. The observed rate constant increased by a factor of a = 0.4±0.1 when increasing the pH by one unit. The data was therefore fitted by equation 5.10:

$$-\frac{d[\mathrm{HOI}]}{dt} = k_8[\mathrm{HOI}][\mathrm{methylglyoxal}][\mathrm{OH}^-]^a \qquad (5.10)$$

Formation of CHI_3 from α-Methyl Carbonyl Compounds. The formation of CHI_3 was measured at pH = 7 and 9 with initial concentrations of 6 μM HOI and 1 μM acetone or methylglyoxal. At pH = 7, acetone yielded no CHI_3 and methylglyoxal resulted in a small CHI_3 formation. At pH = 9, higher CHI_3 concentrations were found. In Fig. 5.3, the experimental data is plotted according to eq. 5.6. At pH = 9, the CHI_3 formation yield q is in the range of 0.05 to 0.1 $M^{-1}s^{-1}$ for both acetone (squares) and methylglyoxal (diamonds). At pH = 7, q is below 0.001 $M^{-1}s^{-1}$ for acetone and about 0.005 $M^{-1}s^{-1}$ for methylglyoxal. For acetone, CHI_3 formation is about 25 % of the value which was expected from the rate constant for HOI consumption. This difference could be due to a retardation of the overall reaction by the final hydrolysis of triiodoacetone. For methylglyoxal, the comparison between the rates of HOI consumption and CHI_3 formation is not possible. HOI consumption was first-order in HOI whereas the formation of CHI_3 was zero-order in HOI. Therefore, the rate-determining step which leads to CHI_3 is different from the step in which HOI is consumed. The results of both acetone and methylglyoxal give an indication that the hydrolysis is the rate-determining step in CHI_3 formation.

Another experiment for the iodination of acetone was performed at pH = 9 in excess of acetone (1-1000 μM) over HOI (1 μM). Under these conditions, the initial HOI addition reacted according to a second-order behavior with a rate constant of 1 $M^{-1}s^{-1}$. This experiment was performed to get information about the ratio of the rate constants of the first, second, and third iodination step as well as the hydrolysis of triiodoacetone. In general, carbon double bonds are more stable when they have more substituents. The additional iodine-atom in iodoacetone would therefore increase the stability of the enol of iodoacetone when compared to acetone and accelerate the second iodination step. Our experimental results support this reasoning. After 16 h reaction, CHI_3 was found even if acetone was in a 1000-fold excess over HOI (see Fig. 5.6, circles). The highest CHI_3 concentration (0.2 μM) was found for a 30-fold excess of acetone. The observed product pattern was also obtained by modeling the rate constant for the second iodination step. The calculated CHI_3 formation for three values of this rate constant is shown in Fig. 5.6 (lines). Best fit resulted when assuming a rate constant of 30 $M^{-1}s^{-1}$ for the second iodination step what is 30 times faster than the first iodination step. The third iodination step required a second-order rate constant of at least 10^3 $M^{-1}s^{-1}$. The hydrolysis of triiodoacetone was at least 10^{-4} s^{-1} to explain our results. Such a rate constant can e.g. be found for the hydrolysis of an ester such as $CH_3COOCH=CH_2$ (Mabey & Mill, 1978).

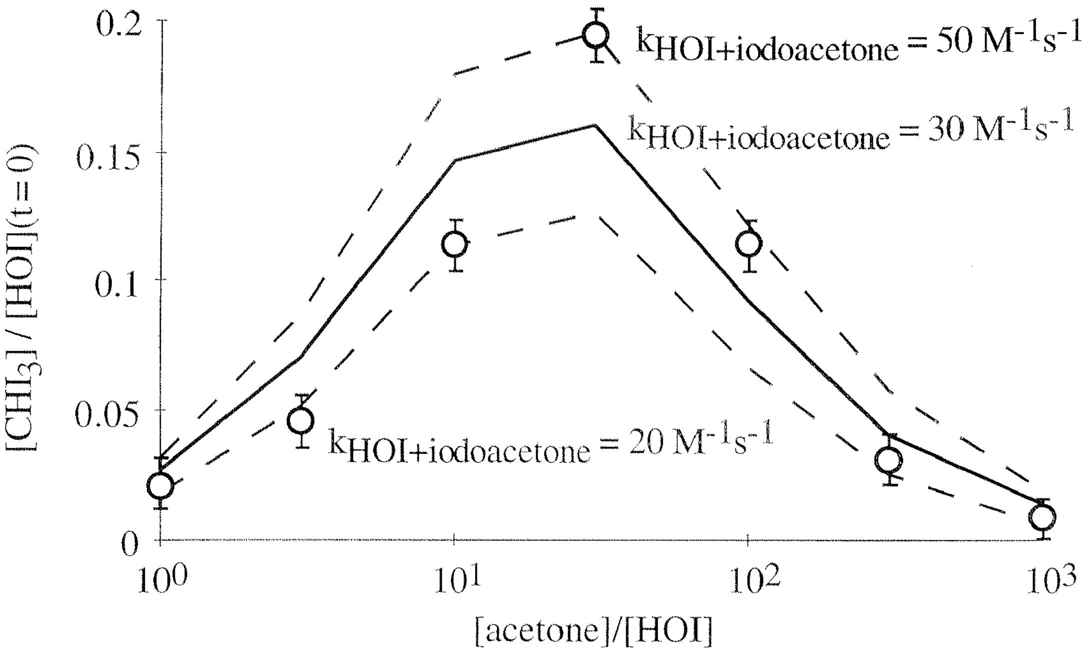

Figure 5.6: Formation of CHI_3 (circles) from acetone and HOI (1 μM) at pH = 9. Lines: Model with varying rate constants for the reaction HOI + iodoacetone.

Consumption of HOI by Other Model Compounds. Besides phenols and carbonyl compounds, other organic model compounds (allyl alcohol, glucosamine, glycine, toluene, and oxalate) were tested for their reactivity toward HOI. Only allyl alcohol and glucosamine showed a measurable reactivity (Table 5.3). For the other compounds, the maximum observed second-order rate constants are given.

The observed rate constant for the reaction of HOI with allyl alcohol, an alkene, increased by a factor of 10 when the pH was decreased by one unit. This behavior was explained by assuming that H_2OI^+ was the reactive iodine species although it was a minor species in the experiments (pH = 6.2 - 8.2). The rate constant k_9 for the reaction H_2OI^+ + allyl alcohol was calculated to be 1.8 x $10^7\ M^{-1}s^{-1}$ (Table 5.3). The half-life for HOI at pH = 7 and a concentration of 1 mg/L of allyl alcohol is about 6 h.

Table 5.3 Rate Constants for the Reaction of Model Compounds with HOI

compound	pK_a	pH range	mM buffer	mM	[HOI](t=0) / μM	n^c	observed rate constants
Allyl alcohol		6.2-8.2	0.5-1	0.25-10	1.5-4.0	11	$k_9 = 1.8 \pm 0.4 x 10^7$ $M^{-1}s^{-1}$
Glucosamine	7.58^a	5.5-9.2	1	3-50	1.8-2.5	11	$k_{10} = 0.27 \pm 0.07$ $M^{-1}s^{-1}$
							$k_{11} = 7 \pm 3 x 10^{-3}$ $M^{-1}s^{-1}$
Glycine	9.78^b	6.1-9.0	0-1	2-1000	0.6-2.5	10	$k_{obs} < 0.1$ $M^{-1}s^{-1}$
Oxalate	1.25, 4.27^b	6.0-8.1	1	10-200	1.7-2.2	7	$k_{obs} < 0.1$ $M^{-1}s^{-1}$
Toluene		4.1-7.3	1	2-4	1.0-2.9	5	$k_{obs} < 1$ $M^{-1}s^{-1}$

a: this work; b: Dean, 1985; c: n = number of kinetic experiments ([HOI] vs. t)

The observed second-order rate constant for the reaction of HOI with glucosamine increased by a factor 10 per pH-unit at pH < 7.5. At pH > 8.5, the rate constant did not depend on the pH any more. This pH-dependence corresponds to the speciation of glucosamine which changes at these pH values ($pK_a = 7.58$). Therefore, glucosamine and protonated glucosamine both reacted with HOI. k_{10} in Table 5.3 is the rate constant for the reaction HOI + glucosamine and k_{11} is the rate constant for the reaction HOI + protonated glucosamine.

5.3.2 Consumption of HOI and Formation of THMs and IO_3^- During Disinfection of Natural Waters

The kinetics of the consumption of HOI and of the formation of iodine-containing disinfection by-products (IO_3^-, I-THMs) was measured during the first 24 h of the oxidation of two natural waters (Lake Zurich, Switzerland and Seine river, France) spiked with I^-. The waters were treated under varying conditions: the standard experiment was performed at pH = 8.0, 0.5 mg/L Cl_2, and 400 nM I^- (50 μg/L). Additional experiments were performed in which one of these parameters was changed. Either was the pH reduced to 6.2, or the chlorine dose was increased to 1 mg/L Cl_2, or the I^- concentration was reduced to 80 nM (10 μg/L), or O_3 or chloramine were used instead of chlorine.

Figure 5.7 shows the evolution of IO_3^-, CHI_3, total I in I-THMs, and other organic I together with the decrease of HOI and chlorine in the standard experiment in lake water. For the calculation of the parameter I in THMs, the concentrations of the single I-THMs are multiplied with the number of iodine atoms they contain. The concentration of other organic I was calculated as the difference of the total iodine (50 μg/L, 400 nM) and the sum of HOI, IO_3^- and the I in THMs. HOI decreased very quickly. More than 90 % had disappeared after 30 min. After 1 h, the IO_3^- concentration had reached the half of its final value. For the I in the THMs and for CHI_3, this time was longer (2 h). The comparison of the development of the concentrations of I in THMs and organic I which is not in THMs shows that the sum of them remains constant during the whole experiment. This shows that the reaction of HOI with the NOM is finished after a short time. After the fast initial iodination however, the I-THMs and especially CHI_3 are not released immediately. As speculated above (CHI_3 formation from acetone), the hydrolysis of the trihalomethyl group could be a slower, rate-determining process in I-THM formation. The formation of iodine-containing disinfection by-products is finished after

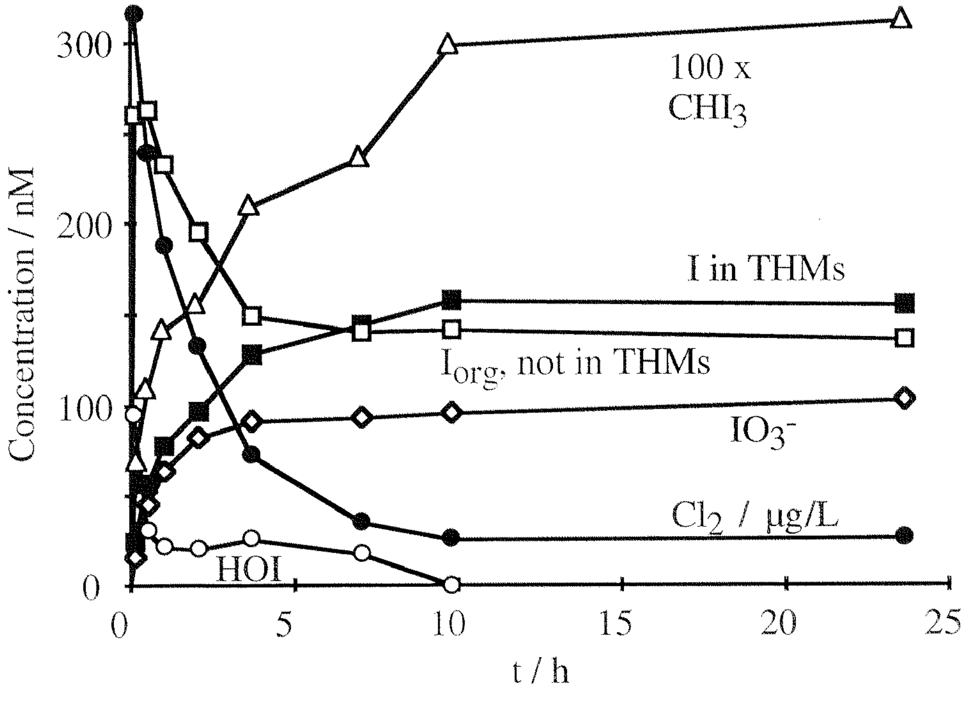

Figure 5.7: Consumption of HOI and chlorine together with the formation of IO_3^-, CHI_3, the sum of I in I-THMs, and I_{org} in a lake water (400 nM I^- (50 µg/L), 15 µg/L Br^-, 1.3 mg/L DOC, 0.5 mg/L Cl_2, pH = 8.0).

10 h. After that time, approximately a third of the initial iodine yielded IO_3^-. Another third was incorporated into THMs and another third into NOM but not into THMs. This distribution depends strongly on the oxidation conditions.

Figure 5.8 shows the final concentrations (24 h after the oxidant addition) of IO_3^-, CHI_3, the total iodine which was incorporated into THMs, the total concentrations of the six I-THMs, and the total concentrations of the four classical THMs. In the following, the results presented in Fig. 5.8 will be discussed together with results of some additional experiments:

Product distribution: IO_3^-, I-THMs, and Other Iodoorganic Compounds. Both IO_3^- and I-THMs were formed in all experiments with exception of the ozonation (Fig. 5.8, exp. E; no I-THMs). The highest IO_3^- concentrations were found in the ozonation (exp. E) and in a chlorination (exp. B) where 90 % and 75 %, respectively of the I^- were transformed to IO_3^-. IO_3^- formation increased with the chlorine dose (see exp. A vs. B or F vs. G). The lowest IO_3^- concentrations were found in chloramination experiments (exp. C, D, H) where IO_3^- formation accounted for less than 3 % of the total iodine.

The highest CHI_3 formation (16 nM CHI_3) was observed when using chloramine (exp. C). 47 nM I or 12 % of the initial I^- (400 nM) were incorporated into CHI_3. CHI_3, $CHClI_2$, $CHCl_2I$, and CHBrClI were found in several experiments but $CHBr_2I$ or $CHBrI_2$ were never detected. The Br^- concentration in the investigated waters was too low to lead to a significant incorporation of bromine into the THMs. CHBrClI was the only bromine-containing I-THM which was detected with a maximum concentration of 24 nM in the chlorinated river water (exp. G).

The sum of IO_3^- and I-THMs accounted for 20 to 90 % of the total iodine in the water. Since HOI had always disappeared after 24 h, iodine which is not found in the I-THMs or as IO_3^- was present as iodoorganic

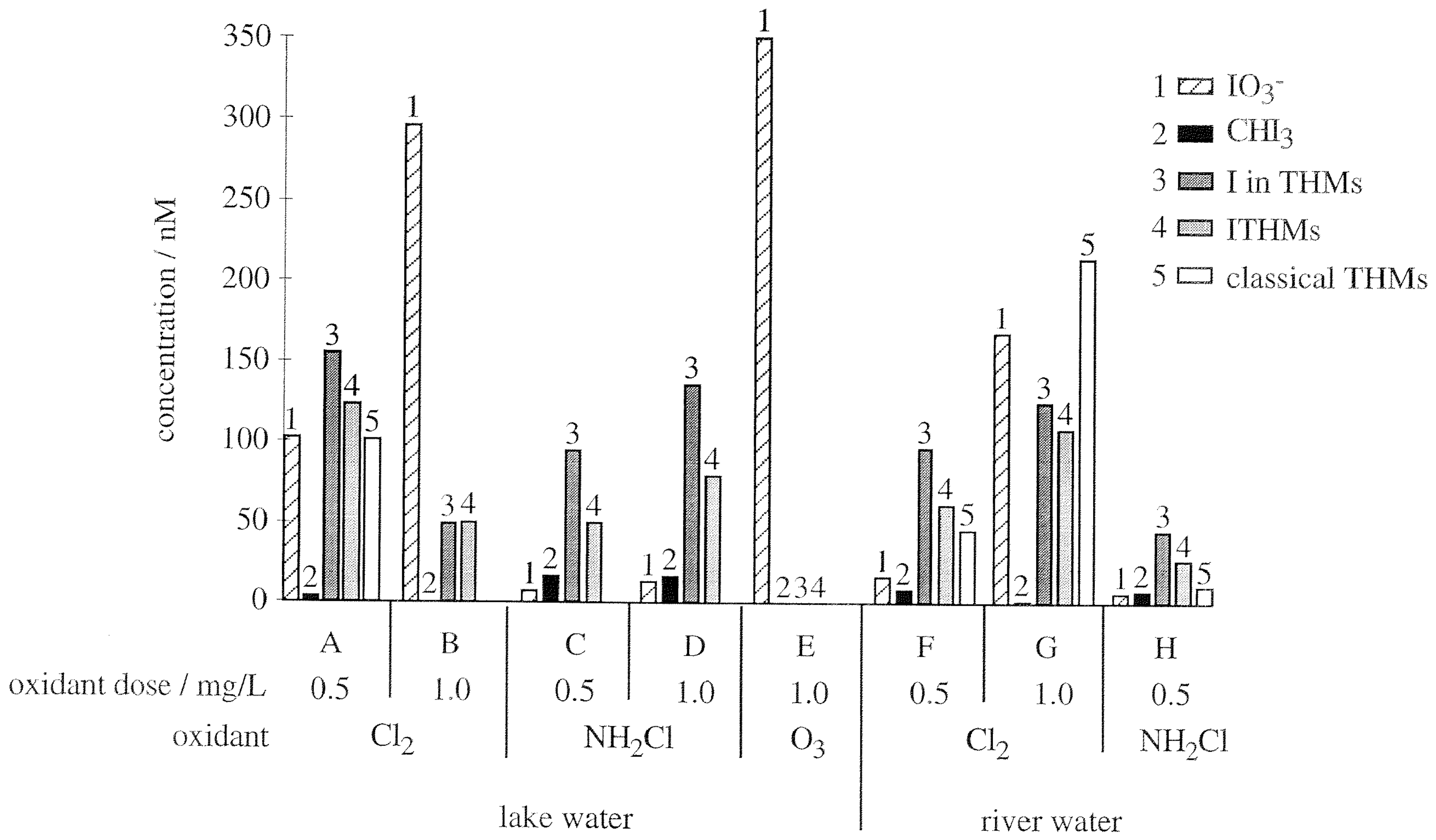

Figure 5.8: Formation of disinfection by-products in the oxidation of natural waters (24 h after addition of the oxidant). pH = 8.0, I^- = 400 nM (50 µg/L). The concentrations of the classical THMs were not measured in the experiments B-E.

compounds other than I-THMs. Low amounts of these compounds (< 30 % of total iodine) were formed during ozonation and chlorination at high dose (exp. B, E, G). Higher concentrations (≥ 60 % of total iodine) were found in the chloramination experiments (exp. C, D, H). This effect can be explained by the fact that HOI is the only halogenating agent in a chloramine-based oxidation. Since the NOM is in excess over HOI, many THM-precursor sites are not fully halogenated in the chloramination. Only in the presence of chlorine can the halogenation of the THM-precursor sites be completed and I-THMs released.

Chloramine vs. Free Chlorine. The smaller chemical reactivity of chloramine compared to chlorine leads to two general differences in the formation of iodine-containing disinfection by-products. Firstly, chloramine is not capable to oxidize HOI to IO_3^- whereas this reaction is significant for chlorine (chapter 4). This explains the higher IO_3^- formation in chlorinations compared to chloraminations (Fig. 5.8). Hence, HOI has a higher life-time in chloramination processes which leads to an increased reaction time with NOM. Secondly, the competition between chlorine and iodine for the incorporation into the THMs is much higher in the presence of chlorine than in the presence of chloramine because of the higher reactivity of HOCl compared to NH_2Cl. This shifts the product distribution from CHI_3 in chloraminations to the mixed I-THMs in chlorinations. Chloramination resulted in 16 nM CHI_3 and 34 nM mixed I-THMs (exp. C). Under the same conditions, chlorine induced the formation of 3 nM CHI_3 and 119 nM mixed I-THMs (exp. A).

Chlorine Concentration. In the chlorinations at 0.5 mg/L, 4 % (exp. F) and 26 % (exp. A) of the iodine were transformed to IO_3^-. A higher chlorine dose resulted in higher IO_3^- production. In the chlorinations at 1 mg/L, 43 % (exp. G) and 75 % (exp. B) of the total iodine were found as IO_3^-. A lower IO_3^- yield was found in the water with the higher

DOC (river water). Because of the lower chlorine stability, less HOI can be oxidized to IO_3^-. In addition, the reaction of HOI with the NOM is more important in the river water than in the lake water. The distribution among the I-THMs was also affected by the chlorine dose. In the river water, 8 nM CHI_3 and 54 nM mixed I-THMs were detected for 0.5 mg/L Cl_2 (exp. F). At a chlorine dose of 1 mg/L, $[CHI_3]$ decreased to 1 nM and the mixed I-THMs increased to 107 nM (exp. G). In the lake water, chlorination with 0.5 mg/L resulted in 3 nM CHI_3 and 119 nM mixed I-THMs (exp. A) whereas no CHI_3 but 46 nM mixed I-THMs were formed for 1 mg/L of chlorine (exp. B). For the prevention of medicinal taste and odor caused by CHI_3, an increased chlorine dose can be a reasonable solution. A drawback of that is the enhanced formation of the classical THMs. The increase of the chlorine dose from 0.5 to 1 mg/L led to an increase in the classical THMs from 45 nM (5.8 μg/L) to 213 nM (29 μg/L) in the river water (exp. F, G).

pH Dependence. A possibility to prevent the formation of both classical and I-THMs is to decrease the pH. At $pH = 6.2$, CHI_3 formation decreased by 75 - 85 % compared to $pH = 8.0$ and $CHCl_3$ formation decreased by 30 - 40 % for the same chlorine dose and stability (data not shown). In Fig. 5.3, the same effect can be observed for resorcinol, methylglyoxal, and acetone. This could be due to a pH-dependent distribution of halogenated organic products. Reckhow & Singer (1984) show that for increasing pH ($5 < pH < 11$), $CHCl_3$ formation increased but formation of trichloroacetic acid decreased. This behavior was explained by a competition of two reactions of the trichlorocarbonyl intermediate. At low pH, oxygenation of the carbonyl group by HOCl and the resulting formation of trichloroacetic acid is favored whereas at high pH, hydrolysis by OH^- leads to $CHCl_3$.

I^- Concentration. All the reported cases of CHI_3 formation in a drinking water occurred at initial I^- concentrations ≥ 50 μg/L. Therefore, we used a concentration of 50 μg/L I^- for most of our experiments. However, such high I^- concentrations are an exception in natural waters. Usually, they lie below 10 μg/L (Fuge & Johnson, 1986). To assess the significance of CHI_3 formation during chlorination at lower I^- concentrations, experiments with 10 μg/L I^- (80 nM) were conducted both in the river and in the lake water (pH = 8.0, 0.5 mg/L Cl_2). Mixed I-THMs, but no CHI_3 could be detected under these conditions. At low I^- concentrations, the competition between HOI and HOCl for the NOM sites favors HOCl. However, $CHCl_2I$ was found at concentrations of up to 26 nM what accounts for 33 % of the total iodine. The percentage of total iodine which is incorporated into THMs or present as IO_3^- does not depend on the initial I^- concentration. In contrast, the distribution of I-THMs is shifted from highly iodinated THMs such as CHI_3 for high $[I^-]$ to less iodinated THMs such as $CHCl_2I$ for low $[I^-]$.

Ozonation. IO_3^- was the only detected iodine-containing by-product in the ozonation experiment (exp. E). However, not all the I^- was transformed to IO_3^- despite of the fast oxidation of HOI by O_3 ($t_{1/2} < 4$ s) (chapter 4). Organic compounds which are highly reactive toward HOI successfully competed with O_3. Such competitors could be phenolic compounds which have a higher apparent rate constant with HOI than O_3. To test this hypothesis, we selected p-methoxyphenol at pH = 6.3 (O_3 + HOI: 3.6×10^4 $M^{-1}s^{-1}$, p-methoxyphenol + HOI: 7.6×10^4 $M^{-1}s^{-1}$). To compete with O_3 which is in excess over the NOM, such a compound has to be present at quite high concentrations. If the p-methoxyphenol concentration is 7 times lower than $[O_3]$, it can react with 25 % of the HOI and therefore reduce the IO_3^- formation to 75 % of the initial $[I^-]$. This was confirmed experimentally (20 μM O_3, 3 μM p-methoxyphenol, 0.4 μM I^-, pH = 6.3). Only 85 % of the initial I^- was found as IO_3^- under these conditions.

Incorporation of Iodine and Chlorine into THMs. Because of the big differences in initial concentrations between HOI (0.4 μM) and HOCl (7 μM) in chlorination processes, it is necessary that iodine reacts much faster with THM-precursors than chlorine to lead to I-THM formation. As shown above, the reaction of HOI with phenols can be 4 to 20'000 times faster than the corresponding reaction of HOCl. This difference in reactivity led to similar incorporation of iodine and chlorine into THMs in the river water. In this experiment, $\int[\mathrm{HOCl}]dt$ was about 15 times higher than $\int[\mathrm{HOI}]dt$. HOI therefore reacted about 15 times faster than HOCl with the THM-precursor groups in the river water.

Apparent Rate Constant HOI + NOM. In the experiments with chloramine as the oxidant, only the NOM reacted with HOI. The absence of the oxidation of HOI by the oxidant allowed the quantification of the kinetics of the reaction of HOI with the NOM. HOI consumption occurred in two phases: an initial, fast (t < 5 min) followed by a second slower process.

After 5 min, only 17 - 34 % of the initial I^- could be found as HOI in the exp. C, D, and H. However, the I^- oxidation by chloramine was not complete after 5 min ($k_{I^- + NH_2Cl} = 240\ M^{-1}s^{-1}$; Kumar et al., 1986). At this point of the reaction, only 40 % (exp. C and H) and 64 % (exp. D) of I^- had been oxidized to HOI. Taking into account the incomplete HOI formation, the rate constants for HOI + NOM (on a C-atom base) in this initial phase were determined as 10 - 90 $M^{-1}s^{-1}$ or 0.7×10^{-6} - $6 \times 10^{-6}\ s^{-1}$ by kinetic modeling. By comparison of these rate constants with the rate constants of HOI with model compounds at pH = 8 (phenols: 3×10^{1} - $6 \times 10^{5}\ M^{-1}s^{-1}$, methylglyoxal: 0.8 $M^{-1}s^{-1}$, glucosamine 0.2 $M^{-1}s^{-1}$, allyl alcohol: 0.04 $M^{-1}s^{-1}$, α-methyl carbonyl compounds: 6×10^{-9} - $5 \times 10^{-7}\ s^{-1}$ on a C-atom base), the observed rate constants in natural waters can only be explained by the presence of phenolic entities in the NOM but not by other compounds.

In a second phase of the reaction ($t > 5$ min), HOI consumption was much slower. Since the decrease of HOI was first-order, it was possible to fit a rate constant for the reaction of HOI with the NOM. The value of this rate constant was 3×10^{-5} $Lmg^{-1}s^{-1}$ in the lake water and 10^{-5} $Lmg^{-1}s^{-1}$ in the river water. The corresponding half-life of HOI was about 5 h for both waters. On a C-atom base, the rate constants amount to 0.4 and 0.1 $M^{-1}s^{-1}$. These values describe the reaction of HOI with NOM_1 which leads to iodoorganic compounds such as I-THMs (eq. 5.11).

$$HOI + NOM_1 = I\text{-}NOM \qquad (5.11)$$

$$HOI + NOM_2 = I^- + NOM_{2,ox} \qquad (5.12)$$

According to eq. 5.12, HOI can also be reduced to I^- by NOM_2. However, this reaction has no influence on the kinetics of the HOI decrease since the formed I^- is quickly reoxidized to HOI by chloramine. The kinetic constants for the reaction of HOI with NOM can again be compared with apparent second-order rate constants of model compounds mentioned above. If the NOM was composed of 12-50 % of methylglyoxal, the observed reaction in the natural water could be explained with this compound. Since this percentage is very high, it is quite unlikely that carbonyl compounds contribute significantly to the HOI consumption and the resulting I-THM formation in these waters. Here again, phenolic entities as part of the NOM could account for the experimental results.

Yield of CHI_3 Formation. CHI_3 formation yield q according to eq. 5.6 was also calculated for the natural waters (see inset Fig. 5.3). Only the experiments with chloramine were taken into consideration where CHI_3 formation was less competed by the formation of mixed I-THMs. In the lake water, q reached a value of ≥ 0.12 $M^{-1}s^{-1}$ for 0.5 mg/L

NH_2Cl (diamonds in inset Fig. 5.3) and $\geq 0.24\ M^{-1}s^{-1}$ for 1.0 mg/L NH_2Cl (triangles in inset Fig. 5.3). Since the fast initial phase of the CHI_3 formation (< 2 h) was not recorded in these experiments, q values can in reality be even higher than that. However, they are higher than what has been achieved with the model carbonyl compounds or with phenol. Only resorcinol yielded enough CHI_3 to account for the results from the lake water. In the river water (squares in inset Fig. 5.3), q was 0.002 to 0.035 $M^{-1}s^{-1}$. The highest values were found at the beginning of the experiment. The observed q values can principally be explained by methylglyoxal or acetone, but only if they account for more than 35 % of the NOM. Since this percentage is quite high, it is more likely that the phenolic groups in the NOM account for the observed CHI_3 formation in the river water.

Conclusions. The experiments in natural waters show that the formation of I-THMs and especially CHI_3 is highly influenced by the disinfectant. Whereas no I-THMs could be detected in the ozonation experiment, chlorine and chloramine induced the formation of these compounds. The main competition reaction to the formation of I-THMs is the formation of IO_3^-. This reaction is important in ozonation processes and in chlorination processes at high doses. Chloramine did not result in IO_3^- formation. Since this competition reaction did not take place in chloramination processes, CHI_3 formation occurred in significant amounts. In the presence of chlorine, the incorporation of chlorine into THMs which resulted in formation of mixed I-THMs such as $CHCl_2I$ was another competition reaction to the formation of CHI_3.

The kinetics of HOI consumption in naturals waters both in the initial fast phase and in the second, slower phase can be explained by phenols but not by carbonyl compounds. The comparison of the CHI_3 formation yields for natural and model waters further supports the hypothesis that carbonyl compounds do not play a key role in CHI_3 formation in oxidative drinking water treatment. Among the compounds which were investigated in this study, only phenolic entities can explain both the observed consumption of HOI and the formation of CHI_3 in natural waters.

5.3.3 Oxidation Kinetics of I-THMs by O_3 and $OH^{\bullet}$

The rate constants of the reactions of I-THMs with molecular O_3 and OH-radicals were determined. With these rate constants, it can be estimated to what extent these compounds are removed in an ozonation or advanced oxidation process.

To determine the rate constants of the reaction of O_3 with the I-THMs, 73 µM (3.5 mg/L) O_3 was added to an acidic solution (pH = 3, 1.2 mM H_3PO_4, 70 mM tert-butanol) of all six I-THMs (10 µg/L). tert.-Butanol is a scavenger for OH-radicals and prevents the radical-induced decay of O_3. After 2 h, no degradation of the I-THMs could be observed. The second-order rate constants of O_3 with the I-THMs were calculated as $< 2\ M^{-1}s^{-1}$ (Table 5.4).

To determine the rate constants of the reaction of OH-radicals with the I-THMs, 10 - 80 µM (0.5 - 4.0 mg/L) of O_3 were added to a basic (pH = 11) solution of 10 µg/L of the I-THMs. Under these conditions, O_3 was quickly transformed to OH-radicals. The initial step in this transformation is the reaction of OH^- with O_3 which leads to the formation of O_2 and HO_2^-. This reacts with another O_3 to HO_2/O_2^- and O_3^-. O_2^- reacts with O_3 and yields O_3^- and O_2. After protonation, O_3^- decays to OH-radicals and O_2. These reactions are described in more details by Hoigné (1998). The decrease of I-THMs in the experiment was measured relative to p-chlorobenzoic acid (pCBA) which does not react with molecular O_3 but with OH-radicals. The rate constant for the reaction of OH-radicals with pCBA is $5.0 \pm 0.8 \times 10^9\ M^{-1}s^{-1}$ (Neta & Dorfman, 1968). The rate constants for the I-THMs could be determined by decrease relative to pCBA. All six I-THMs reacted with approximately the same rate constant (see Table 5.4). Therefore, the degradation of I-THMs during ozonation processes will be dominated by $OH^{\bullet}$.

Table 5.4 Rate Constants for the Reactions of I-THMs with O_3 and $OH^{\bullet}$

	k_{O_3} / $M^{-1}s^{-1}$	$k_{OH^{\bullet}}$ / $M^{-1}s^{-1}$
CHI_3	< 2	7±2 x 10^9
$CHClI_2$	< 2	8±2 x 10^9
$CHBrI_2$	< 2	7±1 x 10^9
$CHCl_2I$	< 2	8±2 x 10^9
$CHBr_2I$	< 2	7±1 x 10^9
CHBrClI	< 2	7±2 x 10^9

5.3.4 Stability of CHI_3 in Model and Natural Waters

Hydrolysis of the carbon-iodine bond is a process which can possibly lead to a removal of halogenated compounds. The half-life of CHI_3 in distilled water (pH = 6-9, 1 mM phosphate) in ambered bottles was found to be higher than 100 d. In a natural water (Lake Zurich, pH = 8.2, 1.3 mg/L DOC), a CHI_3 half-life of 21 d was found. The difference could possibly be due to biological processes. In the literature, the half-life of CH_3I has been reported to be 113 d in distilled water and in sea water what compares well with our result in distilled water (Elliott & Rowland, 1995). Hydrolysis occurs in the range of months and is therefore not a significant pathway for the removal of CHI_3 at drinking-water relevant time scales.

References

Alexander, N.M. (1984). *Iodine*, in "Biochemistry of the Essential Ultratrace Elements", Ed.: E. Frieden. Plenum Press, New York; 33-53.

Amoore, J.E. (1986). *The chemistry and physiology of odor sensitivity.* Journal of the American Water Works Association, **78**(3): 70-76.

Andersen, F.A. (1995). *Final report on the safety assessment of sodium iodate.* Journal of the American College of Toxicology, **14**(3): 231-239.

Anselme, C., J.P. Duguet, and J. Mallevialle (1989). *Treatment of earthy-musty tastes and odors by ozone, hydrogen peroxide, and GAC filtration.* Proceedings of AWWA Seminar on Identification and Treatment of Taste and Odor Compounds; Los Angeles, California; 49-62.

Atwater, J.E., R.L. Sauer, and J.R. Schultz (1996). *Numerical simulation of iodine speciation in relation to water disinfection aboard manned spacecraft I. Equilibria.* Journal of Environmental Science and Health, **A31**(8): 1965-1979.

Awtrey, A.D. and R.E. Connick (1951). *The absorption spectra of* I_2, I_3^-, I^-, IO_3^-, $S_4O_6^{2-}$, *and* $S_2O_3^{2-}$. *Heat of the reaction* $I_3^- = I_2 + I^-$. Journal of the American Chemical Society, **73**: 1842-1843.

Bablon, G., W.D. Bellamy, M.M. Bourbigot, F.B. Daniel, M. Doré, F. Erb, G. Gordon, B. Langlais, A. Laplanche, B. Legube, G. Martin, W.J. Masschelein, G. Pacey, D.A. Reckhow, and C. Ventresque (1991). *Fundamental aspects,* in "Ozone in Water Treatment - Application and Engineering", Eds.: B. Langlais, D.A. Reckhow, and D.R. Brink; Lewis Publishers, Chelsea, Michigan; 11-132.

Bader, H. and J. Hoigné (1981). *Determination of ozone in water by the indigo method.* Water Research, **15**: 449-456.

Bartels, J.H.M., G.A. Burlingame, and I.H. Suffet (1986). *Flavor profile analysis: taste and odor control of the future.* Journal of the American Water Works Association, **78**(3): 50-55.

Barton, A.F.M. and G.A. Wright (1968). *Kinetics of the iodate-iodide reaction: catalysis by carboxylate and phosphate ions.* Journal of the Chemical Society A, 2096-2103.

Bell, R.P. and H.C. Longuet-Higgins (1946). *Kinetics of the halogenation of acetone in alkaline solutions.* Journal of the Chemical Society, 636-638.

Bell, R.P. and E. Gelles (1951). *The halogen cations in aqueous solution.* Journal of the Chemical Society, 2734-2740.

Bellar, T.A., J.J. Lichtenberg, and R.C. Kroner (1974). *The occurrence of organohalides in chlorinated drinking waters.* Journal of the American Water Works Association, **66**(12): 703-706.

Black, A.P., W.C. Thomas Jr., R.N. Kinman, W.P. Bonner, M.A. Keirn, J.J. Smith Jr., and A.A. Jabero (1968). *Iodine for the disinfection of water.* Journal of the American Water Works Association, **60**(1): 69-83.

Brass, H.J., M.A. Feige, T. Halloran, J.W. Mello, and D. Munch (1977). *The national organic monitoring survey: samplings and analyses for purgeable organic compounds*, in "Drinking Water Quality Enhancement through Source Protection", Ed.: R.B. Pojasek; Ann Arbor Science Publishers, Ann Arbor, Michigan.

Bruchet, A., K. N'Guyen, J. Mallevialle, and C. Anselme (1989). *Identification and behaviour of iodinated haloform medicinal odor.* Proceedings of AWWA Seminar on Identification and Treatment of Taste and Odor Compounds; Los Angeles, California; 125-141.

Bunn, W.W., B.B. Haas, E.R. Deane, and R.D. Kleopfer (1975). *Formation of trihalomethanes by chlorination of surface water.* Environmental Letters, **10**(3): 205-213.

Burger, J.D. and H.A. Liebhafsky (1973). *Thermodynamic data for aqueous iodine solutions at various temperatures.* Analytical Chemistry, **45**(3): 600-602.

Burlingame, G.A., R.M. Dann, and G.L. Brock (1986). *A case study of geosmin in Philadelphia's water.* Journal of the American Water Works Association, **78**(3): 56-61.

Buxton, G.V. and R.M. Sellers (1985). *Radiation-induced redox reactions of iodine species in aqueous solution.* Journal of the Chemical Society, Faraday Transactions, **81**: 449-471.

Campos, M.L.A.M., P.D. Nightingale, and T.D. Jickells (1996). *A comparison of methyl iodide emissions from seawater and wet depositional fluxes of iodine over the southern North Sea.* Tellus, **48B**(1): 106-114.

Cancho, B., F. Ventura, and M.T. Galceran (1999). *Solid-phase microextraction for the determination of iodinated trihalomethanes in drinking water.* Journal of Chromatography A, **841**(2): 197-206.

Chang, P.-S., L.-J. Chen, and Y.-C. Wang (1998). *The effect of ultraviolet irradiation, heat, pH, ozone, salinity and chemical disinfectants on the infectivity of white spot syndrome baculovirus.* Aquaculture, **166**(1-2): 1-17.

Chia, Y. (1958). *Chemistry of +I iodine in alkaline solutions.* Thesis, University of California, Berkeley.

Cicerone, R.J. (1981). *Halogens in the atmosphere.* Reviews of Geophysics and Space Physics, **19**(1): 123-139.

Councell, T.B., E.R. Landa, and D.R. Lovley (1997). *Microbial reduction of iodate.* Water, Air, and Soil Pollution, **100**(1-2): 99-106.

Courtois, B. (1813). Annales de Chimie Physique, **1/88**: 304.

Dean, J.A., Ed. (1985). *Lange's Handbook of Chemistry.* 13th ed., McGraw-Hill, New York.

Delange, F., J.T. Dunn, and D. Glinoer, Eds. (1993). *Iodine deficiency in Europe: a continuing concern.* NATO ASI Series. Series A: Life Sciences Vol. 241. Plenum Press, London.

Douillet, P.A. and P.L. Pickering (1999). *Seawater treatment for larval culture of the fish* Sciaenops ocellatus Linnaeus *(red drum).* Aquaculture, **170**(1): 113-126.

Duce, R.A., J.T. Wasson, J.W. Winchester, and F. Burns (1963). *Atmospheric iodine, bromine, and chlorine.* Journal of Geophysical Research, **68**(13): 3943-3947.

Dubois, J.E. and J. Toullec (1971). *Reactivity of the enols of saturated aliphatic ketones: quasi-identity of the rate constants for bromination and iodination.* Tetrahedron Letters, **37**: 3373-3376.

Eckhardt, K., E. Gocke, M.-T. King, and D. Wild (1981). *Mutagenic activity of chlorate, bromate, and iodate.* Mutation Research, **97**: 185.

Eigen, M. and K. Kustin (1962). *The kinetics of halogen hydrolysis.* Journal of the American Chemical Society, **84**: 1355-1361.

Elliott, S. and F.S. Rowland (1995). *Methyl halide hydrolysis rates in natural waters.* Journal of Atmospheric Chemistry, **20**: 229-236.

Ellis, K.V. and H.B.R.J. van Vree (1989). *Iodine used as a water-disinfectant in turbid waters.* Water Research, **23**(6): 671-676.

EU (European Union) (1998). *Richtlinie 98/83/EG des Rates.* Amtsblatt der Europäischen Gemeinschaften.

Fabian, I. and G. Gordon (1997). *The kinetics and mechanism of the chlorine dioxide-iodide ion reaction.* Inorganic Chemistry, **36**(12): 2494-2497.

Fuge, R. and C.C. Johnson (1986). *The geochemistry of iodine - a review.* Environmental Geochemistry and Health, **8**(2): 31-54.

Fuge, R. (1987). *Iodine in the environment: its distribution and relationship to human health.* Trace Substances in Environmental Health, **21**: 74-87.

Fuson, R.C. and B.A. Bull (1934). *The haloform reaction.* Chemical Reviews, **15**: 275-309.

Gallard, H. (1999). Personal communication.

Garland, J.A., A.W. Elzerman, and S.A. Penkett (1980). *The mechanism for dry deposition of ozone to seawater surfaces.* Journal of Geophysical Research, **85**(C12): 7488-7492.

Garland, J.A. and H. Curtis (1981). *Emission of iodine from the sea surface in the presence of ozone.* Journal of Geophysical Research, **86**(C4): 3183-3186.

Gay Lussac, J.L. (1814). *Mémoire sur l'iode.* Annales de Chimie Physique, **1/91**: 5.

Genser, E.E. and R.E. Connick (1973). *Exchange of iodide ion with triiodide ion studied by nuclear magnetic resonance.* Journal of Chemical Physics, **58**: 990-996.

Gerba, C.P., D.C. Johnson, and M.N. Hasan (1997). *Efficacy of iodine water purification tablets against* Cryptosporidium *oocysts and* Giardia *cysts.* Wilderness and Environmental Medicine, **8**: 96-100.

Giese, B., F. Laturnus, F.C. Adams, and C. Wiencke (1999). *Release of volatile iodinated* C_1*-*C_4 *hydrocarbons by marine macroalgae from various climate zones.* Environmental Science & Technology, **33**(14): 2432-2439.

Giger, W., M. Reinhard, C. Schaffner, and F. Zürcher (1976). *Analyses of organic constituents in water by high-resolution gas chromatography in combination with specific detection and computer-assisted mass spectrometry*, in "Identification & Analysis of Organic Pollutants in Water", Ed.: L.H. Keith; Ann Arbor Science, Ann Arbor, Michigan; 433-452.

Gittelman, T.S. and T.L. Yohe (1989). *Treatment of the iodinated haloform medicinal odors in drinking water.* Proceedings of AWWA Seminar on Identification and Treatment of Taste and Odor Compounds; Los Angeles, California; 105-123.

Gottardi, W. (1983). *Iodine and iodine compounds*, in "Disinfection, Sterilization, and Preservation." 3rd ed.; Ed.: S.S. Block; Lea & Febiger, Philadelphia, Pennsylvania; 183-196.

Greenwood, N.N. and A. Earnshaw (1984). *Chemistry of the elements*. Pergamon Press, Oxford.

Gribble, G.W. (1994). *The natural production of chlorinated compounds*. Environmental Science & Technology, **28**(7): 310A-319A.

Gschwend, P.M., J.K. MacFarlane, and K.A. Newman (1985). *Volatile halogenated organic compounds released to seawater from temperate marine macroalgae*. Science, **227**: 1033-1035.

Haag, W.R. and J. Hoigné (1983). *Ozonation of bromide-containing waters: kinetics of formation of hypobromous acid and bromate*. Environmental Science & Technology, **17**: 261-267.

Han, K., W.F. Koch, and K.W. Pratt (1987). *Improved procedure for the determination of iodide by ion chromatography with electrochemical detection*. Analytical Chemistry, **59**: 731-736.

Hansson, R.C., M.J. Henderson, P. Jack, and R.D. Taylor (1987). *Iodoform taste complaints in chloramination*. Water Research, **21**: 1265-1271.

Hetzel, B.S. and G.F. Maberly (1986). *Iodine*, in "Trace Elements in Human and Animal Nutrition", Ed.: W. Mertz; Academic Press, London. 139-208.

Hoffmann, P., N. Pilz, K.H. Lieser, V. Ilmstädter, and M. Griesbach (1987). *Radionuclides from the Chernobyl accident in the environment of Chattia, a region of the FRG*. Radiochimica Acta, **41**(4): 173-179.

Hoigné, J., H. Bader, W.R. Haag, and J. Staehelin (1985). *Rate constants of reactions of ozone with organic and inorganic compounds in water III. Inorganic compounds and radicals*. Water Research, **19**(8): 993-1004.

Hoigné, J. (1998). *Chemistry of aqueous ozone and transformation of pollutants by ozonation and advanced oxidation processes*, in "The Handbook of Environmental Chemistry Vol. 5 Part C, Quality and Treatment of Drinking Water II", Ed.: J. Hrubec; Springer-Verlag, Berlin. 83-141.

Hunt, N.K. and B.J. Mariñas (1997). *Kinetics of* Escherichia coli *inactivation with ozone*. Water Research, **31**(6): 1355-1362.

Ito, K. (1997). *Determination of iodide in seawater by ion chromatography*. Analytical Chemistry, **69**: 3628-3632.

Johnson, J.D. and R. Overby (1971). *Bromine and bromamine disinfection chemistry.* Journal of the Sanitary Engineering Division, **97**(5): 617-628.

Johnson, C.D. (1980). *The Hammett equation.* Cambridge Texts in Chemistry and Biochemistry, Cambridge University Press, Cambridge.

Karpel Vel Leitner, N., J. Vessella, M. Doré, and B. Legube (1998). *Chlorination and formation of organoiodinated compounds: the important role of ammonia.* Environmental Science & Technology, **32**(11): 1680-1685.

Khiari, D. (1999). Report American Water Works Association Research Foundation, in progress.

Kleopfer, R.D. and B.J. Fairless (1972). *Characterization of organic components in a municipal water supply.* Environmental Science & Technology, **6**(12): 1036-1037.

Klick, S. and K. Abrahamsson (1992). *Biogenic volatile iodated hydrocarbons in the ocean.* Journal of Geophysical Research, **97**(C8): 12683-12687.

Krupp, G. and D.C. Aumann (1999). *The origin of iodine in soil I. Iodine in rainfall over Germany.* Chemie der Erde, **59**(1): 57-67.

Kumar, K., R.A. Day, and D.W. Margerum (1986). *Atom-transfer redox kinetics: general-acid-assisted oxidation of iodide by chloramines and hypochlorite.* Inorganic Chemistry, **25**(24): 4344-4350.

Lambert, J.L., G.L. Hatch, and B. Mosier (1975). *Iodide and iodine determination in the parts-per-billion range with leuco crystal violet and N-chlorosuccinimide-succinimide reagents.* Analytical Chemistry, **47**: 915-916.

Langer, P. (1960). *History of goitre,* in "Endemic Goitre"; World Health Organization, Geneva; 9-25.

Laverock, M.J., M. Stephenson, and C.R. Macdonald (1995). *Toxicity of iodine, iodide, and iodate to* Daphnia magna *and rainbow trout (*Oncorhynchus mykiss*).* Archives of Environmental Contamination and Toxicology, **29**: 344-350.

Leigh, G.J., Ed. (1990). *Nomenclature of inorganic chemistry: Recommendations.* Blackbell Scientific Publications, Oxford.

Lengyel, I., I.R. Epstein, and K. Kustin (1993). *Kinetics of iodine hydrolysis.* Inorganic Chemistry, **32**(25): 5880-5882.

Lengyel, I., J. Li, K. Kustin, and I.R. Epstein (1996). *Rate constants for reactions between iodine- and chlorine-containing species: a detailed mechanism of the chlorine dioxide/chlorite-iodide reaction.* Journal of the American Chemical Society, **118**: 3708-3719.

Lovelock, J.E. (1975). *Natural halocarbons in the air and in the sea*. Nature, **256**: 193-194.

Luther III, G.W., J. Wu, and J.B. Cullen (1995). *Redox chemistry of iodine in seawater - frontier molecular orbital theory considerations*, in "Aquatic Chemistry: Interfacial and Interspecies Processes", Eds.: C.P. Huang, C.R. O'Melia, and J.J. Morgan; Advances in Chemistry Vol. 244; American Chemical Society, Washington DC; 135-155.

Mabey, W. and T. Mill (1978). *Critical review of hydrolysis of organic compounds in water under environmental conditions*. Journal of Physical Reference Data, **7**(2): 383-415.

Margerum, D.W., P.N. Dickson, J.C. Nagy, K. Kumar, C.P. Bowers, and K.D. Fogelman (1986). *Kinetics of the iodine monochloride reaction with iodide measured by the pulsed-accelerated-flow method*. Inorganic Chemistry, **25**(27): 4900-4904.

McTaggart, A.R., E.C.V. Butler, P.R. Haddad, and J.H. Middleton (1994). *Iodide and iodate concentrations in eastern Australian subtropical waters, with iodide by ion chromatography*. Marine Chemistry, **47**: 159-172.

Miyake, Y. and S. Tsunogai (1963). *Evaporation of iodine from the ocean*. Journal of Geophysical Research, **68**(13): 3989-3993.

Moisan, T.A., W.M. Dunstan, A. Udomkit, and G.T.F. Wong (1994). *The uptake of iodate by marine phytoplankton*. Journal of Phycology, **30**(4): 580-587.

Moore, R.E. (1977). *Volatile compounds from marine algae*. Accounts of Chemical Research, **10**: 40-47.

Moore, R.M. and R. Tokarczyk (1992). *Chloro-iodomethane in N. Atlantic waters: a potentially significant source of atmospheric iodine*. Geophysical Research Letters, **19**(17): 1779-1782.

Moore, R.M., M. Webb, R. Tokarczyk, and R. Wever (1996). *Bromoperoxidase and iodoperoxidase enzymes and production of halogenated methanes in marine diatom cultures*. Journal of Geophysical Research, **101**(C9): 20899-20908.

Mössinger, J.C., D.E. Shallcross, and R.A. Cox (1998). *UV-Vis absorption cross-sections and atmospheric lifetimes of* CH_2Br_2, CH_2I_2 *and* CH_2BrI. Journal of the Chemical Society, Faraday Transactions, **94**(10): 1391-1396.

Nägeli, F. (1969). *Auswirkungen des Phenolunfalles vom 20. September 1967 im Wasserwerk der Stadt Zürich*. Gas, Wasser, Abwasser, **49**(11): 372-377.

Nagy, J.C., K. Kumar, and D.W. Margerum (1988). *Non-metal redox kinetics: oxidation of iodide by hypochlorous acid and by nitrogen trichloride measured by the pulsed-accelerated-flow method.* Inorganic Chemistry, **27**(16): 2773-2780.

Neta, P. and L.M. Dorfman (1968). *Pulse radiolysis studies. XIII: Rate constants for the reaction of hydroxyl radicals with aromatic compounds in aqueous solutions.* Advances in Chemistry Series, **81**: 222-230.

Palmer, D.A. and M.H. Lietzke (1982). *The equilibria and kinetics of iodine hydrolysis.* Radiochimica Acta, **31**: 37-44.

Paquette, J. and B.L. Ford (1985). *Iodine chemistry in the +1 oxidation state I. The electronic spectra of* OI^-*, HOI, and* H_2OI^+. Canadian Journal of Chemistry, **63**: 2444-2448.

Pearson, R.G. (1969). *Hard and soft acids and bases.* Survey of Progress in Chemistry, **5**: 1-52.

Pethybridge, A.D. and J.E. Prue (1967). *Equilibria in aqueous solutions of iodic acid.* Transactions of the Faraday Society, **63**: 2019-2033.

Pinkernell, U., B. Nowack, H. Gallard, and U. von Gunten (1999). *Photometric determination of reactive bromine and chlorine species using ABTS.* submitted to Water Research.

Pundt, I., J.-P. Pommereau, C. Phillios, and E. Lateltin (1998). *Upper limit of iodine oxide in the lower stratosphere.* Journal of Atmospheric Chemistry, **30**: 173-185.

Rabai, G. and M.T. Beck (1988). *Exotic kinetic phenomena and their chemical explanation in the iodate-sulfite-thiosulfate system.* Journal of Physical Chemistry, **92**(10): 2804-2807.

Ramette, R.W. and R.W. Sandford Jr. (1965). *Thermodynamics of iodine solubility and triiodide ion formation in water and in deuterium oxide.* Journal of the American Chemical Society, **87**(22): 5001-5005.

Reckhow, D.A. and P.C. Singer (1984). *Mechanisms of organic halide formation during fulvic acid chlorination and implications with respect to preozonation,* in "Water Chlorination: Chemistry, Environmental Impact and Health Effects, Vol. 5", Eds.: R.L. Jolley, R.J. Bull, W.P. Davis, S. Katz, M.H. Roberts Jr., and V.A. Jacobs; Lewis Publishers, Chelsea, Michigan; 1229-1257.

Reifenhäuser, W. and K.G. Heumann (1992). *Determinations of methyl iodide in the Antarctic atmosphere and the south polar sea.* Atmospheric Environment, **26A**(16): 2905-2912.

Rook, J.J. (1974). *Formation of haloforms during chlorination of natural waters.* Journal of Water Treatment and Examination, **23**(2): 234-243.

Sammet, V. (1905). *Die Gleichgewichte* $6\ H^+ + 5\ I^- + IO_3^- = 3\ I_2 + 3\ H_2O$ *und* $6\ H^+ + 5\ Br^- + BrO_3^- = 3\ Br_2 + 3\ H_2O$, *chemisch und elektromotorisch bestimmt.* Zeitschrift für Physikalische Chemie, **53**(6): 641-691.

Sano, T., H. Hori, M. Yamamoto, and T. Yasunaga (1984). *Kinetic studies of the polyiodide complex formation in the iodine-iodide solutions.* Bulletin of the Chemical Society of Japan, **57**(2): 575-576.

Shin, H.S., Y.S. Oh-Shin, J.H. Kim, and J.K. Ryu (1996). *Trace level determination of iodide, iodine and iodate by gas chromatography-mass spectrometry.* Journal of Chromatography A, **732**: 327-333.

Soulard, M., F. Bloc, and A. Hatterer (1981). *Diagrams of existence of chloramines and bromamines in aqueous solution.* Journal of the Chemical Society, Dalton Transactions, **12**: 2300-2310.

Sturges, W.T. and L.A. Barrie (1988). *Chlorine, bromine, and iodine in arctic aerosols.* Atmospheric Environment, **22**(6): 1179-1194.

Suez Lyonnaise des Eaux (1993). *Conditions de formation et destruction des trihalométhanes iodés responsables des goûts et odeurs pharmaceutiques.* Internal Report, Lyonnaise des Eaux, Le Pecq, France.

Suffet, I.H., A. Corado, D. Chou, M.J. McGuire, and S. Butterworth (1996). *AWWA taste and odor survey.* Journal of the American Water Works Association, **88**(4): 168-180.

Taurog, A., E.A. Howells, and H.I. Nachimson (1966). *Conversion of iodate to iodide in vivo and in vitro.* Journal of Biological Chemistry, **241**(20): 4686-4693.

Ternes, T.A., R.W. Hirsch, M. Stumpf, T. Eggert, B.F. Schuppert, and K. Haberer (1999). *Nachweis und Screening von Arzneimittelrückständen, Diagnostika und Antiseptika in der aquatischen Umwelt.* ESWE-Institut für Wasserforschung und Wassertechnologie GmbH, Wiesbaden.

Thomas, T.R., D.T. Pence, and R.A. Hasty (1980). *The disproportionation of hypoiodous acid.* Journal of Inorganic & Nuclear Chemistry, **42**: 183-186.

Thompson, A.M. and O.C. Zafiriou (1983). *Air-sea fluxes of transient atmospheric species.* Journal of Geophysical Research, **88**(C11): 6696-6708.

Tian, R.C., J.C. Marty, E. Nicolas, J. Chiavérini, D. Ruiz-Pino, and M.D. Pizay (1996). *Iodine speciation: a potential indicator to evaluate new production versus regenerated production*. Deep-Sea Research I, **43**(5): 723-738.

Troy, R.C., M.D. Kelley, J.C. Nagy, and D.W. Margerum (1991). *Non-metal redox kinetics: iodine monobromide reaction with iodide ion and the hydrolysis of IBr*. Inorganic Chemistry, **30**(25): 4838-4845.

Truesdale, V.W., C. Canosa-Mas, and G.W. Luther III (1994). *Kinetics of disproportionation of hypoiodous acid*. Journal of the Chemical Society, Faraday Transactions, **90**(24): 3639-3643.

Truesdale, V.W. and C. Canosa-Mas (1995). *Kinetics of disproportionation of hypoiodous acid in phosphate and borate buffer at pH < 8.5 modelled using iodide feedback*. Journal of the Chemical Society, Faraday Transactions, **91**(15): 2269-2273.

Truesdale, V.W. (1997). *Kinetics of disproportionation of hypoiodous acid at high pH, with an extrapolation to rainwater*. Journal of the Chemical Society, Faraday Transactions, **93**(10): 1909-1914.

Turner, D.H., G.W. Flynn, N. Sutin, and J.V. Beitz (1972). *Laser Raman temperature-jump study of the kinetics of the triiodide equilibrium. Relaxation times in the 10^{-8}-10^{-7} second range*. Journal of the American Chemical Society, **94**(5): 1554-1559.

Urbansky, E.T., B.T. Cooper, and D.W. Margerum (1997). *Disproportionation kinetics of hypoiodous acid as catalyzed and suppressed by acetic acid-acetate buffer*. Inorganic Chemistry, **36**: 1338-1344.

USEPA (United States Environmental Protection Agency) (1998). *Federal Register Part IV*.

Vollhardt, K.P.C. and N.E. Schore (1994). *Organic Chemistry*. W.H. Freeman, New York.

von Gunten, U. and J. Hoigné (1994). *Bromate formation during ozonation of bromide-containing waters: interaction of ozone and hydroxyl radical reactions*. Environmental Science & Technology, **28**(7): 1234-1242.

Waber, U., H.R. von Gunten, and U. Krähenbühl (1987). *The impact of Chernobyl accident on a river/groundwater aquifer*. Radiochimica Acta, **41**: 191-198.

Wang, Y.L., J.C. Nagy, and D.W. Margerum (1989). *Kinetics of hydrolysis of iodine monochloride measured by the pulsed-accelerated-flow method*. Journal of the American Chemical Society, **111**(20): 7838-7844.

Wayne, R.P., G. Poulet, P. Biggs, J.P. Burrows, R.A. Cox, P.J. Crutzen, G.D. Hayman, M.E. Jenkin, G. Le Bras, G.K. Moortgat, U. Platt, and R.N. Schindler (1995). *Halogen oxides: radicals, sources and reservoirs in the laboratory and in the atmosphere*. Atmospheric Environment, **29**(20): 2675-2881.

Weast, R.C., Ed. (1984). *Handbook of chemistry and physics*. CRC Press: Boca Raton, Florida.

Webster, S.H., M.E. Rice, B. Highman, and W.F. von Oettingen (1957). *The toxicology of potassium and sodium iodates: acute toxicity in mice*. Journal of Pharmacology and Experimental Therapeutics, **120**: 171-178.

Webster, S.H., E.F. Stohlman, and B. Highman (1966). *The toxicology of potassium and sodium iodates III. Acute and subacute oral toxicity of potassium iodate in dogs*. Toxicology and Applied Pharmacology, **8**: 185-192.

Weinberg, H.S. and H. Yamada (1998). *Post-ion-chromatography derivatization for the determination of oxyhalides at sub-ppb levels in drinking waters*. Analytical Chemistry, **70**(1): 1-6.

Wennberg, P.O., J.W. Brault, T.F. Hanisco, R.J. Salawitch, and G.H. Mount (1997). *The atmospheric column abundance of IO: implications for stratospheric ozone*. Journal of Geophysical Research, **102**(D7): 8887-8898.

Whitehead, D.C. (1984). *The distribution and transformations of iodine in the environment*. Environment International, **10**: 321-339.

WHO (World Health Organization) (1993). *Guidelines for Drinking-Water Quality. Vol. 1: Recommendations*. WHO, Geneva.

WHO (World Health Organization) (1996). *Guidelines for Drinking Water Quality. Vol. 2: Health criteria and other supporting information*. WHO, Geneva.

Wolfe, R.L., N.D. Ward, and B.H. Olson (1985). *Inorganic chloramines as drinking water disinfectants: a review*. Journal of the American Water Works Association, **77**(10): 74-88.

Wong, G.T.F. (1991). *The marine geochemistry of iodine*. Reviews in Aquatic Sciences, **4**(1): 45-73.

Wren, J.C., J. Paquette, S. Sunder, and B.L. Ford (1986). *Iodine chemistry in the +1 oxidation state II. A Raman and UV/visible spectroscopic study of the disproportionation of hypoiodite in basic solutions*. Canadian Journal of Chemistry, **64**(12): 2284-2296.

Xin-Min, J., C. Xue-Yi, J. Ji-Yong, M. Tai, D.W. James, M.A. Rakeman, D. Zhi-Hong, M. Mamette, K. Amette, Z. Ming-Li, and G.R. Delong (1997). *Dynamics of environmental supplementation of iodine: Four years' experience of iodination of irrigation water in Hotien, Xinjiang, China.* Archives of Environmental Health, **52**(6): 399-408.

Yokouchi, Y., H. Mukai, H. Yamamoto, A. Otsuki, C. Saitoh, and Y. Nojiri (1997). *Distribution of methyl iodide, ethyl iodide, bromoform, and dibromomethane over the ocean (east and southeast Asian seas and the western Pacific).* Journal of Geophysical Research, **102**(D7): 8805-8809.

Young, W.F., H. Horth, R. Crane, T. Ogden, and M. Arnott (1996). *Taste and odour threshold concentrations of potential potable water contaminants.* Water Research, **30**(2): 331-340.

Appendix A: Overview of Equilibrium and Rate Constants

equilibrium	K	ref.
$I_2 + H_2O = HOI + I^- + H^+$	5.44×10^{-13}	Burger & Liebhafsky, 1973
$3\ HOI = IO_3^- + 2\ I^- + 3\ H^+$	6×10^{-11}	Sammet, 1905
$I_2 + I^- = I_3^-$	725	Burger & Liebhafsky, 1973
$H_2OI^+ = HOI + H^+$	0.04	Bell & Gelles, 1951
$HOI = H^+ + OI^-$	4.0×10^{-11}	Chapter 3
$OI^- + I^- = I_2O_2^-$	0.045	Atwater et al., 1996
$HOI + I^- = I_2OH^-$	300	Chia, 1958
$HIO_3 = IO_3^- + H^+$	0.18	Pethybridge & Prue, 1967
$I_3^- + I^- = I_4^{2-}$	0.184	Genser & Connick, 1973
$I_3^- + I_2 = I_5^-$	9	Ramette & Sandford, 1965
$2\ I_3^- = I_6^{2-}$	0.41	Sano et al., 1984
$ICl_2^- = ICl + Cl^-$	0.013	Wang et al., 1989
$ICl + H_2O = HOI + Cl^- + H^+$	8.2×10^{-5}	Wang et al., 1989
$IBr_2^- = IBr + Br^-$	0.035	Troy et al., 1991
$IBr = I^- + I_2Br^-$	2×10^{-6}	Troy et al., 1991
$IBr + H_2O = HOI + H^+ + Br^-$	2.4×10^{-7}	Troy et al., 1991
$I_2 + Cl^- = I_2Cl^-$	1.7	Margerum et al., 1986

reaction	rate constant	products	ref.
$I_2 + OH^-$	$8 \times 10^8\ M^{-1}s^{-1}$	I_2OH^-	Lengyel et al., 1993
I_2OH^-	$6.9 \times 10^5\ s^{-1}$	I_2, OH^-	Lengyel et al., 1993
$I_2OH^- + H^+$	$2.2 \times 10^{10}\ M^{-1}s^{-1}$	I_2, H_2O	Lengyel et al., 1993
I_2OH^-	$1.3 \times 10^6\ s^{-1}$	HOI, I^-	Eigen & Kustin, 1962
$HOI + I^-$	$5 \times 10^9\ M^{-1}s^{-1}$	I_2OH^-	Eigen & Kustin, 1962
$IO_3^- + 2\ I^- + 2\ H^+$	$3.0 \times 10^8\ M^{-4}s^{-1}$	HOI, OI^-	Barton & Wright, 1968
$I_2 + I^-$	$6.2 \times 10^9\ M^{-1}s^{-1}$	I_3^-	Turner et al., 1972
I_3^-	$8.5 \times 10^6\ s^{-1}$	I_2, I^-	Turner et al., 1972
HOI + HOI	$3 \pm 2 \times 10^{-1}\ M^{-1}s^{-1}$	IO_2^-, I^-	Chapter 3
$HOI + OI^-$	$15 \pm 1\ M^{-1}s^{-1}$	IO_2^-, I^-	Chapter 3
$HOI + HOI + HCO_3^-$	$5 \pm 2 \times 10^1\ M^{-2}s^{-1}$	IO_2^-, I^-	Chapter 3
$HOI + HOI + CO_3^{2-}$	$5.0 \pm 0.5 \times 10^3\ M^{-2}s^{-1}$	IO_2^-, I^-	Chapter 3
$HOI + HOI + B(OH)_4^-$	$1.7 \pm 0.6 \times 10^3\ M^{-2}s^{-1}$	IO_2^-, I^-	Chapter 3
$O_3 + I^-$	$2 \times 10^9\ M^{-1}s^{-1}$	OI^-	Garland et al., 1980
$HOCl + I^-$	$4.3 \times 10^8\ M^{-1}s^{-1}$	HOI	Nagy et al., 1988
$NH_2Cl + I^- + H^+$	$2.4 \times 10^{10}\ M^{-2}s^{-1}$	HOI	Kumar et al., 1986
$ClO_2 + I^-$	$1870\ M^{-1}s^{-1}$	$I^\bullet$	Fabian & Gordon, 1997

reaction	rate constant	products	ref.
HOI + O_3	3.6±1.0 x 10^4 $M^{-1}s^{-1}$	IO_3^-	Chapter 4
OI^- + O_3	1.6±0.5 x 10^6 $M^{-1}s^{-1}$	IO_3^-	Chapter 4
HOI + HOCl + HOCl	8.3±0.8 x 10^4 $M^{-2}s^{-1}$	IO_3^-	Chapter 4
HOI + HOCl	8.2±0.8 $M^{-1}s^{-1}$	IO_3^-	Chapter 4
HOI + OCl^-	52±5 $M^{-1}s^{-1}$	IO_3^-	Chapter 4
HOI + NH_2Cl	< 2 x 10^{-3} $M^{-1}s^{-1}$		Chapter 4
OI^- + NH_2Cl	< 3 $M^{-1}s^{-1}$		Chapter 4
H_2OI^+ + p-methoxy-phenol	5±1x10^4 $M^{-1}s^{-1}$		Chapter 5
H_2OI^+ + p-cresol	4.0±1.5x10^4 $M^{-1}s^{-1}$		Chapter 5
H_2OI^+ + phenol	5±2x10^4 $M^{-1}s^{-1}$		Chapter 5
H_2OI^+ + p-chlorophenol	3±1x10^3 $M^{-1}s^{-1}$		Chapter 5
H_2OI^+ + p-iodophenol	4±1x10^3 $M^{-1}s^{-1}$		Chapter 5
H_2OI^+ + p-cyanophenol	2±1x10^2 $M^{-1}s^{-1}$		Chapter 5
HOI + p-methoxy-phenol	< 100 $M^{-1}s^{-1}$		Chapter 5
HOI + p-cresol	3±1x10^2 $M^{-1}s^{-1}$		Chapter 5
HOI + phenol	1.0±0.3x10^2 $M^{-1}s^{-1}$		Chapter 5
HOI + p-chlorophenol	< 5 $M^{-1}s^{-1}$		Chapter 5
HOI + p-iodophenol	20±8 $M^{-1}s^{-1}$		Chapter 5
HOI + p-cyanophenol	1.5±0.5 $M^{-1}s^{-1}$		Chapter 5

reaction	rate constant	ref.
HOI + p-methoxy-phenol	$7\pm2\text{x}10^{8}\,M^{-1}s^{-1}$	Chapter 5
HOI + p-cresol	$7\pm3\text{x}10^{8}\,M^{-1}s^{-1}$	Chapter 5
HOI + phenol	$2\pm1\text{x}10^{6}\,M^{-1}s^{-1}$	Chapter 5
HOI + p-chlorophenol	$1.6\pm0.5\text{x}10^{5}\,M^{-1}s^{-1}$	Chapter 5
HOI + p-iodophenol	$1.5\pm0.8\text{x}10^{5}\,M^{-1}s^{-1}$	Chapter 5
HOI + p-cyanophenol	$4\pm2\text{x}10^{2}\,M^{-1}s^{-1}$	Chapter 5
acetaldehyde	$9\pm1 \text{ x } 10^{-8}\,s^{-1}$	Chapter 5
pinacolone	$4\pm2 \text{ x } 10^{-9}\,s^{-1}$	Chapter 5
acetone	$1.3\pm0.4 \text{ x } 10^{-8}\,s^{-1}$	Chapter 5
acetaldehyde + OH^-	$0.90\pm0.04\,M^{-1}s^{-1}$	Chapter 5
pinacolone + OH^-	$0.037\pm0.002\,M^{-1}s^{-1}$	Chapter 5
acetone + OH^-	$0.25\pm0.03\,M^{-1}s^{-1}$	Chapter 5
HOI + acetone	$2.5\pm1.0\,M^{-1}s^{-1}$	Chapter 5
OI^- + acetone + OH^-	$3\pm1 \text{ x } 10^{3}\,M^{-2}s^{-1}$	Chapter 5
HOI + methylglyoxal + OH^-	$6\pm2 \text{ x } 10^{2}\,M^{-1.4}s^{-1}$	Chapter 5
H_2OI^+ + allyl alcohol	$1.8\pm0.4 \text{ x } 10^{7}\,M^{-1}s^{-1}$	Chapter 5
HOI + glucosamine	$0.27\pm0.07\,M^{-1}s^{-1}$	Chapter 5
HOI + Hglucosamine^+	$7\pm3 \text{ x } 10^{-3}\,M^{-1}s^{-1}$	Chapter 5

Appendix B: I^- and IO_3^- in Natural and Treated Waters and in Table Salts

	IO_3^- / µg/L	I^- / µg/L	Date
Moos, Zurich			16.10.1998
source water Sihl 401	0.9	1.8	
source water Lorze 402	1.2	2.0	
source water after ClO_2 107	1.0	0.0	
lake water 101/01	0.0	0.3	
lake water preox (Cl_2, ClO_2) 102/02	0.5	0.1	
fast filtration 156	0.4	0.0	
ozonation 110	1.7	0.0	
GAC filtrate 112	1.4	0.2	
finished water 115/01	1.4	0.1	
Le Pecq			19.4.1999
raw water	4.2	10.2	
ozonated water	25.3	1.0	
GAC filtrate	24.9	0.1	
osmosis	0.2	0.3	
Le Pecq			29.4.1999
raw water	1.9	11.2	
ozonated water	24.8	1.9	
GAC filtration	24.0	0.9	
new GAC filter	10.8	0.6	
Croissy/Le Pecq			8.6.1999
raw water	0.8	8.7	
ozonation	20.0	< 0.2	
GAC filtration	22.9	< 0.2	
ground water F1 Le Pecq		10.7	
ground water F4 Le Pecq		12.0	
ground water F6 Le Pecq		1.1	
ground water F7 Le Pecq		17.6	
ground water F9 Le Pecq		21.8	
ground water F1 Mexique		3.2	
ground water F12 Mexique		0.4	
ground water F15 Mexique		< 0.2	
rain water		0.5	

Rainwaters Switzerland	IO_3^- / µg/L	I^- / µg/L	
Chaumont	< 0.1	3.3	27.4.1999
Chaumont	0.5	1.0	29.4.1999
Chaumont	0.1	7.3	30.4.1999
Chaumont	< 0.1	2.8	1.5.1999
Chaumont	< 0.1	1.9	7.5.1999
Chaumont	< 0.1	2.3	8.5.1999
Chaumont	< 0.1	10.8	11.5.1999
Dübendorf	0.4	1.4	29.4.1999
Dübendorf	< 0.1	2.7	30.4.1999
Dübendorf	< 0.1	1.0	6.5.1999
Dübendorf	< 0.1	1.0	7.5.1999
Dübendorf	< 0.1	1.6	8.5.1999
Payerne	< 0.1	5.5	27.4.1999
Payerne	< 0.1	0.5	8.5.1999
Payerne	< 0.1	2.2	11.5.1999
Rigi	< 0.1	4.4	27.4.1999
Rigi	0.6	3.7	29.4.1999
Rigi	0.3	0.7	30.4.1999
Rigi	< 0.1	0.7	5.5.1999
Rigi	< 0.1	2.3	6.5.1999
Tänikon	< 0.1	1.5	21.4.1999
Tänikon	< 0.1	4.7	23.4.1999
Tänikon	< 0.1	5.2	24.4.1999
Tänikon	< 0.1	3.7	27.4.1999
Tänikon	0.2	2.8	30.4.1999
Tänikon	< 0.1	0.8	6.5.1999

Mimizan (french Atlantic coast)			Aug. 99
rain water	0.2	< 0.3	
drinking water	3.5	< 0.3	

Table salts India	IO_3^- / mg/kg	I^- / mg/kg	May 99
A	27.7	1.7	
B	36.3	8.5	
C	31.2	6.1	

Appendix C: Kinetic Raw Data

Raw data: oxidation of HOI by chlorine and ozone

pH	[HOCl]$_{tot}$ / µM	k / s^{-1}
5.30	5.1	2.45e-5
5.40	35.3	4.78e-4
5.40	20.4	1.95e-4
5.40	19.8	1.80e-4
5.40	15.0	1.71e-4
5.40	10.1	8.36e-5
5.40	4.9	2.30e-5
5.40	19.8	3.73e-4
5.50	100.8	2.17e-3
5.50	71.0	1.36e-3
5.50	69.5	9.52e-4
5.58	433.0	2.08e-2
5.60	375.5	1.26e-2
5.62	289.0	1.10e-2
5.64	254.8	7.23e-3
5.69	144.0	2.09e-3
5.70	145.0	1.88e-3
6.20	15.0	1.28e-4
6.20	10.0	9.89e-5
6.20	5.0	1.86e-5
6.26	375.5	1.14e-2
6.29	240.3	4.57e-3
6.30	20.4	1.97e-4
6.35	114.0	9.24e-4
7.18	341.2	1.21e-2
7.20	39.6	6.16e-4
7.20	20.4	2.90e-4
7.20	20.2	5.83e-4
7.20	15.3	5.26e-4
7.20	15.3	6.05e-4
7.20	10.2	1.08e-4
7.20	5.1	6.26e-5
7.23	170.4	4.46e-3
7.28	83.1	2.45e-3
8.14	41.3	1.81e-3
8.16	123.8	6.02e-3
8.17	82.5	3.97e-3
8.20	20.4	8.01e-4
8.20	15.0	5.94e-4
8.20	19.8	4.29e-4
8.20	19.8	1.35e-3
8.21	9.6	5.08e-4
8.22	254.1	1.05e-2
8.24	10.2	3.51e-4
8.25	5.1	2.17e-4
8.26	131.8	5.89e-3
8.28	63.8	3.22e-3
8.50	19.9	1.28e-3
8.58	29.3	1.90e-3
8.71	40.3	2.21e-3
8.75	49.4	3.66e-3
8.75	49.2	2.74e-3
8.75	10.1	5.84e-4
8.80	40.3	3.36e-3
8.80	15.0	7.62e-4
8.80	5.0	2.52e-4
8.90	249.3	1.02e-2
8.90	150.1	5.90e-3
8.90	59.9	5.53e-3
8.90	49.8	3.25e-3
8.90	20.4	1.14e-3
8.91	102.0	4.48e-3
8.93	198.3	7.34e-3

pH	ozone: k / M^{-1}s^{-1}
5.99	29100
6.00	36200
6.00	30400
6.05	25345
6.36	29921
6.38	25300
6.39	50000
6.40	56300
6.68	35400
6.70	37500
6.96	32900
7.00	42100
7.00	52800
7.38	50600
7.40	54700
7.80	59100
7.81	37900
7.82	59900
8.24	57100
8.36	34200
8.39	50435
8.42	66300
8.46	46150
8.77	53490
9.17	113700
9.21	123700
9.43	172900
9.50	181900
9.56	187090
9.56	182600
9.61	231900
9.62	232400
9.74	387000
9.74	377000

Raw data: disproportionation

k_Σ / $M^{-1}s^{-1}$	pH	borate / M
1.28	7.65	3.00e-3
1.04	7.66	2.94e-3
2.95	7.95	2.49e-2
1.89	8.18	3.04e-3
2.04	8.18	2.94e-3
4.88	8.21	1.23e-2
6.19	8.21	2.17e-2
1.41	8.21	3.01e-3
2.68	8.33	3.00e-3
6.89	8.39	1.21e-2
3.31	8.52	3.01e-3
3.21	8.90	2.73e-3
5.43	8.94	2.91e-3
8.32	8.96	2.99e-3
6.86	8.96	2.96e-3
11.18	8.96	3.00e-3
32.42	8.97	2.40e-2
6.14	8.98	2.93e-3
5.79	8.98	2.93e-3
5.66	8.98	2.93e-3
5.73	8.99	2.93e-3
12.14	9.0	4.32e-3
9.12	9.0	4.32e-3
8.42	9.0	4.32e-3
4.46	9.0	2.86e-3
18.74	9.0	1.20e-2
6.07	9.03	3.00e-3
7.23	9.04	3.01e-3
12.80	9.73	2.96e-3
11.32	9.95	3.01e-3
12.40	9.96	3.04e-3
50.16	9.97	2.10e-2
53.97	9.97	2.10e-2
32.20	9.98	1.23e-2
33.98	9.98	1.20e-2
8.40	10.0	2.00e-3
13.30	10.44	2.96e-3
10.66	10.61	3.00e-3

k_Σ / $M^{-1}s^{-1}$	pH	carbonate / M
2.13	8.46	3.00e-3
2.25	8.46	3.00e-3
2.15	8.48	3.00e-3
2.02	8.48	3.00e-3
3.93	8.94	3.00e-3
29.52	8.97	2.98e-2
21.33	8.99	2.09e-2
13.40	8.99	1.19e-2
4.07	8.99	3.00e-3

k_Σ / $M^{-1}s^{-1}$	pH	carbonate / M
4.17	9.00	3.00e-3
9.24	9.01	2.98e-3
4.75	9.07	3.00e-3
18.64	9.07	2.11e-2
9.80	9.13	1.21e-2
1.21	9.19	3.02e-3
8.02	9.47	3.00e-3
8.62	9.49	3.00e-3
27.43	9.51	1.21e-2
9.09	9.53	3.00e-3
13.62	9.69	3.02e-3
10.64	9.85	2.97e-3
35.36	9.96	1.19e-2
56.10	9.97	2.07e-2
12.71	9.97	3.00e-3
14.61	9.98	3.00e-3
14.90	9.98	3.00e-3
15.30	10.01	3.00e-3
61.83	10.02	2.11e-2
40.04	10.04	1.21e-2
16.57	10.18	3.02e-3
17.69	10.42	3.00e-3
15.17	10.43	3.00e-3
15.91	10.49	3.00e-3
15.05	10.51	3.00e-3
8.96	10.86	2.96e-3
10.15	10.88	3.00e-3
9.80	10.92	3.00e-3
9.47	10.95	3.00e-3
9.22	10.98	3.00e-3
14.98	10.99	1.19e-2
12.45	11.00	3.02e-3
13.54	11.02	1.21e-2
16.77	11.06	2.07e-2

k_Σ / $M^{-1}s^{-1}$	pH	ammonia / M
2.07	8.29	1.98e-3
2.19	8.32	9.89e-3
1.67	8.33	4.94e-2
4.90	8.79	9.98e-4
0.87	8.98	4.99e-2
0.77	8.98	9.98e-2
1.07	9.07	2.48e-2
2.49	9.08	3.40e-3
1.56	9.08	1.46e-2
2.75	9.96	1.98e-3
1.09	10.00	9.68e-3
0.55	10.15	4.88e-2

Raw data: reaction of HOI with phenols

pH	p-iodophenol / M	k / s^{-1}
0.47	1.00e-5	2.80e-2
0.96	1.00e-5	3.15e-2
1.43	1.00e-5	2.04e-2
1.94	2.00e-5	1.52e-2
3.09	5.00e-5	5.03e-3
3.35	2.00e-4	1.06e-2
4.09	2.00e-5	4.60e-4
4.27	2.00e-4	6.36e-3
5.05	2.00e-5	4.23e-4
5.11	6.00e-5	2.23e-3
5.38	2.00e-5	5.22e-4
5.57	2.00e-5	5.96e-4
6.27	2.00e-5	5.03e-3
7.29	1.00e-4	2.20e-1
7.29	2.00e-4	4.69e-1
8.23	2.50e-5	2.42e-1

pH	p-cresol / M	k / s^{-1}
2.45	1.00e-5	3.87e-2
2.49	1.00e-5	4.08e-2
2.79	1.00e-5	2.96e-2
3.24	1.00e-5	9.33e-3
3.24	1.00e-5	1.28e-2
3.48	1.00e-5	1.01e-2
4.05	1.00e-5	5.33e-3
4.88	1.00e-5	3.95e-2

pH	p-methoxyphenol / M	k / s^{-1}
3.1	1.00e-5	1.36e-2
3.16	1.00e-5	1.08e-2
3.26	1.00e-5	8.85e-3
3.27	1.00e-5	9.45e-3
3.49	1.00e-5	5.80e-3
3.5	1.00e-5	6.77e-3
3.7	1.00e-5	5.22e-3
4.07	1.00e-5	5.07e-3
4.07	2.00e-5	1.62e-2
4.51	1.00e-5	1.38e-2
4.68	1.00e-5	2.43e-2

pH	phenol / M	k / s^{-1}
3.09	1.00e-5	1.37e-2
3.26	1.00e-5	1.23e-2
3.71	1.00e-5	4.47e-3
3.98	4.00e-5	7.90e-3
4.0	2.00e-5	3.75e-3
4.49	6.00e-5	1.17e-2
4.5	1.00e-4	1.25e-2
4.53	2.00e-5	2.99e-3
4.91	2.00e-5	2.58e-3
5.15	4.00e-4	7.71e-2
5.43	5.00e-4	1.88e-1
5.48	2.00e-5	8.18e-3
5.8	1.25e-4	6.01e-2
6.25	1.00e-4	1.71e-1
6.28	5.00e-4	7.70e-1
6.29	1.25e-4	2.01e-1
7.02	1.00e-4	5.06e-1
7.66	5.00e-5	8.01e-1
7.68	2.50e-5	3.99e-1
7.8	5.00e-5	5.78e-1
7.91	2.50e-5	5.04e-1
7.97	2.50e-5	4.46e-1
8.08	2.50e-5	4.97e-1
8.16	2.50e-5	8.71e-1
8.18	2.50e-5	6.92e-1
8.33	2.50e-5	9.08e-1
8.55	2.50e-5	1.55e+0

pH	p-cyanophenol / M	k / s^{-1}
-0.04	1.00e-5	6.03e-2
0.54	1.00e-5	1.33e-2
1.02	1.00e-5	6.17e-3
1.02	1.00e-5	6.42e-3
1.48	2.00e-5	5.26e-3
1.86	1.00e-4	7.99e-3
1.91	5.00e-5	7.04e-3
2.44	5.00e-4	8.83e-3
3.24	1.00e-3	5.18e-3
4.09	1.00e-3	1.52e-3
4.11	5.00e-4	8.50e-4
4.56	5.00e-4	9.66e-4
4.58	1.00e-3	2.05e-3
5.03	5.00e-4	1.22e-3
5.07	1.00e-3	2.63e-3
5.54	1.00e-3	4.68e-3
6.25	2.00e-4	3.74e-3
6.27	1.00e-4	1.86e-3
7.27	2.00e-5	1.69e-3
7.29	1.00e-5	9.00e-4
7.63	1.00e-5	1.31e-3
7.66	2.00e-5	2.45e-3
8.19	1.00e-5	1.28e-3
8.41	2.00e-5	3.07e-3

pH	p-chlorophenol/M	k / s^{-1}	pH	p-chlorophenol/M	k / s^{-1}
1.49	1.00e-5	2.20e-2	5.07	2.00e-4	1.95e-3
1.95	2.00e-5	1.05e-2	5.86	1.00e-4	6.07e-3
2.37	1.00e-5	2.72e-3	6.83	5.00e-5	2.57e-2
3.26	2.00e-4	7.01e-3	7.26	1.00e-5	1.18e-2
3.88	2.00e-4	2.31e-3	7.27	2.00e-5	2.72e-2
4.49	2.00e-4	8.98e-4	7.67	1.00e-5	2.30e-2
4.75	2.00e-4	1.35e-3	7.70	1.00e-5	2.23e-2

Raw data: reaction of HOI with carbonyl compounds, first-order in HOI

pH	methylglyoxal / M	k / s^{-1}
3.85	2.00e-3	1.12e-4
4.23	2.00e-3	1.54e-4
4.72	2.00e-3	2.83e-4
6.08	2.00e-3	6.06e-4
7.13	2.00e-3	1.44e-3
7.2	1.00e-3	7.65e-4
7.76	1.00e-3	1.74e-3
7.95	1.00e-3	2.28e-3
8.09	3.00e-4	5.96e-4
8.19	3.00e-4	8.83e-4
8.41	1.00e-4	2.60e-4
8.46	3.00e-5	1.16e-4
8.51	1.00e-4	3.76e-4

pH	methylglyoxal / M	k / s^{-1}
8.72	1.00e-4	5.82e-4
9.12	3.00e-5	3.54e-4

acetone / M	pH	k / s^{-1}
5.00e-3	9.08	6.61e-3
8.38e-3	9.3	1.54e-2
4.71e-3	9.61	1.04e-2
4.41e-3	10.04	9.85e-3
5.00e-3	10.48	1.17e-2
5.00e-3	10.69	1.30e-2
5.00e-3	10.87	1.40e-2
2.00e-3	11.3	1.04e-2
2.00e-3	11.59	1.76e-2

Raw data: reaction of HOI with carbonyl compounds, zero-order in HOI

pH	acetaldehyde / M	k / M/s
8.05	8.85e-4	1.48e-10
7.78	1.00e-2	5.35e-9
8.04	3.00e-3	2.43e-9
8.11	1.00e-3	1.00e-9
7.15	1.00e-2	2.42e-9
7.26	3.00e-3	8.17e-10
6.75	3.00e-2	4.31e-9
8.17	3.00e-3	3.80e-9
8.51	1.00e-3	2.74e-9
8.62	3.00e-4	1.19e-9

pH	pinacolone / M	k / M/s
8.41	1.00e-2	9.05e-10
8.77	1.00e-2	2.48e-9
8.10	1.00e-2	7.47e-10
6.29	1.00e-2	1.31e-10
4.80	1.00e-2	3.02e-10
8.79	1.00e-2	2.11e-9
8.64	1.00e-2	1.59e-9

pH	pinacolone / M	k / M/s
8.79	1.00e-2	2.37e-9
8.74	3.00e-2	5.15e-9
8.88	3.00e-3	9.66e-10
8.92	1.00e-3	3.29e-10
7.30	3.00e-2	3.38e-10
7.28	1.00e-1	8.98e-10
7.31	1.00e-2	1.40e-10

acetone / M	pH	k / M/s
5.00e-2	5.98	2.71e-10
4.07e-2	6.55	9.36e-10
3.06e-2	6.84	1.14e-9
6.42e-2	7.29	3.11e-9
3.34e-2	7.33	1.94e-9
5.50e-2	7.33	3.10e-9
5.09e-2	7.61	4.83e-9
5.00e-2	7.92	1.18e-8
5.00e-2	8.25	2.21e-8

Curriculum Vitae

Yves Bichsel
born December 30, 1971 in Zurich
Citizen of Eggiwil, Switzerland
Married

1978-1984	Primary school, Zurich
1984-1990	High school, Zurich (Kantonsschule Zürich-Oerlikon)
1990	Matura type C
1991-1995	Undergraduate studies in chemistry, Swiss Federal Institute of Technology Zurich (ETHZ, Abt. IV)
1995	Diploma in General Chemistry (Analytical Chemistry, Physical Chemistry, Environmental Chemistry, Inorganic Chemistry, Organic Chemistry)
	Diploma thesis at the Swiss Federal Institute of Environmental Science and Technology EAWAG (in the group of Prof. Dr. René Schwarzenbach), 'Triphenyltin: Analytics and Sorption on SiO_2 and Kaolinite'
1995-1999	Doctoral thesis, EAWAG (in the group of Dr. Urs von Gunten), 'Behavior of iodine species in oxidative processes during drinking water treatment.'
1996-1999	Teaching assistant, EAWAG/ETH